Title

The Geography of Long Term Exposure to Particulate Matter 2.5 and COVID-19 Mortality; An Assessment of the Fragility and Spatial Sensitivity of a Significant Finding

Author

Badger, Jennifer

Publication Date

2022

Peer reviewed|Thesis/dissertation

UNIVERSITY OF CALIFORNIA

Los Angeles

The Geography of Long Term Exposure to Particulate Matter$_{2.5}$ and COVID-19 Mortality

An Assessment of the Fragility and Spatial Sensitivity of a Significant Finding

A thesis submitted in partial satisfaction of the requirements for the degree Master of Arts in Geography

by

Jennifer Beth Badger

2022

ABSTRACT OF THE THESIS

The Geography of Long Term Exposure to Particulate Matter$_{2.5}$ and COVID-19 Mortality

An Assessment of the Sensitivity and Spatial Processes of a Significant Finding

by

Jennifer Beth Badger

Master of Arts In Geography

University of California, Los Angeles, 2022

Professor Michael E. Shin, Chair

Air pollution is directly linked to death. In December 2020, a UK coroner ruled that air pollution was the cause of a fatal asthma attack that led to the 2013 death of nine-year-old Ella Adoo-Kissi Debrah who lived adjacent to a busy motorway (BBC News, 2022). The assignment of air pollution as the official cause of death on a death certificate was the first of its kind in the world (Reynolds, 2020). Though this was the first official assignment of air pollution as a cause of death, there are numerous studies linking air pollution exposure with mortality all over the world. Before the COVID-19 pandemic, the air pollutant $PM_{2.5}$ was identified as the "largest environmental risk factor in the United States" (Goodkind et al. 2019, p. 8780) and the cause of more annual premature deaths than traffic accidents and homicides combined (Goodkind et al. 2019).

With the onset of the COVID-19 pandemic, researchers began assessing the impact of air pollution exposure on COVID-19 incidence and death. In a widely received, nationwide study linking air pollution exposure to COVID-19 mortality, Harvard T.H. Chan School of Public Health researchers, Wu et al., produced significant findings linking the impact of long term

exposure to $PM_{2.5}$ to COVID-19 mortality across the contiguous United States. This 2020 study, published in *ScienceAdvances,* has been cited over 600 times, covered by 131 news outlets and downloaded over 15,000 times. Georeferenced data is routinely used in public health research such as this, however, the substantive influence of geography in the relationship between the treatment and outcome variable is often not considered in the model specifications, research design, nor the sampling strategy (Goldhagen et al., 2005; Matisziw, Grubesic, and Wei 2008). Additionally, the mechanism of data aggregation to an administrative unit may spatially misrepresent the data (Delmelle et al., 2022). As air pollution is a local, regional, and transboundary phenomenon (Nordenstam et. al, 1998; Goodkind, 2019), spatial autocorrelation, or spatially similar values, in the long term exposure to $PM_{2.5}$ among U.S. counties is likely. Despite the inclusion of maps indicating strong spatial trends in the long term exposure to $PM_{2.5}$ and COVID-19 mortality, the possible presence of spatial autocorrelation at the local level or spatial heterogeneity at the regional level was not investigated by the authors.

Epidemiological studies invoking large, areal units may misrepresent the underlying, spatial processes of environmental health-hazards and produce unreliable treatment effect estimates when relating air pollution exposure to disease (Fotheringham and Wong, 1991; Kolak and Anselin, 2019). In this thesis, the fragility of the Wu et al. treatment effect estimate to unobserved confounding is assessed utilizing an alternative sensitivity analysis framework. This framework revealed that the estimate derived by Wu et al. (2020) is much more fragile to confounding than reported by the authors. Spatial analysis was then applied to investigate the possibility of spatial regimes (e.g. hotspots) in the treatment and outcome variables which may contribute to biased or inefficient treatment effect estimates. Strong levels of spatial autocorrelation and regional spatial heterogeneity in the long term exposure to $PM_{2.5}$, and to a lesser extent in the COVID-19 mortality rate, were confirmed by both computational and

exploratory spatial data analysis. The highly variable associations between long term exposure to $PM_{2.5}$ and COVID-19 Mortality per U.S. Census Region or EPA Climatically Consistent Region delivered the expected result that the relationship between the treatment and outcome variable changes with changes in the sub-National definition of place. An understanding of the geography of the ubiquitous, locally variable and far-reaching $PM_{2.5}$, and its related health-hazard risks can contribute to an uncovering of the politics, power relations, and socioenvironments that coproduce differential access to clean air and the resulting uneven health burdens experienced by Black, LatinX, Asian-American, and immigrant communities. This is an essential step towards disentangling the relationships rendering clean air no longer an “open-access good” (Véron, 2006).

The thesis of Jennifer Beth Badger is approved.

Susanna B. Hecht

Kathleen Bawn

Michael E. Shin, Committee Chair

University of California, Los Angeles

2022

TABLE OF CONTENTS

1. Introduction..... pp. 1-13

2. Research Questions.....p. 13

3. Literature Review.....pp. 13 - 29

4. Data and Methods.....pp. 30 - 56

5. Results.....pp. 57 - 107

6. Discussion.....pp. 108 - 115

7. Appendix.....pp. 116 - 118

7. Bibliography.....pp. 119 - 136

LIST OF FIGURES

i	U.S. Census Regions	p. 16
ii	County-level decrease in ambient PM2.5 concentrations	p. 19
1a	Conditional Ignorability	p. 36
1b	Common Support	p. 36
2a	Reworked Outcome Variable	p. 37
2b	Reworked OLS Main Model	p. 37
2c	Ozone OLS Model	p. 39
3	Global Moran's I Formula	p. 49
4	Local Moran's I Formula	p. 50
5	Spatial Lag Formula	p. 51
6	Spatial Error Formula	p. 52
7	Spatial Durbin Formula	p. 53
8	U.S. Census OLS Model	p. 54
9	EPA Climatically Consistent Regions	p. 55
10	EPA OLS Model	p. 56
11	Megalopolis, U.S. Census Bureau, 2021 (Appendix)	p. 118

LIST OF TABLES

1	Wu et al.'s Negative Binomial "Main Model"	p. 57
2	OLS reworking: "OLS Main Model"	p. 57
3	OLS Treatment Model	p. 59
A	Sensitivity of OLS Main Model treatment effect to confounding	p. 60
4	Ozone subset OLS Model	p. 65
5	Ozone subset OLS Treatment Model	p. 66
B	Sensitivity of the Qzone Subset to confounding	p. 67
6a	Global Moran's I for treatment, outcome and model residuals	p. 80
6b	Monte Carlo Simulation of Moran's I (Appendix)	p. 117
7	OLS Main Model Breusch-Pagan Test Results	p. 88
8	LM Tests, OLS Main Model	p. 89
9	OLS Main Model vs. Spatial Lag vs. Spatial Error	p. 92
10	Spatial Durbin Model Results	p. 94
11a	One Way ANOVA results, Census Regions	p. 96
11b	LM Test Results: Census Region Model	p. 97
12	Census Region OLS(1) vs. Spatial Lag (2) and Spatial Error (3) Models	p. 99
13	Spatial Durbin Model Results	p. 102
14a	One Way ANOVA results, EPA Regions	p. 103
14b	LM Test Results: EPA Region Model	p. 104
15	EPA Climatically Consistent Region OLS vs. Spatial Lag and Spatial Error Models	p. 105
16	Spatial Durbin Impacts- EPA Region	p. 106

LIST OF PLOTS

A_i	Sensitivity of OLS Main Model treatment effect to confounding	p. 60
A_{ii}	Sensitivity of OLS Main Model t-value	p. 63
1	Original sample vs. Ozone subset	p. 64
B_i	Sensitivity of the *Ozone Subset* to confounding	p. 67
B_{ii}	Sensitivity of OLS Ozone Model t-value	p. 69
2	Ozone ppb vs. COVID-19 Mortality Rate	p. 70
3	Correlation Between $PM_{2.5}$ and Ozone (Appendix)	p. 116
4a, 4c, 4e	Density Distributions of Mean $PM_{2.5}$, COVID-19 Mortality Rate, OLS Main Model Residuals	p. 71
4b, 4d, 4f	Q-Q Plots of Mean $PM_{2.5}$, COVID-19 Mortality Rate, OLS Main Model Residuals	p. 71
5a	Long term Exposure to $PM_{2.5}$ Amongst U.S. Counties	p. 74
5b	COVID-19 Mortality Prevalence Amongst U.S. Counties	p. 75
5c	OLS Main Model Residuals Amongst U.S. Counties	p. 76
5d	2020 Population Density per U.S. County (Appendix)	p. 116
5e	*America's Economic Output in 2018* (Appendix)	p. 117
6a-6c	Global Moran's I Plots: $PM_{2.5}$, COVID-19 Mortality, OLS Main Model Residuals	p. 79
7a-7c	Local Moran's I $PM_{2.5}$, COVID-19 Mortality, OLS Main Model Residuals	pp. 83-85
8	OLS Main Model Fitted Values vs. Residuals	p. 88
9	National Long Term Exposure to PM 2.5 vs COVID-19 Mortality by County	p. 94
10a	Long Term Exposure to PM 2.5 vs COVID-19 Mortality by Census Region	p. 95
10b	Tukey Honest Significant Difference Test Census Regions	p. 97
11	Long Term Exposure to PM 2.5 vs COVID-19 Mortality by EPA Region	p. 102

1. Introduction

1.1 *Air Pollution and Mortality*

Air pollution is directly linked to death. In December 2020, a UK coroner ruled that air pollution was the cause of a fatal asthma attack that led to the 2013 death of nine-year-old Ella Adoo-Kissi Debrah who lived adjacent to a busy motorway: “[t]he inquest into Ella's death found levels of nitrogen dioxide near her [South London] home exceeded World Health Organization and European Union guidelines” (BBC News, 2022). The assignment of air pollution as the official cause of death on a death certificate was the first of its kind in the world (Reynolds, 2020). Though this was the first official assignment of air pollution as a cause of death, there are numerous studies linking air pollution exposure with mortality all over the world. A meta-analytic summary across North America, Europe, and Asia of twenty-five years of cohort studies on the effects of long term exposure to $PM_{2.5}$ by Pope et al. found substantial evidence of “adverse PM2.5-mortality associations for all-cause mortality, cardiopulmonary mortality, and lung-cancer mortality” (2020, p. 7). $PM_{2.5}$, also referred to as fine particulate matter, refers to a broad category of inhalable, microfine solids and liquids that are 2.5 μm in diameter or smaller (US EPA, 2016b). Before the onset of the COVID-19 pandemic, $PM_{2.5}$ was identified as the “largest environmental risk factor in the United States” (Goodkind et al. 2019, p. 8780) and the cause of more annual premature deaths than traffic accidents and homicides combined (Goodkind et al. 2019).

With the onset of the COVID-19 pandemic, researchers began assessing the impact of air pollution exposure on COVID-19 incidence and death. An individual level study focused on Mexico City, by López-Feldman, Heres and Marquez-Padilla (2021) found that exposure to $PM_{2.5}$ increases the probability of dying from COVID-19 and that this effect is most likely driven by long-term exposure while results are robust to the “inclusion of confounders at the municipal

and individual-level" (p.8) including individual characteristics such as age and comorbidities (López-Feldman, Heres and Marquez-Padilla, 2021). Researchers Zhu et al. observing '[d]aily confirmed cases, air pollution concentration and meteorological variables in 120 cities throughout China found "a significant relationship between air pollution and COVID-19 infection including "[p]ositive associations of $PM_{2.5}$, PM_{10}, CO, NO_2 and O_3" (2020, p. 3). A UCLA Fielding School of Public Health spatial analysis of COVID-19 and traffic related air pollution found that chronic exposure to nitrogen dioxide is "associated with COVID-19 incidence and mortality in Los Angeles County neighborhoods" (Lipsitt et al., 2021, p. 5) and that neighborhoods occupied by higher levels of Latinx and Black people experience higher levels of pollution (Lipsitt et al., 2021). Similarly, studies from Italy, England, and the United States found associations between air pollution exposure and COVID-19 incidence and death (Lipsitt et al., 2021).

1.2 *$PM_{2.5}$ and COVID-19 Mortality: A Widely Received Study*

Epidemiological studies rely on observational data in order to formulate critical public health interventions; research on the developing, worldwide COVID-19 pandemic is no exception. Especially in the case of a pandemic in progress, observational studies are published before the event is over, while the data is incomplete, and the mechanisms for spread and vulnerability are still being understood. In a widely received, nationwide study linking air pollution exposure to COVID-19 mortality, Harvard T.H. Chan School of Public Health researchers, Wu et al., produced significant findings linking the impact of long term exposure to $PM_{2.5}$ to COVID-19 mortality across the contiguous United States. This study was published in a November 2020 edition of *ScienceAdvances.* Almost two years after its publication, it has been cited over 600 times, covered by 131 news outlets and downloaded over 15,000 times.

The research in question by Wu et al. found that "higher historical $PM_{2.5}$ exposures are positively associated with higher county-level COVID-19 mortality rates after accounting for many area-level confounders" (2020, p. 1). The study specifically conducted a U.S.-wide

ecological regression analysis, where data is aggregated to an areal administrative unit to infer individual-level health outcomes, on county-level COVID-19 mortality and historical $PM_{2.5}$ concentrations between 2000 - 2016. Their causal story regarding the linkages between long term exposure to $PM_{2.5}$ and COVID-19 is as follows: "[i]t has been hypothesized that because long term exposure to $PM_{2.5}$ adversely affects the respiratory and cardiovascular systems and increases mortality risk, it may also exacerbate the severity of COVID-19 symptoms and worsen the prognosis of this disease" (Wu et al., 2020, p. 1). They found "an increase of 1 $\mu g/m^3$ in the long term average $PM_{2.5}$ is associated with a statistically significant 11% (95% CI, 6 to 17%) increase in the county's COVID-19 mortality rate" (Wu et al., 2020, p. 1). They also found statistical significance when evaluating predictor variables such as population density, median household income, educational attainment, age distribution, and percent Black residents (Wu et al., 2020).

Importantly, Wu et al. highlight the limitations of an ecological regression analysis throughout the study but argue that area level conclusions can still be used to inform public health policy actions (Wu et al., 2020, p.3). Given the tentative nature of the Wu et al. findings and their potential influence on public health policy, this thesis employs two strategies for evaluating the reliability of their treatment effect estimate: sensitivity analysis and spatial analysis within a geographic framework. The purpose is to first assess the fragility of the Wu et al. estimate to unobserved confounding using a sensitivity framework alternative to the approaches used by the authors, and next to utilize spatial analysis to investigate the possibility of spatial regimes (e.g. hotspots) in the treatment and outcome variables. Finally, the influence of geography on the health-hazard relationship is explored by varying model covariates representing the delineation of space into alternate socioeconomic and climatic units (e.g. substituting a state covariate for a U.S. Census region) to assess whether differing treatment effect estimates emerge with differing definitions of place.

1.3 *Sensitivity Analysis: Assessing Fragility in a Treatment Effect Estimate*

The most popular strategy across disciplines for identifying causal relationships using observational data is linear regression with a set of “observed covariates deemed sufficient to control for confounding” (Cinelli, Ferwerda, and Hazelett, 2020, p.1). In order to defend their conclusions, researchers must argue that no unobserved confounders interfere with the causal relationship that is represented by a regression coefficient (Cinelli, Ferwerda, and Hazelett, 2020; Reich et al. 2021), an “impossible assumption to defend in most applied settings” (Cinelli, Ferwerda, and Hazelett, 2020, p.2). In response, Hazlett and Parente (2020) advocate for a sensitivity based approach that quantifies and explicitly states the degree of confounding that would be required to meaningfully alter research conclusions alongside treatment effect estimates and harnesses domain knowledge to determine whether this degree of confounding is plausible.

Broadly, sensitivity analysis can be described as the study of how the inputs of a system, often expressed as one or more mathematical models, affect the outputs (Razavi et al., 2021, p.2) and provides a framework for assessing whether unmeasured confounding is strong enough to alter causal conclusions (Ding and VanderWeele 2016). The application of sensitivity analysis to health-hazard studies can be traced back to its inception in 1959 by Cornfield et al. in the linking of cigarette smoking to lung cancer (Ding and VanderWeele 2016). The suite of tools, methods, and deliverables used in sensitivity vary across disciplines and approaches (Razavi et al., 2021), with epidemiological studies favoring use of the E-value.

In this thesis, a sensitivity analysis framework, as developed by Cinelli and Hazlett (2019), is applied to the Wu et al. data as an alternative to the E-value. It is used to quantify and explicitly state their treatment effect estimate’s sensitivity to unobserved confounding and

consider whether or not this degree of confounding is plausible. Cinelli and Hazlett's (2020) sensitivity analysis framework is used to assess the strength of the Wu et al. causal claim using a readily interpretable statistic without requiring assumptions regarding the "functional form of the treatment effect assignment mechanism nor the distribution of the unobserved confounder" (p. 40). Employing an alternate measure to assess the strength of a causal claim made by a widely received study is especially useful given the study's potential influence on COVID-19 pandemic policy response. Bounding procedures are used in order to consider the plausibility of such an unobserved confounder by comparing its relative strength with known, influential covariates. Once sensitivity statistics were estimated for the Wu et al. treatment effect, background knowledge was then applied in order to propose and explore the plausibility of the air pollutant and unexplored confounder, ozone.

1.4 *Spatial Analysis: The Effect of Place on a Treatment Effect Estimate*

At its core, Geography concerns itself with phenomena defined by space and/or place (Tuan, 1979). Though there are variable definitions of each, space can generally be defined by locational attributes such as latitude and longitude or euclidean measures of area and distance (Yang, Ye, and Sui, 2016) while place refers to a unique spatial entity often characterized by a locational definition of any size and a matrix of sociocultural, political, economic and historical contexts (Cresswell, 2004; Tuan, 1979). Place has been described by Lukermann (1964) as an emergent 'special ensemble' (p. 170) and by Agnew (1987) as consisting of three essential elements that comprise these 'meaningful locations': location, locale and sense of place. The subdiscipline of Health Geography examines human environment interactions and acknowledges that "geography and health are intrinsically linked" (Dummer, 2008, p. 1177) while acknowledging that space and place are not merely "containers for epidemiological processes" (Curtis, 2016, p.6) but rather substantially contribute to the processes governing health variation among individuals and populations (Curtis, 2016; Cutchin, 2007; Morello-Frosch

and Lopez, 2006). In contrast to epidemiology which focuses on the spread of disease in a biomedical context (Dummer, 2008), Health Geography examines health, well-being, and exposure to environmental hazards as shaped by the spatial, climatic, social, political and cultural contexts of the places that we live, work, and recreate in (Dummer, 2008; Sittner 2021).

Spatial analysis in epidemiology and public health have a long history most commonly traced back to 1854 with the story of Dr. John Snow and the dot-map he used to identify a London water pump as the source of a Cholera outbreak (Tulchinsky, 2018). Although georeferenced data is now ubiquitously deployed in modern public health research, the substantive influence of geography is often not considered in the model specifications nor the sampling strategy (Goldhagen et al., 2005; Matisziw, Grubesic, and Wei 2008) or is masked by the mechanism of data aggregation to an administrative, geographic unit which, in turn, spatially misrepresents the data (Delmelle et al., 2022). Jones and Moon (1993) critique aggregate analysis in medical geography, the sub-disciplinary antecedent to health geography, as "incapable of distinguishing the contextual- the difference a place makes- from the compositional- what is in a place" (p. 519). They argue that aggregate studies may also overlook important within-area variability and call for the mutual consideration of macro and micro scales as one component to a more comprehensive medical geography (Jones and Moon, 1993).

Though there is a strong geographical component to the Wu at. al study with national maps of historical $PM_{2.5}$ concentrations and COVID-19 mortality rates at the forefront and demographic, socioeconomic, climatic and political factors accounted for in their primary and secondary analysis, a deeper consideration of the spatial distribution of the treatment and outcome variables as well as the geographic context for their production is missing. The Wu et al. study relies heavily on the aggregation of data to a spatial unit, the U.S. County, in order to

make inferences at the National level. With the U.S. county as the unit of analysis and the contiguous U.S. as the macro-level political entity, important sub-County variation is lost and the potential for detecting differences in regional-level long term exposure to $PM_{2.5}$ is overlooked. According to their data, there is clear evidence of spatial clustering of $PM_{2.5}$ and COVID-19 mortality at the regional level, which is left uninvestigated.

While a sensitivity analysis framework can be used to consider the strength of confounding required to alter a research conclusion, spatial analysis can complement the investigation of unobserved confounders by potentially revealing spatial structure in the treatment-outcome relationship. For example, “the treatment at one location may influence the outcomes at nearby locations, a phenomenon known as spillover or interference” (Reich et al. 2021, p. 605). When spatial effects are not explicitly included in model specifications, standard statistical measures of fit may become biased or unreliable (Kolak and Anselin 2019). Exploratory Spatial Data Analysis (ESDA) can be used to identify disease and environmental hazard patterns in a geographic context. ESDA is utilized in studies where the data is geolocated in order to visually probe the geographic distribution of the health-hazard relationship and identify spatial patterns, such as the clustering of like values, and can motivate the inclusion of a spatially lagged variable in a modeling approach. In this thesis, significant clustering among counties with high levels of $PM_{2.5}$ and moderate clustering among counties with COVID-19 mortality was discovered. A variety of spatial lag models were then estimated to account for these spatial regimes and compare the effects of the inclusion of these spatial processes in the treatment effect estimate.

An understanding of the geographic context producing the health-hazard relationship can be used to help explain the spatial patterns identified (Cutchin, 2007). For instance, geographically characterizing the accessibility of health services as well as variability in the

location and regulation of pollutant emitting facilities is one way in which geography can inform the “interrelations inherent in many health related exposures” (Dummer, 2008). This can bolster treatment effect estimates against confounding through the analysis and integration of the effects of space and place into model specifications (e.g., spatial econometrics), sampling strategies (e.g. identifying high-risk populations and environmental riskscapes), or research hypotheses (e.g. using spatially located development histories to form place specific inquiries). Spatial pattern identification in the health-hazard relationship can also inform future model iterations or study design by, for example, constraining model coverage to a geographic extent that captures important regional or local variability influenced by specific place-based histories of residential segregation or other political and economic forces governing the distribution of health hazards.

Air pollution exposure is both a local and transboundary health hazard (Goodkind, 2019) with economic, climatic and political drivers. The health risks associated with $PM_{2.5}$ “vary widely depending on where emissions are released” (Goodkind et al. 2019, p. 8775). The largest share of the health burden occurs in or near densely populated areas in close proximity to emission sources with “large spatial gradients in damages, including within county and within urban” (Goodkind et al. 2019, p. 8780) yet a stunning twenty-five percent of the health burden from emissions can “occur more than 256 km away” (Goodkind et al. 2019, p. 8775). According to Sergi et al. (2020) “[a]round 30% of all US counties receive 90% of their health damages from emissions in other counties, and these damage-importing counties also tend to have lower median incomes” (p.1). An exception to this observation is Fairfield County, Connecticut which records the highest ozone pollution in the eastern half of the U.S., in part due ozone and ozone precursors transported from the Midwest (American Lung Association, 2021). Differential access to clean air may also be exacerbated along the U.S. border. In an analysis of transboundary air pollution in the U.S., Konisky and Woods found that “states perform fewer enforcement actions

in counties adjacent to international borders" (2009). Acknowledging that "air pollution is a transboundary problem" Nordenstam et. al, suggest that boundary dependent air pollution policy regimes do not accurately address the resulting environmental issues that do not constrain their manifestation to "human designated jurisdictions" (1998, p. 231).

Researchers Clay, Muller, and Wang found that after a steady decline in $PM_{2.5}$ across the U.S. between 2008 and 2016, a sharp increase occurred over the next two years (2021). Further examination of $PM_{2.5}$ across U.S. Census regions uncovered a different story. Though the overall National trend was positive, two of the four U.S. Census Regions had actually stopped declining while vast increases in $PM_{2.5}$ pollution across the West and Midwest regions were the source of the positive Nationwide trend (Clay, Muller, and Wang, 2021). The increase in these two regions were likely stimulated by place-based economic activity, wildfires and Clean Air Act enforcement actions (Clay, Muller, and Wang, 2021). The American Lung Association's multi-year *State of the Air* publication reports that the geographic distribution of ozone has also moved west since 2016 where increased temperatures, climate change, and an increase in oil and gas extraction in the Southwest have all led to more Western cities experiencing ozone exceedances (2021). In the Eastern U.S., ozone exceedances are attributed to ozone and ozone precursors transported upwind from the Midwest (American Lung Association, 2021).

Much like the spatial distribution of air pollution is linked to climatic, political, economic, and sociocultural factors, COVID-19 incidence and death has also been linked to such factors by numerous studies. Grekousis et al. (2022) identified regional differences in eight local risk factors in the COVID-19 death rate, half of which were socioeconomic. The leading local risk factor identified was lack of health insurance, mostly concentrated within the Midwest and South regions while counties throughout California, Oregon, Washington and parts of the South region were distinguished by lack of physical activity as the primary local risk factor. Romano et al.

(2021) found that the “racial/ethnic distribution of hospitalized COVID-19 patients differed among U.S. Census regions” (p.561) with Hispanic patients representing the highest cumulative proportion across all regions. Likely contributors to these geographic and temporal disparities include differential access to healthcare, occupational safety, safe transit and housing stability (Romano et al., 2021). Other studies have shown that one’s occupational status designation as essential worker is associated with a disproportionate risk of COVID-19 incidence and mortality and that these workers are more likely to identify as racial and ethnic minorities or immigrants (Fielding-Miller, Sundaram, and Brouwer, 2020). Garcia et al. (2022) found differential treatment effects in a statewide Calfornian study when evaluating long term exposure to $PM_{2.5}$ and COVID-19 mortality across different seasons with the highest positive associations occurring during the spring and summer months.

One of the factors that have shaped the course of the COVID-19 pandemic has been the timing, uptake, and politicization of public health interventions such as statewide stay-at-home orders, social distancing guidelines and public masking policies (Neelon et al., 2021). The political affiliation of a state’s governor was found by Adolph et al. to be the primary determinant of the timing of statewide mask mandates with Republican governors, on average, delaying the low-cost public health intervention for an estimated 98 days (2021). States with Democratic governors were found to have lower test positivity rates in the second half of 2020 suggesting that state leaders with these party affiliations imposed stricter containment strategies (Neelon et al., 2021) and that gubernatorial political affiliation is associated with the likelihood of exposure.

The landmass defining the contiguous U.S. is more than a backdrop: “geographers know well….that culture is written on the landscape and that the landscape reflexively affects people” (Cutchin, 2007, p. 4). Its area is conceptually divided into sub-national administrative units such as states, counties, census tracts and neighborhoods that provide a bounded definition of place

for representative government, the implementation of laws, economic development, creation of livelihoods, and sociocultural identities. The widespread use of large, aggregate administrative units such as counties and states to examine health-hazard relationships in epidemiology speaks to both the availability of data and the convenience of their use for modeling. When health-hazard studies exclude important local variability, they may miss the complex relationship between air pollution and the excessive burden borne by communities of color, for instance, in the contribution of "diverse legacies of discrimination [that] shape current spatial distributions of pollution sources" (Morello-Frosch and Lopez, 2006). While states and counties represent sub-national administrative units with shared governance, another set of commonly used conceptual boundaries used in statistical analyses to capture larger scale health-hazard relationships are U.S. Census regions and divisions.

U.S. Census regions and divisions are sub-national geographic entities that provide a framework for defining our large and diverse Nation with units that share common attributes such as "historical development, population characteristics, and economy" (U.S. Dept. of Commerce, 1994, p. 6-1). In addition to U.S. Census regions, Environmental Protection Agency (EPA) Climatically Consistent Regions provide another framework for considering the definition of place. They are sub-national geographic entities organized on the basis of temperature and precipitation and are considered by the EPA (2016a) to be a relevant way to assess regional trends in air quality. They are commensurate with National Oceanic and Atmospheric Administration (NOAA) climatically consistent regions which align with "areas containing similar emissions source types" (Simon et al., 2015) which suggest that these regions may also share similar histories of development.

The consideration of the geographic context for the production of $PM_{2.5}$, as well as COVID-19 mortality can be used to better understand the health-hazard relationship and the

defining role of place in shaping exposures and outcomes. In this thesis, the Wu et al. data is used to iterate through model specifications utilizing varying sub-national boundaries in order to evaluate the effects of these varying definitions of place on the treatment effect estimates. State fixed effects are substituted with U.S. Census regions in order to evaluate the effect of regional histories of development, economic and demographic factors on the distribution on $PM_{2.5}$ and COVID-19 mortality. The influence of climatic parameters governing the $PM_{2.5}$ and COVID-19 mortality health-hazard relationship is considered by substituting state fixed effects with EPA Climatically Consistent Regions. By redefining the contiguous U.S. landscape into alternate, socioeconomically and climatically defined sub-national, space-place entities, the difference in the framing of the health-hazard relationship is expected to yield differing treatment effect estimates.

The goal of this thesis is to illustrate that place makes a difference when estimating the effects of $PM_{2.5}$ on COVID-19 mortality and should be considered when estimating air pollution health-hazard risks. As expected, when the sub-national definitions of place applied to the Wu et al. study data were changed, so did the treatment effect estimates. When researchers adjust the apertures of their study to include spatial extents and definitions of place that capture important variability in health-hazard relationships, this can produce more locally accurate and relevant treatment effect estimates. With a deeper understanding of the context producing the health-hazard relationship, more effective, place-specific policy interventions can then be deployed.

2. Research Questions

My research questions for examination in this thesis are as follows:

a. *Is there a geography to $PM_{2.5}$? If so, can geography meaningfully be accounted for when estimating National models of air pollution exposure risks?*

   H_1: Long term exposure to $PM_{2.5}$ and associated health risks are spatially heterogeneous across the contiguous U.S. and are the result of diverse histories of development, political, socioeconomic, and climatic forces defining place and operating at various scales. Treatment effect estimates made at the National level may be sensitive to confounding due to misalignment of process and scale.

   H_0 : Long term exposure to $PM_{2.5}$ estimates and associated health risks are homogeneous across the contiguous U.S. Treatment effect estimates at the National level are not subject to spatial regimes and are not affected by alternate definitions of sub-national place.

b. *Can an understanding of the geographic context producing the health-hazard relationship help to inform public health research questions and modeling strategies?*

Why are these questions important? Because clean air is no longer an “open-access good” (Véron, 2006). An understanding of the geographies of air pollutants, including the ubiquitous, locally variable and far-reaching $PM_{2.5}$, can contribute to an uncovering of the politics, power relations, management strategies and socioenvironments that coproduce differential access to clean air and the resulting uneven health burdens due to both direct exposure and related illnesses experienced by Black, LatinX, immigrant, and communities of color.

3. Literature Review

3.1 Health and Place

Health Geography is a subdiscipline of Human Geography focusing on the spatial, temporal, and place-based processes that shape interactions between human health and the environment (Dummer, 2008; Sittner, 2021). It is the sub-disciplinary descendant of Medical Geography and differs from Epidemiology in that it also considers the influence of the social,

cultural, and political contexts that define place, unique entities with history and meaning (Lukermann, 1964), on human health (Glass, 2000; Cutchin, 2007; Curtis, 2016). Health Geography offers a more holistic view of human health hazards, well-being, and disease by exploring how both space and place contribute to health variation among individuals and populations (Glass, 2000; Dummer, 2008; Curtis, 2016; Sittner, 2021). The incorporation of geographic context to interactions between human health and the environment is essential to the creation of effective public health policy and the identification of environmental riskscapes rooted in inequality (Jones and Moon, 1993; Dyck, 1995; Morello-Frosch and Lopez, 2006; Cutchin, 2007; Curtis, 2016).

Though there are a multitude of studies exploring the relationship between COVID-19 and air pollution exposure, most rely on large, aggregate data units to make inferences. Studies exploring health hazard risks using large, spatial units of analysis may be subject to ecological fallacy that makes incorrect assumptions about individuals based on aggregate data about their communities, resulting in misaligned health policy (Dummer, 2008). Few studies utilize the geography of $PM_{2.5}$ to functionally inform their research design or sampling strategy nor do they explore the potentially confounding effects of scale or explicitly express the fragility of their findings in the face of unobserved confounders. The goal of this thesis is to address the dearth of studies exploring the effects of space and place on the relationship between COVID-19 and air pollution exposure by first quantifying the fragility of a widely received treatment effect estimate identified by Wu et al. (2020), then using spatial analysis and alternate definitions of subnational place to explore the influence of space and place on the treatment effect of the long term exposure to $PM_{2.5}$ on COVID-19 mortality. Through the lens of Health Geography, a better understanding of the spatial and place-based contexts governing $PM_{2.5}$ pollution production and exposure can be used to guide more effective health policy interventions.

3.2 The Geography of $PM_{2.5}$

$PM_{2.5}$ is the chimera of pollutants. Unlike most other prominent air pollutants, it is variable in its composition (Hinojosa-Baliño, Vásquez, and Vallejo 2019) with common constituents including elemental carbon, organic carbon, ammonium, sulfate, and nitrate (Amini et al., 2022). The presence of $PM_{2.5}$ is spatially, temporally and climatically dependent (Cheng et al., 2015; Zalakeviciute, López-Villada and Rybarczyk, 2018; Amini et al., 2022) thus complicating its role in the connections between health and place and the environmental riskscapes it shapes. It can penetrate lung tissues and enter the bloodstream imparting numerous and well documented adverse human health impacts (Bell 2012; Makar et al. 2107; Chen et al. 2018; Zhang, Rui, and Fang, 2018; Hinojosa-Baliño, Vásquez, and Vallejo 2019; US EPA, 2016) including, but not limited to, cardiopulmonary disease (Garcia et al., 2016), lung cancer (Thind et al., 2019) and premature mortality (Goodkind et al., 2019). It is considered the "largest environmental risk factor in the United States" (Goodkind et al. 2019, p. 8780) and can originate from a variety of sources such as fuel combustion, wildfires, cooking, heating, fugitive dust (US EPA 2018, NY State Dept. of Health 2018), electricity generation and agricultural activities (Goodkind et al., 2019). Individual particles themselves are not visible, though a critical mass of particulate matter contributes to a reduction in visibility (Kumar, Chu and Foster, 2007). Over fifty-four million Americans live in areas subject to unhealthy spikes in particle pollution, a number that has substantially risen since 2017, while over twenty million experience year-round particle pollution that exceeds national air quality limits (American Lung Association, 2021).

The spatial distribution of the air pollutant $PM_{2.5}$ and its toll on human health varies geographically due to differential vectors of production, population density, its regulation, and the climatic and geophysical conditions affecting its spread (Colmer, 2020). It is a complicated pollutant given its variability in its constituents, its ability to be emitted directly or formed in the

atmosphere from precursors (US EPA, 2018; Amini et al., 2022), and its tendency to be deposited both locally and hundreds of miles away (US EPA, 2018; Goodkind et al., 2019). Tobler's First Law of Geography states that "everything is related to everything else, but near things are more related than distant things" (1970, p. 236); it can be reasonably applied to $PM_{2.5}$ but doesn't fully relate the more complicated picture of its spread. $PM_{2.5}$ is capable of traveling hundreds of miles (US EPA, 2018) yet also, in the case of traffic emissions, exists in concentrations harmful to human health as a function of distance to highway (Pierce et. al, 2019). Goodkind et al. (2019), found that over one third of marginal damages from premature mortality related to $PM_{2.5}$ exposure occurred within "8km of emission sources" (p. 8775) with marginal damages varying by "over an order of magnitude within a single county" (p. 8775) and another twenty-five percent of marginal damages occurring over 256 km away, indicating the need to consider both fine-scale and multi-scalar impacts.

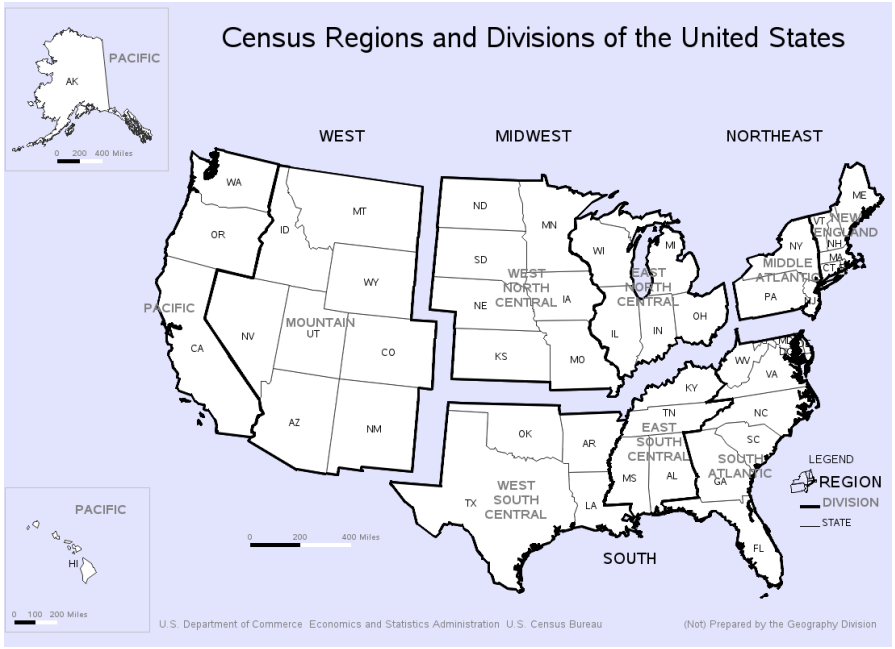

Figure i : U.S. Census Regions. From Census.gov; Public Domain.

The geography of $PM_{2.5}$ differs among U.S. Census regions and divisions. U.S. Census

regions and divisions are commonly used constructs of the U.S. Census Bureau in order to "provide a larger geographic framework for comparative statistical analysis" (U.S. Dept. of Commerce 1994 p. 6-1) of the same groups of states over time and are organized on the basis of "historical development, population characteristics, and economy" (1994 p. 6-1). Between 1981 and 2016, substantial and absolute reductions in $PM_{2.5}$ concentrations have occurred in the U.S. though these reductions are not isotropic across the country (Colmer et al., 2020). The absolute reductions and increases in $PM_{2.5}$ concentrations across the Nation are in large part spatially contiguous (Colmer et al., 2020). Over this time period, portions of the East Coast and the East North Central, East South Central and South Atlantic U.S. Census divisions have all experienced a relative reduction in $PM_{2.5}$ concentrations while California, Arizona, and portions of the West South Central, East South Central and the southernmost portion of the South Atlantic U.S. Census divisions became relatively more polluted (Colmer et al., 2020). Strikingly, the disparities in absolute $PM_{2.5}$ concentrations have largely been maintained with many of the most burdened census tracts in 1981 remaining the most burdened in 2016 (Colmer et al., 2020). Improved air quality was associated with whiter, higher income, more populated and less Hispanic census tracts (Colmer et al., 2020). In all regions but the West, Clay, Muller, and Wang (2021) observed a reduction in the $PM_{2.5}$ precursor, sulfate, between 2009 - 2018, likely linked to a decline in coal-fired power generation. Meanwhile the West region has also experienced recent, elevated exposures to $PM_{2.5}$ related to wildfires and extreme heat, linking particle pollution exposure risks to a changing climate (American Lung Association, 2021; Clay, Muller, and Wang, 2021).

In addition to between region variability, within region variability in $PM_{2.5}$ concentrations have been found. Lee et al. (2012) utilized a combination of remotely sensed and ground based monitoring station data to derive $PM_{2.5}$ mass concentrations across a nine year period in the New England region. They identified "heterogeneous $PM_{2.5}$ spatial patterns in the study region"

(Lee et al., 2012, p.1) despite previous studies indicating low spatial variability across the same study area (Lee et al., 2012). The distribution of these concentrations “clearly exhibited densely populated and high traffic areas” (Lee et al., 2012, p. 1) and may speak to the increase in the ability to observe fine-scale variability as measurement and estimation methods improve their resolution. In another within region study, Garcia et al. (2016) found larger treatment effects in rural areas than urban areas when analyzing the impacts of long term exposure to $PM_{2.5}$ on cardiovascular disease, cardiopulmonary disease and all-cause mortality within California. Bravo et al. (2016) found that $PM_{2.5}$ concentrations were consistently higher in urban census tracts than rural census tracts and that tracts with high degrees of racial isolation also experienced higher average $PM_{2.5}$ concentrations regardless of their urbanicity. This trend held in all regions with the exception of rural census tracts in the West (Bravo et al., 2016). When characterizing geographies of health, Jones and Moon (1993) argue that the inclusion of multiple scales of analysis and the place-based sets of relations shaping human health hazards can move geographic inquiry into human health patterns beyond location as a “mere container of measurable events” (p. 515). Strategies such as this can help to uncover the difference a place makes by, for instance, revealing important within-area sociospatial inequalities, such as community-level stressors that augment vulnerability to an environmental health hazard (Morello-Frosch and Lopez, 2006), or health hazard patterns tied to regional histories of development. By uncovering the nature of these spatial and place-based relations, more locally precise and equitable public health interventions can be developed.

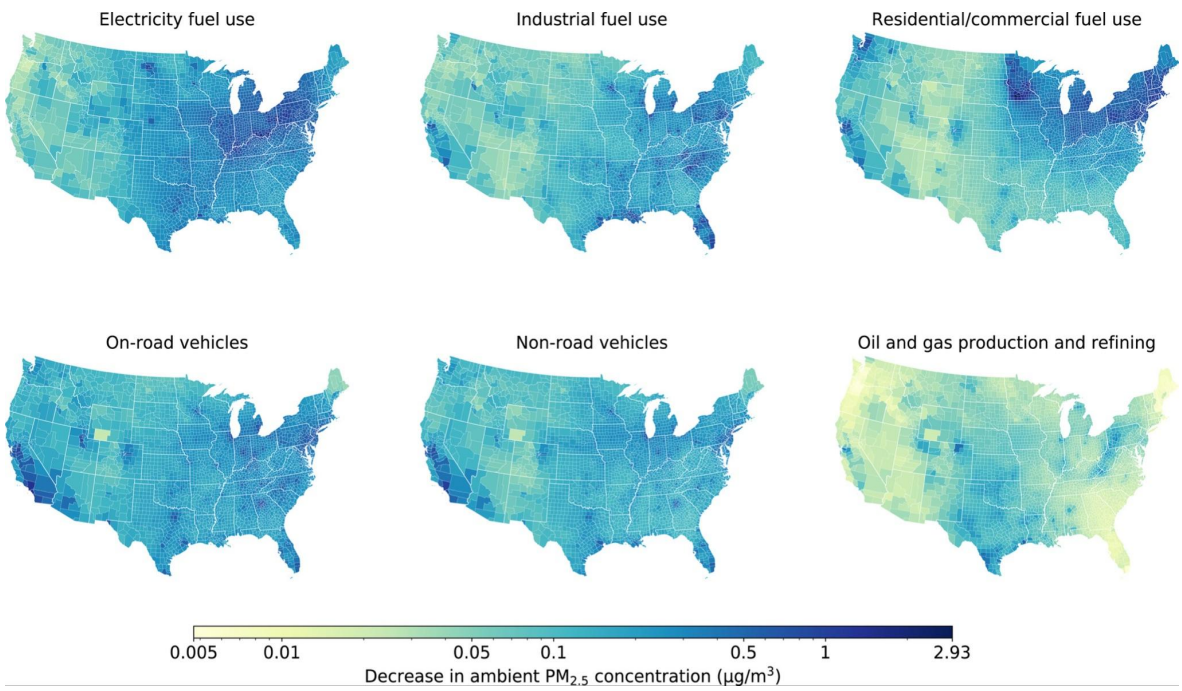

Figure ii : County-level decrease in ambient $PM_{2.5}$ concentrations from the independent removal of $PM_{2.5}$, SO_2, and NO_x emissions in each of the six energy-related sectors (Mailloux et al., 2022)

The heterogenous geography of $PM_{2.5}$ is, in part, due to differential governance. 1963 marks the initiation of the Federal Clean Air Act (CAA) which, along with its many amendments, standards, and programs regulates the levels of air pollution that can be present in U.S. air (US EPA, 2021d). Since 1970, the enforcement of the CAA has been enacted through the Environmental Protection Agency (Currie and Walker, 2019). The National Ambient Air Quality Standards (NAAQS) of the CAA sets thresholds for the ground level concentrations of six common pollutants associated with adverse human health effects commonly referred to as criteria pollutants including $PM_{2.5}$ (US EPA, 2021c). Additionally, a constellation of other regulatory mechanisms aimed at industrial and transportation related pollution including interstate air pollution transport (US EPA, 2022) and the Regional Haze Program (US EPA, 2021b) operate in tandem.

Particulate matter, including $PM_{2.5}$, are regulated with primary and secondary National Ambient Air Quality Standards which correspond to thresholds for health and welfare respectively (US EPA, 2021a). The primary annual average $PM_{2.5}$ of 12.0 $\mu g/m^3$, secondary annual (15.0 $\mu g/m^3$) and 24-hour $PM_{2.5}$ (35 µg/m3) standards of 15.0 $\mu g/m^3$ were established (primary annual) or maintained (secondary annual, 24-hour) in 2013 (US EPA, 2013). The most recent review of the primary and secondary National Ambient Air Quality Standards for particulate matter occurred in December of 2020, during the final months of the Trump administration's aggressive rollback of federal environmental protections (Baker, 2020) and resulted in the maintenance of primary and secondary standards (US EPA, 2021a). After President Biden took office, reconsideration of this ruling was announced in June of 2021 resulting in an October 2021 *Draft Policy Assessment of the Particulate Matter National Ambient Air Quality Standards* (Tsirigotis, 2021) opening the door to a reevaluation of the health and welfare thresholds. When analyzing the health benefits of removing energy-related emissions across the contiguous U.S, Mailloux et al. (2022) found that nationwide clean energy policies targeting energy-related sectors could prevent over 50,000 premature deaths each year. Projected regional reductions in ambient $PM_{2.5}$ differed depending on the energy-related sector analyzed (e.g. on-road vehicles vs electricity fuel use) (Mailloux et al., 2022; see Figure ii) thus highlighting how place-based regional histories of development can inform regional air pollution policy.

Though the NAAQS for particulate matter operates as a baseline for their regulation in the U.S., state governments can elect to impose stricter standards, including the 2022 restoration of California's rights to set its own standards for tailpipe emissions temporarily revoked under the Trump administration (Davenport, 2022). There is some evidence that differential enforcement of clean air standards across the Nation unsurprisingly follows the political affiliations of state elected officials. Utilizing a regression discontinuity design,

researchers Beland and Boucher found that air pollution levels were lower in states with Democratic governors (2015). Similarly, researchers Farzin and Bond substantiated intrastate variability in California air quality as associated with political leadership, however, a significant effect was only identifiable in the pollutants NO_2 and O^3 (2013).

Differential histories of development and current economic activity also contribute to the heterogenous geography of $PM_{2.5}$ (Colmer et al., 2020). In the West region, a 2016-2018 increase in elemental carbon, a precursor to $PM_{2.5}$ is likely attributed to an increase in diesel miles traveled (Clay, Muller, and Wang, 2021), an indicator of economic activity and sprawl. Cities throughout the Nation with high power plant emissions such as New York, Houston, and Detroit consistently log the worst year-round particle pollution (American Lung Association, 2021) while an increase in oil and gas extraction in the Southwest is associated with an increase in ozone (American Lung Association, 2021), a heat-driven $PM_{2.5}$ co-pollutant (Schnell and Prather, 2017; Zhu et al., 2019). Inter-state air pollution also constitutes regional variability in human health. $PM_{2.5}$ pollution and precursor emissions from out of state electricity generation makes a substantial contribution to health risks including premature mortality with some states considered net importers of harm from this sector while others are considered net exporters of harm (Thind et al., 2019). Again, highlighting the need for an understanding of regional air pollution patterns in order to direct regionally specific policy targeting transboundary interstate pollution.

Access to clean air in the U.S. is unevenly distributed and, in the context of $PM_{2.5}$, is disproportionately allocated to disadvantaged communities (Morello-Frosch and Lopez, 2006; Miranda et. al 2011; Bravo et al. 2016; Nardone et al., 2018) in particular non-Hispanic black communities (Miranda et. al 2011; Thind et al., 2019). Geographer René Véron argues that “air quality with its complex sociospatial patterns plays a significant part in the coproduction of urban

socioenvironments" (2006, p. 2093); that the uneven distribution of "good air" is not merely "a matter of proper management but equally one of power and politics" (2006, p. 2093). He furthers that the "indirect and partial commoditization of air quality" (2006, p. 2096) through [urban] property values has rendered clear-air no longer an "open-access good" (2006, p. 2096). Geographer Peter Adey contends that the "constellation of megacity inequality" can be found in the "testimony of pollutants and choking effluvium" as evidenced by the analysis of air (2013, p. 291). With regard to air pollution in the US, low-income, Black, Indigenous, LatinX, Asian American, and immigrant communities bear a disproportionate burden of exposure and related adverse health effects (Miranda et al., 2011; Nardone et al., 2018). Recent findings from researchers Namin et. al (2020) have connected 1930s discriminatory neighborhood grading by the Home Owners' Loan Corporation across major U.S. cities with a statistically significant increase in the likelihood of contemporary exposure to airborne carcinogens and respiratory hazards. Structural racism refers to "the totality of ways in which societies foster racial discrimination through mutually reinforcing systems of housing, education, employment, earnings, benefits, credit, media, health care, and criminal justice" (Bailey et al., 2017, p. 1453) and is evidenced in the distribution of health inequalities in the U.S., including strong associations with racial/ethnic inequalities in COVID-19 mortality (Lundberg et al., 2022). Through unveiling the space and place based patterns of health hazard risks, the underlying structural inequities that produce and reinforce health inequality can be exposed and addressed.

3.3 The Geography of COVID-19 Mortality

COVID-19 incidence and mortality across the U.S. has varied geographically and demographically over time during the course of the pandemic (Oster et al., 2020; Murthy et al., 2021; Lundberg et al., 2022; Nguyen et al. 2022). It is impossible to relate variation in COVID-19

incidence and death across the United States without referring to racial and ethnic disparities as racial and ethnic minorities bear a disproportionate burden of COVID-19 incidence and severe outcomes including death (Chih and Ojede 2020; Rossen et al., 2020; Romano et al., 2021). For example, Nguyen et al. (2022) found that early in the pandemic (April through August 2020), the Middle Atlantic Census division reported the highest in-hospital mortality with overrepresentation in hospitalization and severe outcomes in Black non-Hispanic patients. When assessing excess deaths associated with COVID-19 by race and ethnicity, Rossen et al. (2020) found the largest association among Hispanic persons with significant increases in excess deaths among Black, Asian, and non-Hispanic American Indian or Alaska Natives. When analyzing the demographics of approximately three hundred thousand unique patients diagnosed with COVID-19 between March and December of 2020, Romano et al. (2021) found that in the early stages of the pandemic, "the racial/ethnic distribution of hospitalized COVID-19 patients differed among U.S. Census regions" (p. 561) with Hispanic patients representing "the highest cumulative proportion of hospitalized patients with COVID-19" (p. 561) across all U.S. Census regions.

In a study focused on retrospective and prospective analysis of COVID-19 hotspot counties between early March and mid-July 2020, Oster et al. (2020) found that the percentage of counties meeting hotspot criteria differed over time and among U.S. Census regions. From March - April, 2020 COVID-19 hotspot counties were found primarily in the Northeast while the percentage of counties within the South and West regions meeting hotspot criteria significantly increased from June - July (Oster et al., 2020). Pre-existing social determinants of health (Romano et al, 2021) such as health care access, household crowding, and occupational segregation (Lundberg et al., 2022) as well as an area's urbanicity were early drivers of COVID-19 transmission (Oster et al., 2020). Similarly, outbreaks in congregant settings such as long-term care facilities and food processing facilities were also early drivers of COVID-19 transmission (Oster et al., 2020).

As the pandemic progressed, community transmission (Oster et al., 2020) and demographic and geographic variation in vaccine uptake (Lundberg et al., 2022) increased as contributing factors to its spread. As the pandemic continued so did the shift in the geographic spread of COVID-19. By September 2020 COVID-19 incidence in rural counties surpassed that of urban counties (Murthy et al., 2021). Geographic risk patterns continued to change through 2021 as the pandemic continued to move into increasingly rural areas and white COVID-19 death rates increased (Lundberg et al., 2022).

The difference a place makes in determining health outcomes is traceable across the COVID-19 pandemic. In the absence of federal guidelines to limit the spread of COVID-19, U.S. states and territories individually implemented mandatory stay-at-home orders of varying duration and enforcement (Neelon et al., 2021; Nguyen et al. 2022) contributing to geographic variation in incidence and death (Nguyen et al., 2022). Republican state governors were found to delay pandemic mitigation mandates longer than Democratic governors linking state gubernatorial affiliation with COVID-19 health outcomes (Adolph et. al, 2021; Neelon et al., 2021).

Fielding-Miller, Sundaram, and Brouwer (2020) found that larger populations, higher density, percentage of residents living in poverty, percentage of population over 65 and higher percentage of farmworkers were all predictive of COVID-19 mortality in counties across the Nation, however, in a sub-analyses by U.S. Census region “distinct spatial patterns emerged” (p. 7) and the percentage of farmworks was no longer predictive of COVID-19 mortality in the West South Central, Mountain and Pacific States. Chih and Ojede (2020) identified a positive relationship between the percentage of Black and Hispanic persons in a county and the rate of COVID-19 infection. They employed a spatial model to estimate this relationship given that the

spread of COVID-19 is not expected to exhibit spatial independence considering “the free movement of people across US counties and states” (Chih and Ojede, 2020, p.6). Their results showed that not all regions exhibited the same spatial dependency with counties in the Mid-Atlantic and South Atlantic regions having the highest spatial diffusion of COVID-19 incidence and death (Chih and Ojede, 2020).

Spatial diffusion is described by Morrill, Gaile, and Thrall (1988) as “the process by which behavior or characteristics of the landscape change as a result of what happens elsewhere earlier” (p.7). Regionally higher concentrations of vulnerable racial/ethnic minorities were also associated with higher risks of COVID-19 incidence and death such as African Americans in the Deep South and Native Americans in the Mountain regions (Chih and Ojede, 2020). Chih and Ojede (2020) also cite a sub-regional and sub-county disproportionate impact of COVID-19 on Black communities in older industrial cities such as New York, Philadelphia, Milwaukee, Chicago and Detroit.

New York City (NYC) was considered a COVID-19 epicenter in the spring of 2020 during the early outbreak of the virus with the highest rates of incidence in death occurring amongst populations over seventy-five years of age, those with pre-existing conditions, high poverty areas and communities of color (Thompson et al, 2020). Another NYC based study found that “average temperature, minimum temperature, and air quality are significantly correlated with COVID-19 pandemic” (Bashir et al., 2020, p.3) which could motivate the use climatically consistent regions when investigating the relationship between exposure to air pollution and COVID-19 mortality. A NYC zip code level analysis by Cordes and Castro (2020) found spatial clusters of high positivity rates and that a high proportion of positive tests was associated with public transportation use. They also found lower testing rates but higher positivity rates in the lower-income neighborhood of Eastern Brooklyn and Flushing, Queens and point to structural

inequalities in the city such as medical racism, residential and occupational segregation, and racialized social networks as contributing factors to uneven rates of COVID-19 testing and spread (Cordes and Castro, 2020).

Los Angeles was also considered one of the global epicenters of the virus (Lipsitt et al., 2021). Even amongst widespread infection rates, certain LA County communities have bore the burden of unevenly distributed risk of COVID-19 infection and mortality. For example, according to the NY Times, by late winter 2021, L.A. County data showed that the primarily LatinX neighborhood of Pacoima had one of the highest case rates in the nation; notably Pacoima's case rate was five times that of Santa Monica's (Cowan and Bloch, 2021). In another NY Times article describing the one of the "peak periods of the virus," South L.A.'s MLK Community Hospital was credited with "treat[ing] more Covid patients than some Los Angeles hospitals three to four times its size" (Fink and Kosofsky, 2021). Their chief executive, Elaine Batchlor, described "the inequities in disease and death from Covid as reflecting those long present in the community" (Fink and Kosofsky, 2021). She furthered that "chronic shortages of primary care doctors and other health services" helped to shape the medical desert that coincides with these patient's communities (Fink and Kosofsky, 2021). A 2021 UCLA Geffen School of Medicine study by Vijayan et al. examining COVID-19 positivity rates within L.A. County, found similarly uneven burdens in the distribution of COVID-19 incidence and death: "there are significant local variations in test positivity" (p. 2970) and "several socio-structural determinants" (p. 2970) including race/ethnicity, poverty and household density as underlying ongoing disparities. The study concludes that "public health interventions, beyond shelter in place, are needed to address and target such disparities" (Vijayan et al., 2021, p. 2970).

In response to the uncovering of racial and ethnic COVID-19 disease disparities, Chowkwanyun and Reed (2020) stress the importance of contextualizing findings that discover

disparities in disease distribution along racial or socioeconomic lines in order to prevent narratives that may ensue such as territorial stigmatization or biologic explanations for racial health disparities. They further that “one can highlight place-based risks and resource deficits that might explain [the] spatial distribution, along racial lines, of Covid-19” (Chowkwanyun and Reed, 2020, p. 203) including the “uneven geographic distribution of preventive care services or the concentration of respiratory hazards and toxic sites in [such] neighborhoods” (Chowkwanyun and Reed, 2020, p. 203). Strategies such as this can also help to avoid paternalistic policy response to the identification of comorbidities such as obesity, which puts the onus of responsibility for adverse health outcomes on the individual rather than the broader context of inequities which has allowed COVID-19 to flourish in vulnerable communities.

3.4 Long Term Exposure to $PM_{2.5}$ and COVID-19 Mortality

Studies specifically linking the effects of air pollution exposure on COVID-19 mortality are still emerging all over the world. Several have established a positive association with exposure to long term concentrations of $PM_{2.5}$ and COVID-19 incidence and death while others report a wide range of results including inverse relationships and non-significant findings (Berg, Present and Richardson, 2021). One of the most widely received studies thus far is the aforementioned 2020 Wu et al. study under examination in this thesis. Wu et al. specifically conducted an Nationwide ecological analysis and found “an increase of 1 $\mu g/m^3$ in the long term average $PM_{2.5}$ is associated with a statistically significant 11% (95% CI, 6 to 17%) increase in the county’s COVID-19 mortality rate” (Wu et al., 2020, p. 1). Alternatively, a nationwide, county level analysis by Liang et al. (2020) using both single and multi-pollutant models found a positive association between COVID-19 mortality and long term exposure to the traffic related pollutant NO_2, but only a marginal association with $PM_{2.5}$ and ozone.

Studies employing various geographic and temporal scales report differential treatment

effect estimates of long term exposure to $PM_{2.5}$ on COVID-19 incidence and mortality. In 2022, researchers Garcia et al. published a California study on the relationship between long term exposure to air pollution and COVID-19 mortality based on the observation that most of the studies of these associations to date “were ecological studies at the county or regional level which disregard important local variability” (p. 2). They “evaluated whether long-term ambient air pollution was related to weekly COVID-19 mortality at the census tract-level during the first 12 months of the pandemic” (Garcia et al., 2022, p. 1) and found a positive association between long term exposure to $PM_{2.5}$ and COVID-19 mortality in California during the spring and summer seasons with a more attenuated effect in the winter months (Garcia et al., 2022). Konstantinoudis et al. (2021) conducted an even higher resolution investigation of the relationship between air pollution and COVID-19 mortality, also as a counter to ecological studies which “neglect the strong localized air pollution patterns" (p.1) and the confounding effects of large spatial units. Their study, based in England using high resolution geographic units and a longer temporal window than previous studies, found limited evidence of a treatment effect for long term exposure to $PM_{2.5}$: “[c]ompared to the previous studies, our results are the smallest in magnitude, likely because of the high geographical precision that allows more accurate confounding and spatial autocorrelation adjustment” (Konstantinoudis et al., 2021, p. 6) suggesting that the effects of scale and spatial autocorrelation need to be accounted for when modeling air pollution exposures.

An intra-state study on Texas by Xu et al. (2022) found “no consistent evidence or significant correlations between historic county-average $PM_{2.5}$ concentration and COVID-19 incidence or death” (p.1), though they did uncover a strong correlation between a given county’s percent Black and Hispanic residents and COVID-19 incidence and death. Similarly, Berg et. al (2021) found a positive, but non-statistically significant, increase in COVID-19 mortality in response to increases in long term exposure to $PM_{2.5}$ among Colorado census tracts. In

contrast, Zhu et al. (2020) identified a significant, positive association between COVID-19 confirmed cases and ambient air pollution, including $PM_{2.5}$ and ozone, when analyzing over 120 cities throughout China, suggesting that treatment effect estimates may be sensitive to differential definitions of place and that more research is needed to confirm the effects of air pollution on COVID-19 mortality.

In a 2015 study published in *Environmetrics,* researchers Lee and Sarran (2015) report that the health impact of long-term exposure to air pollution is now being "routinely estimated using spatial ecological studies" (p. 477) thanks to the influx of georeferenced health and pollution data. They contend that the "[a]real unit study design presents a number of statistical challenges, which if ignored have the potential to bias the estimated pollution–health relationship" (Lee and Sarran, 2015, p. 478). In particular, the pollution-health relationship estimates can be biased by "spatial autocorrelation present in the data after accounting for the known covariates" (Lee and Sarran, 2015, p. 477). By re-evaluating the Wu et al. (2020) ecological-level study of the effect of long term exposure to $PM_{2.5}$ on COVID-19 mortality in the contiguous U.S. and accounting for spatial autocorrelation with spatial econometric methods, this thesis attempts to address whether there is a geography to $PM_{2.5}$ and if so, whether geography can meaningfully be accounted for when estimating National models of air pollution exposure risks? Additionally, the Wu et al. (2020) treatment effect estimate's sensitivity to confounding is quantified using a sensitivity based framework alternative to the methods employed by the authors in order to offer another perspective on the reliability of this widely received estimate. Lastly, this thesis evaluates the effects of various regional scales on the treatment effect estimate in order to consider whether an understanding of the geographic context producing the health-hazard relationship can help to inform future public health research questions and modeling strategies.

4. Data and Methods

4.1 Data

The primary data used for this analysis is the data utilized by Wu et al. in the research study *"*Air pollution and COVID-19 mortality in the United States: Strengths and Limitations of an Ecological Regression Analysis," published in the November 2020 edition of *ScienceAdvances.* The data and code were accessed via the publicly available GitHub link provided by the authors in service to the reproduction of their analysis: https://github.com/wxwx1993/PM_COVID. County level ozone data in parts per billion (ppb) was obtained from the EPA and TIGER/lline shapefiles derived from U.S. Census Bureau data for the contiguous U.S. administrative boundaries were obtained from the R package *tigris*. The use of this data is a unique opportunity to illustrate the potential for the treatment effect estimates of public health studies to change with changes in model specifications and the consideration of geographical context. Additionally, the availability of this data provides the opportunity to reconsider the fragility of the author's treatment effect estimate to confounding using alternative sensitivity analysis methods.

4.2 Methods

The organization for the analysis in this section is in service to first evaluating the reliability of Wu et al. (2020) treatment effect estimate and next utilizing various methods in an effort to bolster this effect against confounding, reduce bias, and consider whether differing effect estimates of the long term exposure to $PM_{2.5}$ on COVID-19 mortality emerge with differing definitions of place. This is done using a sensitivity based framework alternative to the methods employed by the authors in order to offer another perspective on the reliability of this widely received estimate. Once fragility to confounding is discovered, then a revised model with the co-pollutant ozone, expressed as a model covariate, is estimated in order to evaluate the ability of the new model specification to reduce unobserved confounding. With both models indicating

room for explanatory improvement, exploratory spatial data analysis is then deployed in order to uncover spatial regimes, potential sources for unmeasured confounding, in the treatment and outcome variables. Spatial econometric models are then estimated to account for such spatial processes, such as spatial heterogeneity, that may contribute to unobserved confounding (Baller et al., 2001). Finally, the influence of geography on the health-hazard relationship is explored by varying model covariates representing the delineation of sub-National space into alternate socioeconomic and climatic regional units.

Sensitivity Analysis

Sensitivity analyses include a wide variety of methods and tools that assist researchers in exploring how the outputs of a system are influenced by the inputs (Razavi et al., 2021). They help to establish which assumptions must remain intact for a causal claim to be sustained (Hazlett and Parente, 2020). In observational studies, linear regression with a set of observed covariates believed to be sufficient to control for confounding is among the most popular strategies for identifying a causal relationship, however, the identification of a treatment effect often relies on the assumption of no unobserved confounders (Reich et al., 2021), a difficult to defend claim in most applied settings (Cinelli, Ferwerda, and Hazlett, 2020; Hazlett and Parente, 2020).

Observational studies using spatially referenced data, such as epidemiological studies evaluating environmental human health risks, face analytic challenges due to both treatment and outcome variables exhibiting spatial correlation and interference, “where the treatment applied at one location affects the outcomes at other locations” (Reich, 2021, p. 606). In a sensitivity based framework, the research emphasis moves away from definitively identifying a treatment effect to instead considering how strong confounding would need to be in order to alter a study’s causal claim (Hazlett and Parente, 2020). In the context of observational studies,

sensitivity analysis can be used to quantify the strength of an unmeasured covariate necessary to alter a research conclusion and whether this level of confounding is plausible (Rosenbaum 2005; Cinelli, Ferwerda, and Hazlett, 2020); a useful approach considering the influence of human health research conclusions on public health policy.

There is untapped potential in the application of sensitivity analysis to research modeling human environment interactions that are affected by confounding variables (Razavi et al., 2021). Despite originally being developed by Cornfield et al. in the mid-20th Century and further developed by others (Greenland, 1996), sensitivity analysis remains underutilized in many disciplines (Cinelli and Hazlett, 2020), including Human Geography. A June 2022 search within the archives of the *International Journal of Geographic Information Science* for the term "sensitivity analysis" yielded two hundred eleven search results from a database of just under 2,700 articles dating back to 2007. A search for the terms “sensitivity analysis” and “robustness value” from the same journal and over the same time period, yielded no results indicating that while sensitivity analyses may be deployed in the field of Geography to some extent, this particular framework has yet to be adopted widely. Within the field of epidemiology, the use of the E-value has quickly become among the most popular strategies for assessing sensitivity (VanderWeele, Martin, and Mathur, 2020).

E-value: Concerns Over Quantifying Uncertainty in Epidemiological Studies

The 2017 introduction of the E-value by VanderWeele and Ding allowed epidemiologists to quantify the degree of confounding on the risk-ratio scale that would “fully explain away a specific treatment-outcome association, conditional on the measured covariates” (p. 2). This method of model assessment has experienced widespread uptake by the epidemiological research literature, however, E-values have been prone to misinterpretation as “[n]o general rule

can exist about what is a "small enough" E-value, and users of the biomedical literature are not familiar with how to interpret a range of E-values" (Hamra, 2019; Ioannidis, Jones, Tan, and Blum, 2019, p. 108; Blum, Tan and Ioannidis, 2020; Fox, Arah, and Stuart, 2020). In this context, the sensitivity of a given treatment effect to confounding is not expressed explicitly alongside treatment effect estimates but rather as a function of the treatment effect that is "worked into" a reported risk ratio. Acknowledging that "confounding is a concern" in their analyses, Wu et al. calculated an E-value which was then worked into their outcome variable, Mortality Rate Ratio, following the conclusion that "that any unmeasured confounder would need to have a confounding effect substantially larger than any of our observed confounders in order to explain away the relationship between $PM_{2.5}$ and COVID-19 mortality rate" (2020, "Supplementary Materials" p. 11).

Wu et al. also conducted "over 80 sensitivity analyses to assess the robustness of the findings to various model assumptions" (2020, "Supplementary Materials" p. 9), however, it is important to note that their sensitivity analyses consist of a variety of model specifications and inclusion of the E-value. I posit that sensitivity statistics would be better expressed explicitly and should be reported alongside treatment effect estimates. Additionally, the treatment effect estimate of a widely received, observational study with public health policy implications can benefit from an alternative assessment of its fragility to confounding. In order to first investigate the potentially tentative nature of findings by Harvard T. Chan School of Public Health researchers, Wu et al., I utilize a sensitivity analysis framework developed by Cinelli and Hazlett (2020) to test the fragility of their treatment effect estimate.

Assessing the Sensitivity of a Treatment Effect Estimate within a Partial R^2

Sensitivity Analysis Framework

The omitted variable bias framework works within the mechanics of linear regression to explore the change in a coefficient estimate of interest that occurs when an omitted covariate is included (Cinelli and Hazlett, 2020). The approach to sensitivity deployed in this thesis, as developed by Cinelli and Hazlett (2020), extends the omitted variable bias framework and harnesses expert background knowledge to assess a research conlusion's fragility to unobserved confounders (Cinelli and Hazlett, 2020). While other sensitivity methods "impose complicated and strong assumptions regarding the nature of the unobserved confounder," (Cinelli, Ferwerda, and Hazlett, 2020, p. 2) this approach is more flexible. It does not require assumptions regarding the confounders' distribution, the linearity of its effect on the treatment or outcome, nor the "functional form of the treatment assignment mechanism" (Cinelli and Hazlett, 2020, p. 40), such as *as-if random*. Working within the widely used regression framework, it addresses how much unobserved confounding it would take to substantially alter a research conclusion by invoking two novel sensitivity measurements and a bounding procedure using known covariates (Cheng, 2019; Cinelli and Hazlett, 2020).

The sensitivity measurements utilized within this framework include the robustness value ($RV_{q=1}$), which uses partial R^2 values to assess the overall robustness of a treatment effect estimate to confounding, and $R^2_{Y\sim D|X}$ which describes "the proportion of variation in the outcome explained uniquely by the treatment" (Cinelli and Hazlett, 2020, p. 40). In the $R^2_{Y\sim D|X}$ sensitivity measurement, Y represents the outcome, D represents the treatment and X represents the model covariates. The portion of the $R^2_{Y\sim D|X}$ subscript, $D|X$, is read as D conditional on X and represents the treatment effect after accounting for model covariates. R^2 is a commonly used summary statistic to to determine the goodness of fit of a statistical model

and can be conceived of as *variance explained* (Nakagawa and Schielzeth, 2013), the proportion of variance in an outcome variable that is explained by the model covariates (Nagelkerke, 1991).

While variance is a measure of variability in a dataset, residual variance can be conceived of as the *unexplained variance,* or the variance that cannot be explained by model covariates. $RV_{q=1}$ considers a confounder that has equal partial R^2 values with both the treatment and outcome" (Cheng, 2019, p. 11) as a useful, overall benchmark to denote the amount of residual variance in both the treatment and outcome variables that would be required to reduce the treatment effect estimate to zero (Cinelli and Hazlett, 2020; Hazlett and Parente, 2020). Similarly, the $RV_{q=1\ ,\ \alpha=0.05}$ denotes the amount of residual variance in both the treatment and outcome variables that would be required to reduce the treatment effect estimate to the boundary of statistical significance at the $\alpha = 0.05$ level (Cinelli, Ferwerda, and Hazlett, 2020, p.5; Hazlett and Parente, 2020). A confounder this strong would render previously significant findings unpublishable. The q subscript of the RV values specifies the fraction of the treatment effect estimate which would need to be explained away by unobserved confounders to be troublesome, with $q = 1$ denoting a treatment effect estimate reduction of 100%, or rather, a treatment effect estimate of zero (Cinelli, Ferwerda, and Hazlett, 2020). The observed treatment effect estimate then, would be due to bias (Hazlett and Parente, 2020). For the purposes of this thesis, a generalized version of the definition of bias, as elaborated by Hazlett and Parente (2020), will be used: the difference in the observed treatment effect estimate and the "true" treatment effect estimate, if unobserved confounding had instead been accounted for with additional model covariates in an ideal, hypothetical model.

Deploying Sensitivity Analysis

The identification strategy deployed in this analysis to determine the treatment effect of long term exposure to $PM_{2.5}$ on COVID-19 mortality is Selection on Observables (S.O.O.). The assumptions associated with S.O.O. in this context are as follows, with an analogous definition available in *Foundations of Agnostic Statistics* by Aronow and Miller (2019; pp. 247-248):

1. Conditional Ignorability: Conditional Ignorability can be described as among units with the same covariate, X , treatment is as-if random. In this case, treatment is continuous; every COVID-19 mortality associated with a particular $PM_{2.5}$ exposure value (d) is independent of exposure to $PM_{2.5}$ (D) amongst members of a given unit with the same covariate value $(X_i = x)$ (Figure 1a).
$$Y_{di} \perp\!\!\!\perp D_i \vert X_i = x \; for \; all \; d$$
Figure 1a: Conditional Ignorability

2. Common Support: For units with any particular value of X, there is some probability of these units having any level of exposure (Figure 1b).
$$0 < Pr(D_i = d \vert X_i) < 1 \; for \; x \in \mathcal{X}$$
Figure 1b: Common Support

In order to generate the sensitivity measurements, RV, $RV_{\alpha=0.05}$, and $R^2_{Y\sim D|X}$, the Wu et al. (2020) model was reworked into an Ordinary Least Squares (OLS) linear regression, a common strategy for estimating unknown parameters, in order to accommodate the sensitivity framework (Table 2). The authors' original model specification was also re-run with the reconstructed data (Table 1). The population covariate was shifted into the denominator of the outcome variable and a log transformation was applied in order to account for the likely exponential increase in the mortality rate (Figure 2a). Hereinafter, the outcome variable will be referred to in this text as the outcome variable, COVID-19 mortality, or as the COVID-19 mortality rate, the OLS reworking of the Wu et al. main model will be referred to as the OLS Main Model (Figure 2b), and the treatment variable is referred to as such and also

interchangeably as mean $PM_{2.5}$, long term exposure to $PM_{2.5}$ and long term average $PM_{2.5}$.Lastly, the authors' state covariate accounting for state-specific random effects was converted to a simplified state covariate accounting for state-specific fixed effects, such as predominant political affiliations influencing mask and social distancing policies and attitudes. The resulting OLS Main Model is enumerated in Figure 2b.

$$log\left(\frac{deaths+1}{population}\right)$$

Figure 2a: Reworked Outcome Variable

$$log\left(\frac{deaths+1}{population}\right) = mean.pm25 + factor(q:popdensity) + scale(poverty) + scale(log(median.house.value)) + scale(log(med.household.income)) + scale(pct.owner.occ) + scale(education) + scale(pct.blk) + scale(hispanic) + scale(older.pecent) + scale(prime.pecent) + scale(mid.pecent) + scale(date.since.social) + scale(date.since) + scale(beds/population) + scale(obese) + scale(smoke) + scale(mean.summer.temp) + scale(mean.winter.temp) + scale(mean.summer.rm) + scale(mean.winter.rm) + state$$

Figure 2b: Reworked OLS Main Model

Bounding the Sensitivity Analysis

This particular sensitivity analysis framework also allows the researcher to bound the degree of plausible confounding with existing, influential model covariates serving as benchmarks to assist in considering whether a confounder of this strength could exist in one's study (Cinelli and Hazlett, 2020; Hazlett and Parente, 2020). These benchmarks allow the researcher to consider the relative strength of an unobserved confounder using known covariates to argue whether or not this degree of confounding is plausible (Cinelli and Hazlett,

2020) and produce contour plots visualizing this relationship. A treatment version of the model, with long term exposure to $PM_{2.5}$ designated as the outcome variable, was run in order to determine which covariates most strongly predict long term exposure to $PM_{2.5}$ in addition to COVID-19 mortality and would therefore be useful to bound the degree of plausible confounding. The results of all three linear models including the negative binomial mixed model, referred to as the Wu et al. Main Model, OLS, and treatment model were then reported in separate tables (Tables 1, 2, 3 respectively). After identifying the benchmarking covariate, *percent Black residents,* the partial R^2 sensitivity measurements and contour plots were evaluated to explore the degree of confounding that would need to exist in order to destabilize the OLS version of Wu et al.'s treatment effect estimate (Table and Plot A_i). Once fragility to confounding was established, the ubiquitous pollutant ozone was explored as a potential confounder.

Possible Confounder: Ozone

$$log\left(\frac{deaths+1}{population}\right) = mean.pm25 + ozoneppb$$
$$+factor(q:popdensity) + scale(poverty)$$
$$+scale(log(median.house.value)) + scale(log(med.household.income))$$
$$+scale(pct.owner.occ) + scale(education) + scale(pct.blk)$$
$$+scale(hispanic) + scale(older.pecent) + scale(prime.pecent)$$
$$+scale(mid.pecent) + scale(date.since.social) + scale(date.since)$$
$$+scale(beds/population) + scale(obese) + scale(smoke)$$
$$+scale(mean.summer.temp) + scale(mean.winter.temp)$$
$$+scale(mean.summer.rm) + scale(mean.winter.rm) + state$$

Figure 2c: Ozone OLS Model

Ozone

Ozone is presented as a potential confounder due its health implications as well as its documented co-presence with $PM_{2.5}$, however, RNA viruses such as COVID-19 are unstable in the presence of ozone (Manjunath et al., 2021) and ozone has been used in medical studies to treat COVID-19 with an associated effect in the reduction of days on ventilator (Hernández et al. 2021). In considering ozone as a potential confounder, it is important to note the differential effects between tropospheric ozone exposure and exposure to ozone therapy in a medical context. Medically administered ozone can be beneficial to COVID-19 patients (Cattel et al., 2021) in that it is a "precise concentration and therapeutic dosage" that is "calibrated against the antioxidant capacity of blood" (Bocci, 2007, p. 255) while tropospheric ozone is considered toxic (Bauer, Diaz-Sanchez and Jaspers, 2012) and even deadly (American Lung Association, 2001).

Ozone's associated public health risks are widely accepted and well documented. The

Asthma and Allergy Foundation of America, or AAFA, (2015) states that ozone is a main contributor to adverse respiratory effects including lung irritation and reduced function. Its concentration is directly related to the frequency of asthma attacks and asthma related Emergency Department visits (AAFA, 2015). As a result, it has articulated to a complex web of regulatory compliance mechanisms and public health imperatives across the U.S. Ground level ozone is subject to both the Federal NAAQS and California state agency regulations that surpass national standards as administered by state agencies such as the California Air Resources Board. It is considered one of the EPA's six most common air pollutants (US EPA, 2015).

Ozone and $PM_{2.5}$ have a relationship in space and time. In the American West, the meteorologically dependent presence of ozone and primarily wildfire-generated $PM_{2.5}$ co-occurrences have been investigated as "[t]he frequency, spatial extent, and temporal persistence of extreme $PM_{2.5}$/ozone co-occurrences have increased significantly between 2001 and 2020, increasing annual population exposure to multiple harmful air pollutants by ~25 million person-days/year" (Kalashnikov, 2022, p. 1). Researchers David et al. question the future of the implementation of EPA NAAQS standards in U.S. regions such as the American West where wildfire-driven days of exceptional ozone and $PM_{2.5}$ events have grown to such an extent that it would threaten a region's attainment status (2021). They also point to regionally specific variations in the presence of these exceptional events: "[w]estern states appear to experience far more wildland fires and stratospheric O3 intrusions relative to other areas" (David et al., 2021, p. 6). The meteorological drivers, namely extreme heat, of the co-occurrences of ozone and particulate matter in the eastern U.S. and Canada were investigated by Schnell and Prather (2017) who concluded that "the hottest temperatures" were drivers for the "highest levels of pollution" (p. 2854), a sobering realization in the context of a changing climate. In a 2019 study on the correlations between $PM_{2.5}$ and ozone over China, Zhu et al. found strong positive

correlations between the presence of the two pollutants during most seasons, particularly the warm seasons, noting that the correlations were likely due to “the promoting effect of high O_3 concentration and active photochemical activity on secondary particle formation” (p.1). The inclusion of ozone as a model covariate is expected to reduce unmeasured confounding in the OLS Main Model therefore producing a more accurate treatment effect of the long term exposure to $PM_{2.5}$ on COVID-19 mortality.

Once the sensitivity analysis for the OLS Main Model was assessed, a model including the potentially relevant confounder ozone (O_3) was then estimated (Ozone OLS Model, Figure 2) to consider whether explicitly including ozone as a covariate strengthened the treatment effect against confounding. County level ozone data in parts per billion (ppb) was obtained from the EPA and the daily maximum 8-hour concentration was averaged over three years for years 2017, 2018, and 2019. The sample size was reduced from approximately 3000 observations to approximately 800 observations in response to the availability of ozone monitored on a continuous scale. Effectively, the ozone portion of this analysis proceeded with a different sample, referred to as *ozone subset*.

Considering that counties included in the EPA’s monitoring of ozone on a continuous scale are likely to be more populous than those that weren’t included, the population density of the original sample was plotted against the *ozone subset* (Plot 1, See Appendix). The limitation of using a subset of more populous counties excludes variation that may be present in the treatment-outcome relationship amongst rural counties, or between rural and populous counties. A treatment model (Table 5) was again estimated and sensitivity measurements quantified in order to consider the degree of confounding that would need to exist in order to destabilize the treatment effect of long term exposure to $PM_{2.5}$ on COVID-19 mortality with ozone expressed as a covariate (Tables and Plots B-C). The correlations between ozone and the treatment and outcome variable are visualized in Plots 2 and 3, respectively (See Appendix) in order to

consider the underlying reasons for the effect estimate of ozone on COVID-19 mortality.The replication of the OLS Main Model with ozone as a model covariate is essential in exploring how the inclusion of this co-pollutant can strengthen the treatment effect of the long term exposure to $PM_{2.5}$ on COVID-19 mortality against confounding. The limited spatial and temporal scales utilized in this approach, however, provide obstacles to obtaining a full account of the environmental health hazards these pollutants pose. Once the ozone model was assessed, spatial analysis was then utilized to uncover underlying spatial processes as potential sources of confounding.

Assessing the Spatial Sensitivity of a Treatment Effect Estimate with ESDA

Spatial analysis can be used as a complementary strategy to sensitivity for exposing potential sources of confounding in epidemiological air pollution studies. Chen et al. (2017) state that air pollutants are often linked with spatial spillover effects as “air pollutants are apt to diffuse and migrate across different regions” (p. 917) and have a “strong negative spatial spillover effect on public health” (Chen et al., 2017, p. 922). As the continuous rather than episodic presence of $PM_{2.5}$ (industrial and traffic related emissions vs. wildfires) is tied to places characterized as urban centers, the distribution of long term $PM_{2.5}$ exposure estimates across geographic units, such as U.S. counties, are likely to not be independent; i.e. the $PM_{2.5}$ exposure values in a given unit are likely to influence the values of neighboring units. Despite the inclusion of maps indicating strong spatial trends in their treatment and outcome variable, the possible presence of spatial autocorrelation at the local level or spatial heterogeneity at the regional level was not investigated by Wu et al. in their 2020 research publication connecting the effects of long term exposure to $PM_{2.5}$ to COVID-19 mortality.

The Case for Space

Often, despite the ubiquitous use of georeferenced data in public health research, the substantive influence of geography in the relationship between the treatment and outcome variable is either not considered in the model specifications nor the sampling strategy (Goldhagen et al., 2005; Matisziw, Grubesic, and Wei 2008) or is masked by the mechanism of data aggregation to an administrative, geographic unit which, in turn, spatially misrepresents the data (Delmelle et al. 2022;). Anselin (1988) contends that "aggregate spatial data are characterized by dependence (spatial autocorrelation) and heterogeneity (spatial structure)" (p.1). Ignoring the presence of spatial dependence in model specifications can produce biased and inconsistent estimates of classical regression models including Ordinary Least Squares (OLS) which assumes identically and independently distributed observations (i.i.d) (Anselin and Bera, 1998; Baller et al., 2001; LeSage 2008; Messner et al, 1999).

Spatial dependence refers to the clustering of similar values of a given variable across space (Shin and Ward, 1999) while spatial autocorrelation is described as occurring when a given variable at a particular location "is determined by the values of the same variable at other locations in the system" (Anselin, 2003, p. 310). For instance, positive spatial autocorrelation can be defined as occurring when like values of a given variable are also locationally similar (Anselin, 1996a). The term spatial dependence is often used interchangeably with the term spatial autocorrelation though there are disciplinary disagreements regarding whether these terms are actually distinct or not (Anselin and Bera, 1998; Chi and Zhu, 2019). Spatial heterogeneity is considered by Anselin and Getis to be a "special case of spatial dependence" (1992, p. 24) where the spatial effects are not uniform across the study area (Anselin and Getis, 1992). Shin and Agnew (2011) use the term spatial heterogeneity to specify regional scale spatial variation as opposed to spatial dependence or positive spatial autocorrelation which is

defined by the authors as specifically pertaining to the clustering of similar values at a local level, also known as hotspots. The identification of hotspots may assist in geographically directing one's research focus for further inquiry (Shin and Ward, 1999). Shin and Ward (1999) point out that spatial dependence and heterogeneity are not necessarily mutually exclusive and that the consideration of regional context may shed light on this particular configuration of spatial relationships within a given study area. For the purpose of this thesis, I will use the terms spatial dependence and spatial autocorrelation interchangeably. As spatial dependence can cause biased and inconsistent treatment effect estimates, this can complicate a researcher's ability to make a causal claim.

The Rubin Causal Model (RCM) is described as a "formal mathematical framework for causal inference" (Imbens and Rubin, 2010, p. 229). It is "part of the foundational framework for empirical treatment effect analysis" (Kolak and Anselin, 2019, p.128) and is utilized to identify causal effects in observational studies based on three essential concepts: units, treatments and potential outcomes (Imbens and Rubin, 2010). A unit is a physically definable object, while the treatment constitutes "an action that can be applied or withheld from a unit" (Imbens and Rubin, 2010, p. 231). The two potential outcomes for each unit can be conceptualized as an outcome variable Y_i where Y_{1i} is the apriori, theoretical treatment potential outcome and Y_{0i} is its non-treatment potential outcome counterpart, also known as the control potential outcome (Imbens and Rubin, 2010). One of the assumptions of the Rubin causal model is the stable unit treatment value assumption, or SUTVA (Imbens and Rubin, 2010). SUTVA maintains that "the potential outcomes of individuals be unaffected by changes in the treatment exposures of all other individuals" (Morgan and Winship, 2015, p. 48). SUTVA itself contains two assumptions, described as well-defined treatments and no-interference, the latter indicating that the treatment status of any particular unit does not affect the treatment status of other units (Imbens and Rubin, 2010).

When spatial effects are not explicitly included in model specifications, standard statistical measures of fit may become biased or unreliable (Kolak and Anselin, 2019). For instance, “spatial interaction and heterogeneity between units at individual or group levels can violate both components of the SUTVA" (Kolak and Anselin, 2019, p. 131) and when such spatial effects are excluded, researchers can inappropriately allocate treatment effect estimates (Kolak and Anselin, 2019). Researchers commonly address this violation by aggregating observational data to macrolevel units, such as administrative or political units, so that the SUTVA assumption can be maintained (Imbens and Rubin in Kolak and Anselin, 2019). This presents problems when the treatment's causal effects in question work at a finer or disaggregated spatial resolution: “spatial effects violate the so-called stable unit treatment value assumption advanced by Rubin” (Kolak and Anselin, 2019, p. 128).

Ecological studies linking pollutant exposures to disease at large, aggregate scales may suffer from the modifiable areal unit problem, or MAUP, where “the scale of the grid cell has an imperfect match with the scale of the process studied, various types of misspecification may result” (Anselin and Getis, 1992, p. 42). Treatment effect estimates obtained from multivariate analysis may vary with the level of data aggregation or the spatial nature of the administrative unit to which they are aggregated, suggesting that areal data may be unreliable or sensitive to a change in geographic unit (Fotheringham and Wong, 1991). Public health research relating air pollution exposure to disease incidence often rely on areal data aggregated to large administrative units to infer population-level associations that force these spatially continuous phenomena into arbitrary units (Lee et al. 2020). In a paper examining the effect of MAUP on population-level air pollution and disease incidence associations, Lee et al. (2020), however, found that the modifiable areal unit problem does not dramatically alter treatment effect estimates when the pollution concentrations are spatially autocorrelated and the number of

areal units is high.

Application of ESDA to Unveil Spatial Relationships

A commonly employed strategy for spatial pattern recognition and evaluation of the spatial distribution of a variable of interest is a set of methods known as exploratory spatial data analysis (ESDA) (Anselin, 1996a; Anselin and Getis, 1992; Chi and Zhu, 2019; Shin and Ward, 1999). ESDA's strength is in its ability to reveal spatial patterns and structures to "help determine the extent of data dependence and heterogeneity" (Anselin and Getis, 1992, p.28.). Here, I utilize ESDA methods in order to visualize any spatial trends present in the data. Broadly, this commonly includes the production of maps of the distribution of the outcome variable and the OLS model residuals as well as the calculation of the global Moran's I and affiliated Moran Scatterplots. Once global measures of spatial autocorrelation are established, Local Indicators of Spatial Association are typically computed and visualized in the context of a map in order to further investigate and locate areas of spatial nonstationarity or "hotspots" (Anselin, 1995).

Specifically, ESDA often begins with data visualizations in a geographic setting, such as a map, in order to look for the existence or lack of spatial regimes (Chi and Zhu, 2019). Before cartographically visualizing the data, the distribution of long term exposure to $PM_{2.5}$, COVID-19 mortality, and the OLS Main Model residuals were visualized through the production of a variety of plots. The quantile-quantile plot, which compares the distribution of the observed values with that of a normal distribution, and the Mean Density Plot, displaying the probability density of observed values per U.S. County, can be found in the Appendix (Plots 4a through 4f). These data visualizations were used in tandem with ESDA methods to unveil spatial nonstationarity in both the outcome and treatment variables, as well as the OLS model residuals.

Visualizing Data Values Geographically

The goal of the production of data distribution maps was to first visually determine whether their values are distributed randomly across the contiguous U.S., or if there are visually definable spatial patterns "as human eyes are good at recognizing spatial patterns from graphical presentations of data" (Chi and Zhu, 2019, pp. 43-44). Maps of the distribution of the long term average $PM_{2.5}$ exposure values and the COVID-19 mortality values across the contiguous U.S. were produced using the Fisher-Jenks classification algorithm and $n = 5$ classes (Plots 5a-5b). For the OLS Main Model residuals, values were binned using the classification algorithm equal-interval (5c).

Study Area and Neighborhood Construction

The study area for this portion of the analysis generally retains the same extent as the Wu et al. (2020) study area, i.e. the contiguous, lower forty-eight U.S. states and District of Columbia (D.C.), excluding the five New York City boroughs (the Bronx, Brooklyn, Manhattan, Queens and Staten Island) from the study region as outliers. Some reconfiguration of the study area was necessary for the creation of a continuous surface in order to proceed with spatial analysis (Anselin and Getis, 1992). The Geographic Information System (GIS) open-source software, QGIS, and the k-nearest neighbor method was used to interpolate nineteen counties' missing values from the ten nearest counties and excluded three county-island observations (Duke, Nantucket, and San Juan Island). Since counties that share borders and/ or vertices are considered spatially contiguous in terms of the ability of particulate matter to be transported through the airspace of adjacent counties, the Queen's contiguity matrix is applied in order to define the "neighborhood" for the dataset.

Global Measures of Spatial Autocorrelation

Once the spatial weights matrix was established, global Moran's I values and scatterplots were produced for COVID-19 mortality, long term exposure to $PM_{2.5}$, and the OLS Main Model residuals (Table 6a and Plots 6a- 6c). The global Moran's I is used in order to test for spatial autocorrelation between the observed values, typically expressed in terms of the outcome variable, y, and the weighted average of neighboring values, W_y, also known as the spatial lag (Anselin 1996b). Specifically, the global Moran's I statistic measures the degree of linear association between a variable value at a given location and the weighted average of the same variable at neighboring locations (Chi and Zhu 2020), producing a single statistic for the entire study area with "a null hypothesis of spatial randomness" (Anselin, 2020). It can be conceived of as the slope of the regression line between the unit value and neighborhood value (Pacheco and Tyrrell 2002) and is interpreted similarly to the Pearson's correlation coefficient where weak correlations are represented by numbers close to zero and high positive or negative correlations are represented by numbers close to 1 or -1, respectively (Chi and Zhu, 2019). The expected value of the Moran's I under the null hypothesis approaches zero as the sample size increases (Boots and Tiefelsdorf, 2000).

The global Moran's I formula, first developed by Moran in 1948 and elaborated by Chi and Zhu (2020, p. 44), is expressed in Figure 3 where n denotes the number of areal units, y_i denotes the value of a variable at a given areal unit i for $i = 1 \rightarrow n$, i and j index n areal units, W_{ij} represents the spatial weight of areal units i and j and $\overline{y}$ is the mean of attribute y_i across all areal units. In order to test the likelihood of the Moran's I statistic randomly occurring, p-values were computed from Monte Carlo simulations for the treatment variable, outcome variable and Main Model OLS residuals (Table 6b, see Appendix). This computational approach, also operating under the null hypothesis of spatial randomness, does not require assumptions of

normality in the data values and is more robust, yet limited in its interpretability with regard to the sample itself (Anselin, 2020), however, it serves as a complement to the Moran's I statistic. In addition to a dataset-wide, global measure of spatial autocorrelation, local indicators of spatial association are useful in identifying spatial regimes.

$$I = \left(\frac{n}{\sum_{i=1}^{n} \sum_{j=1}^{n} w_{ij}} \right) \frac{\sum_{i=1}^{n} \sum_{j=1}^{n} w_{ij}(y_i - \overline{y})(y_j - \overline{y})}{\sum_{i=1}^{n} (y_i - \overline{y})^2}$$

Figure 3: Global Moran's I Formula

Local Measures of Spatial Autocorrelation

Once spatial dependence is discovered visually across the dataset, local indicators of spatial association (LISA) were used in order to assess the degree of statistically significant hotspots and coldspots. Much like the Moran Scatterplot, LISA statistics such as the Local Moran's I allow for "the indication of pockets of spatial nonstationarity, or the suggestion of outliers or spatial regimes" (Anselin, 1995, p. 94). As opposed to producing one statistic for the entire dataset, the Local Moran's I focuses one specific area at a time, the ith areal unit, and its neighboring values (Boots and Tiefelsdorf, 2000; Chi and Zhu, 2019). Given that exposure to $PM_{2.5}$ is both a local, regional, and transboundary phenomenon, LISA analysis was expected to uncover spatial dependence among adjacent units and regional spatial regimes linked to differing histories of development and present day economic activity. Spatial dependence in COVID-19 mortality among U.S. counties was also expected given the likely distribution of the treatment, community spread, and regional, climatic or statewide political conditions contributing to its expansion or abatement. The Local Moran's I, as elaborated by Chi and Zhu (2020, p. 47),

is expressed in Figure 4. Its output is extensive and best visualized in the context of a map (Chi and Zhu, 2019; Plots 7a-7c). It can be thought of as a decomposition of the global Moran's I (Anselin, 1995) as "[t]he arithmetic mean over all Local Moran's I_is equals the global Moran's I" (Boots and Tiefelsdorf, 2000, p. 325).

In order to identify hot and cold spots in the data, long term exposure to $PM_{2.5}$ and COVID-19 mortality county values were standardized to their means and the Local Moran's I county values to their means and then assigned each significant county value (p-value < 0.05) to a quadrant based on their joint relationship to zero (Plots 7a-7c). For instance, when the standardized $PM_{2.5}$ county mean is greater than zero and the Local Moran's I county value is greater than zero, the value is assigned to the "High- High" quadrant. When counties classified as High-High are spatially contiguous for both the treatment and outcome variable, this could indicate spatial spillover, where long term exposure to $PM_{2.5}$ in a given county results in a COVID-19 mortality in another and may result in a biased or inefficient treatment effect estimate.

$$I_i = (y_i - \overline{y}) \sum_{j=1, j \neq i}^{n} w_{ij}(y_j - \overline{y})$$

Figure 4: Local Moran's I Formula

Spatial Econometrics

Standard linear regression models generally require that observations are independent of one another (LeSage, 2014). Similarly, OLS requires that residuals are i.i.d (independently and identically distributed), and normally distributed with a mean zero and constant variance in

order for the parameter estimates to be unbiased and efficient (Chi and Zhu, 2019). If the data in question exhibits spatial dependence, then the parameters may be unreliable (Chi and Zhu, 2019, LeSage 2008). For instance, in the context of OLS, the parameter estimate β can be inefficient if the error terms are spatially dependent (Chi and Zhu, 2019). LeSage (2008) observes that "it is commonly observed that sample data collected for regions or points in space are not independent but rather spatially dependent" (p. 19). In order to bolster the treatment effect estimate of long term exposure to $PM_{2.5}$ against confounding and produce more reliable estimations of its effect on COVID-19 mortality, underlying spatial processes such as spatial dependence must be accounted for in the model specifications.

Spatial econometrics is a field which extends traditional linear regression techniques by allowing for the incorporation of spatial dependence among observations usually in the form of a spatially lagged variable (LeSage 2008). Spatial autoregressive models, also known as spatial lag models, incorporate a spatially lagged dependent variable ρWy where ρ is a spatial autoregressive coefficient, y is a $Nx1$ vector of dependent variable observations, Wy is the lagged dependent variable for weights matrix W and the remaining two terms, $X\beta$ and ε are analogous to an OLS interpretation. Using Anselin and Bera's formal expression (1998, p. 246), the spatial lag model can be found in Figure 5. The expectation that the long term exposure to $PM_{2.5}$ and COVID-19 mortality exhibit spatial structure in their distribution motivates the inclusion of a spatially lagged dependent variable in subsequent models.

$$y = \rho Wy + X\beta + \varepsilon$$

Figure 5: Spatial Lag Formula

Another way to incorporate spatial dependence in model specification is through incorporating a spatial processes in the error term (Anselin and Bera, 1998) and can be found in Figure 6 as a reproduction of the formula expression used in Anselin and Bera (1998, p. 248) where the linear model with error vector ε consists of the spatial autoregressive coefficient λ, the error lag $W\epsilon$, and the homoskedastic error term ξ. The error term represents the portion of the relationship between the long term exposure to $PM_{2.5}$ and COVID-19 mortality that cannot be explained by model covariates, The possibility of spatial processes occurring in the error term, for instance from the lack of inclusion of co-pollutants such as ozone, motivates the inclusion of this model.

$$y = X\beta + \varepsilon$$

$$\varepsilon = \lambda W\varepsilon + \xi$$

Figure 6: Spatial Error Formula

While “the problems of spatial heterogeneity can for the most part be solved by means of standard econometric techniques" (Anselin, 1988, p. 9), a spatial econometric approach must be taken in order to address issues of spatial dependence (Anselin, 1988). OLS Main Model residuals were investigated for heteroscedasticity, also known as unequal scatter, which could suggest, among other possibilities, an important omitted variable. Spatial correlation in the error term is commonly found when spatial spillover among the independent and dependent variables in the model, such as the expected spatial spillover of the long term exposure to $PM_{2.5}$. In response, Lagrange Multiplier diagnostics for spatial dependence in the residuals and outcome variable of the OLS Main Model were estimated (Table 8). Once substantive evidence for spatial dependence was confirmed in the OLS Main Model residuals (weak) and outcome variable

(stronger), Maximum Likelihood functions were then used to estimate spatial lag and spatial error models in order to produce more reliable treatment effect estimates.

A comparison of the OLS Main Model, spatial lag and spatial error model outputs can be found in Table 9. Model fit was compared on the basis of the goodness-of-fit Akaike Information Criterion (AIC) values, often used for likelihood models (Chi and Zhu, 2019). As there is strong evidence for spatial dependence in the treatment variable, the prevalence of COVID-19 mortality in a given county may also be dependent on neighboring treatment variable values due to the negative spatial spillover effects of air pollution on public health (Chen et al. 2017). For this reason, a spatial Durbin model is also considered (Figure 7) which allows for the inclusion of the spatially lagged dependent variable and spatially lagged explanatory variables. The spatial Durbin formal expression in Figure 7 is adapted from Yang, Noah and Shoff (2015, p. 24) where WX denotes the spatially lagged explanatory variable and θ consists of a $kx1$ vector of the effects of WX. The spatial Durbin model output includes spatially lagged COVID-19 mortality as well as long term exposure to $PM_{2.5}$ (Table 10).

$$y = \alpha + \rho W y + X\beta + WX\theta + \varepsilon$$

$$\varepsilon \sim N(0, \sigma^2)$$

Figure 7: Spatial Durbin Formula

$$log(deaths+1/population) = mean.pm25+ozoneppb+factor(q:popdensity)+ scale(poverty)+scale(log(median.house.value))+scale(log(med.household.income))+ scale(pct.owner.occ)+scale(education)+scale(pct.blk)+scale(hispanic)+ scale(older.pecent)+scale(prime.pecent)+scale(mid.pecent)+scale(date.since.social)+ scale(date.since)+scale(beds/population)+scale(obese)+scale(smoke)+ scale(mean.summer.temp)+scale(mean.winter.temp)+scale(mean.summer.rm)+ scale(mean.winter.rm)+CR_{mw}+CR_s+CR_{ne}$$

Figure 8: U.S. Census OLS Model

In consideration of the MAUP, the confounding effects of spatially dependent data, and the growing critique of epidemiological air pollution studies that aggregate disease incidence and pollution data to arbitrary area units in order to make population level public health inferences (Lee et al., 2020), the impact of scale on the treatment effect estimate of long term exposure to $PM_{2.5}$ on COVID-19 mortality was also explored. Regional dummy variables replaced state model covariates (Figures 8 and 10) effectively changing the definition of subnational place as well as the scale of place-based covariates. Lagrange Multiplier tests (Tables 11 and 14) and spatial lag models were estimated (Tables 12, 13, 15, 16) to account for spatial regimes in the data, and offset its spatial structure. For this portion of the analysis, the Wu et al. data was first subset into U.S. Census regions (Figure i, Intro), commonly used to delineate space and define place in epidemiological studies. With regard to the regional variables, Census Region West is assigned as the reference group while the Census Region Midwest variable, C_{mw} takes a value of 1 when the census tract falls within the Midwest Census Region, and 0 otherwise. Similar logic can be applied to the Census Region dummy variables for the South Census Region C_s and Northeast Census Region C_{ne}. In order to further investigate the possibility of differing trends in the relationship between the treatment and outcome variable among regions, long term exposure to $PM_{2.5}$ vs. COVID-19 mortality was

also plotted by county on a National scale without subnational delineations (Plot 9) and then by Census Region against the National mean, expressed as *National* (Plot 10a).

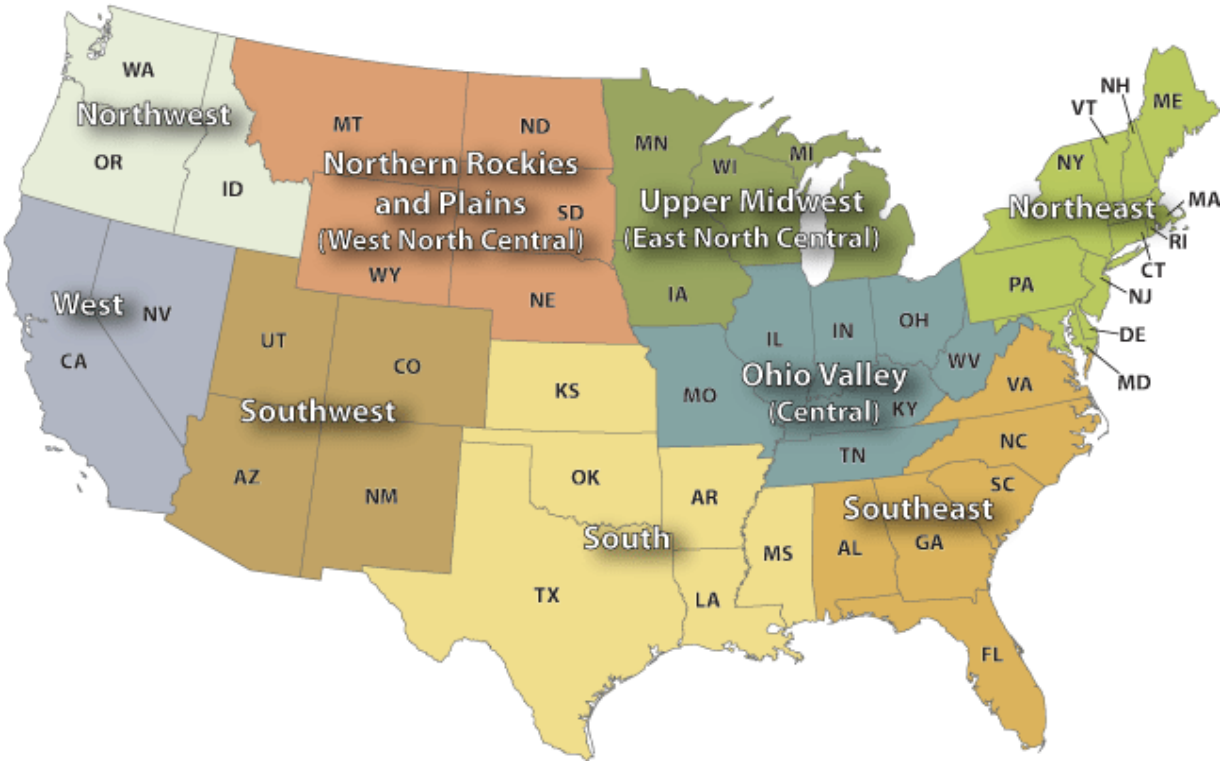

Figure 9: EPA Climatically Consistent Regions. From EPA.gov (2016); Public Domain

The sub-national investigation of the impact of scale, and climatically defined place, on the $PM_{2.5}$ and COVID-19 mortality health-hazard relationship was investigated by subsetting the Wu et al. (2020) data into EPA climatically consistent regions (Figure 9) which are delineated on the basis of similar climatic regimes of temperature and humidity. Long term exposure to $PM_{2.5}$ vs. COVID-19 mortality by EPA Climatically Consistent Region was also plotted against the Mean values for the contiguous U.S. named *National* (Plot 11) in order to again investigate the possibility for differences in trends among regions. The EPA dummy variables were similarly structured with the EPA West region serving as the reference group, EPA Northwest represented by EPA_{nw} and rest of the variables following a similar naming strategy (Figure 10).

$$log(deaths+1/population) = mean.pm25+ozoneppb+factor(q:popdensity)+ scale(poverty)+scale(log(median.house.value))+scale(log(med.household.income))+ scale(pct.owner.occ)+scale(education)+scale(pct.blk)+scale(hispanic)+ scale(older.pecent)+scale(prime.pecent)+scale(mid.pecent)+scale(date.since.social)+ scale(date.since)+scale(beds/population)+scale(obese)+scale(smoke)+ scale(mean.summer.temp)+scale(mean.winter.temp)+scale(mean.summer.rm)+ scale(mean.winter.rm)+EPA_{nw}+EPA_{nrp}+EPA_{sw}+EPA_{s}+EPA_{ov}+ EPA_{umw}+EPA_{SE}+EPA_{ne}$$

Figure 10: EPA OLS Model

In order to quantify regional differences in the relationship between COVID-19 mortality and the long term exposure to $PM_{2.5}$, I perform a one-way analysis of variance test and Tukey Honest Significant Difference for each set of subnational delineations.. The null hypotheses for these tests are equivalent Census Region or EPA Climatically Consistent Region means. The differences in treatment effect estimates through the inclusion of spatial and place based processes are discussed in the Results section.

5. Results

5.1 Sensitivity Analysis

Table 1: Wu et. al Main Model

	Dependent variable:
	Deaths
mean_pm25	0.102*** (0.026)
factor(q_popdensity)2	−0.088 (0.122)
factor(q_popdensity)3	−0.082 (0.125)
factor(q_popdensity)4	−0.287** (0.130)
factor(q_popdensity)5	−0.062 (0.148)
scale(poverty)	0.042 (0.037)
scale(log(medianhousevalue))	0.115* (0.068)
scale(log(medhouseholdincome))	0.182*** (0.066)
scale(pct_owner_occ)	0.108*** (0.038)
scale(education)	0.188*** (0.045)
scale(pct_blk)	0.398*** (0.039)
scale(hispanic)	0.057 (0.046)
scale(older_pecent)	0.049 (0.057)
scale(prime_pecent)	−0.253*** (0.074)
scale(mid_pecent)	−0.276*** (0.055)
scale(date_since_social)	0.183 (0.122)
scale(date_since)	0.871*** (0.078)
scale(beds/population)	−0.004 (0.036)
scale(obese)	−0.032 (0.035)
scale(smoke)	0.117* (0.062)
scale(mean_summer_temp)	0.098 (0.080)
scale(mean_winter_temp)	−0.166 (0.108)
scale(mean_summer_rm)	−0.039 (0.077)
scale(mean_winter_rm)	−0.058 (0.051)
Constant	−10.124*** (0.242)
Observations	3,089
Log Likelihood	-7,498.726
Akaike Inf. Crit.	15,051.450
Bayesian Inf. Crit.	15,214.410
Note:	*p<0.1; **p<0.05; ***p<0.01

Table 2: OLS Reworking of Wu et. al Main Model

	Dependent variable:)
	log(deaths+1/population)
mean.pm25	0.069*** (0.017)
factor(q_popdensity)2	−0.579*** (0.062)
factor(q_popdensity)3	−0.816*** (0.067)
factor(q_popdensity)4	−0.976*** (0.071)
factor(q_popdensity)5	−0.723*** (0.086)
scale(poverty)	0.028 (0.020)
scale(log(medianhousevalue))	0.025 (0.036)
scale(log(medhouseholdincome))	0.084** (0.035)
scale(pct_owner_occ)	−0.005 (0.022)
scale(education)	0.051** (0.026)
scale(pct_blk)	0.309*** (0.026)
scale(hispanic)	0.044* (0.027)
scale(older_pecent)	−0.039 (0.029)
scale(prime_pecent)	−0.308*** (0.024)
scale(mid_pecent)	−0.058** (0.024)
scale(date_since_social)	0.402*** (0.121)
scale(date_since)	−0.106*** (0.020)
scale(beds/population)	0.008 (0.017)
scale(obese)	−0.075*** (0.021)
scale(smoke)	−0.002 (0.036)
scale(mean_summer_temp)	0.101** (0.050)
scale(mean_winter_temp)	−0.117 (0.078)
scale(mean_summer_rm)	−0.101* (0.056)
scale(mean_winter_rm)	−0.044 (0.034)
Constant	−9.246*** (0.177)
Observations	3,089
R^2	0.422
Adjusted R^2	0.408
Residual Std. Error	0.849 (df = 3017)
F Statistic	30.995*** (df = 71; 3017)
Note:	*p<0.1; **p<0.05; ***p<0.01
Note: state variables exluded for space considerations	

Tables 1 and 2: Wu et al.'s Negative Binomial "Main Model" vs. the OLS reworking: "OLS Main Model"
*State covariates are excluded from all tables for space considerations.
**Of note, treatment covariates mean_pm25 and mean.pm25 are equivalent.

The regression results returned from the author's negative binomial, mixed model are expressed in Table 1 with the Wu et al. Main Model returning a value of 10.74% (p<0.01) increase in the COVID-19 mortality rate for every 1 ug/m^3 increase in the long term average $PM_{2.5}$, similar to the result reported by Wu et al. Importantly this metric was not calculated with

an associated E-value. Also of note, upon running the Wu et al. Main Model, R generated a return message “[m]odel is nearly unidentifiable” indicating that the result is barely identified and therefore unreliable. Of note, state variables are excluded from all tables for space considerations and the long term exposure to $PM_{2.5}$ is expressed as *mean.pm25*. Interestingly, the results returned from the OLS reworking of the Wu et al. Main Model displayed in Table 2 resulted in the estimation of a significantly lower treatment effect : a 1 ug/m^3 increase in the long term exposure to $PM_{2.5}$ is associated with a statistically significant 7.16% ($p<0.01$) increase in COVID-19 mortality, expressed as mean.pm25

The treatment model results expressed in Table 3 indicate that the pre-treatment, racial demographic covariate *percent black* is strongly predictive of long term exposure to $PM_{2.5}$: a one percent increase in Black residents is associated with a 0.21 ug/m^3 ($p<0.01$) increase in the long term exposure to $PM_{2.5}$. Additionally, this covariate is also strongly predictive of the outcome, COVID-19 mortality, for every 1 ug/m^3 increase in the long term average $PM_{2.5}$ there is a 36.2% increase in the COVID-19 mortality rate ($p<0.01$) making it an unfortunately useful benchmark for bounding the plausibility of any unmeasured confounding.

Table 3: Treatment Model, OLS Reworking of Wu et. al Main Model

	Dependent variable:
	mean.pm25
factor(q_popdensity)2	0.620^{***} (0.064)
factor(q_popdensity)3	0.895^{***} (0.068)
factor(q_popdensity)4	1.178^{***} (0.072)
factor(q_popdensity)5	1.988^{***} (0.083)
scale(poverty)	-0.015 (0.021)
scale(log(medianhousevalue))	0.093^{**} (0.037)
scale(log(medhouseholdincome))	0.074^{**} (0.037)
scale(pct_owner_occ)	-0.090^{***} (0.023)
scale(education)	0.164^{***} (0.027)
scale(pct_blk)	0.205^{***} (0.027)
scale(hispanic)	0.026 (0.028)
scale(older_pecent)	-0.007 (0.031)
scale(prime_pecent)	0.075^{***} (0.025)
scale(mid_pecent)	0.041 (0.025)
scale(date_since_social)	1.820^{***} (0.122)
scale(date_since)	0.095^{***} (0.021)
scale(beds/population)	-0.032^{*} (0.017)
scale(obese)	0.039^{*} (0.022)
scale(smoke)	-0.075^{**} (0.037)
scale(mean_summer_temp)	0.817^{***} (0.051)
scale(mean_winter_temp)	-0.148^{*} (0.082)
scale(mean_summer_rm)	0.377^{***} (0.058)
scale(mean_winter_rm)	-0.215^{***} (0.036)
Constant	8.201^{***} (0.109)
Observations	3,089
R^2	0.878
Adjusted R^2	0.875
Residual Std. Error	0.890 (df = 3018)
F Statistic	310.456^{***} (df = 70; 3018)
Note:	*p<0.1; **p<0.05; ***p<0.01

Table 3: OLS Treatment Model

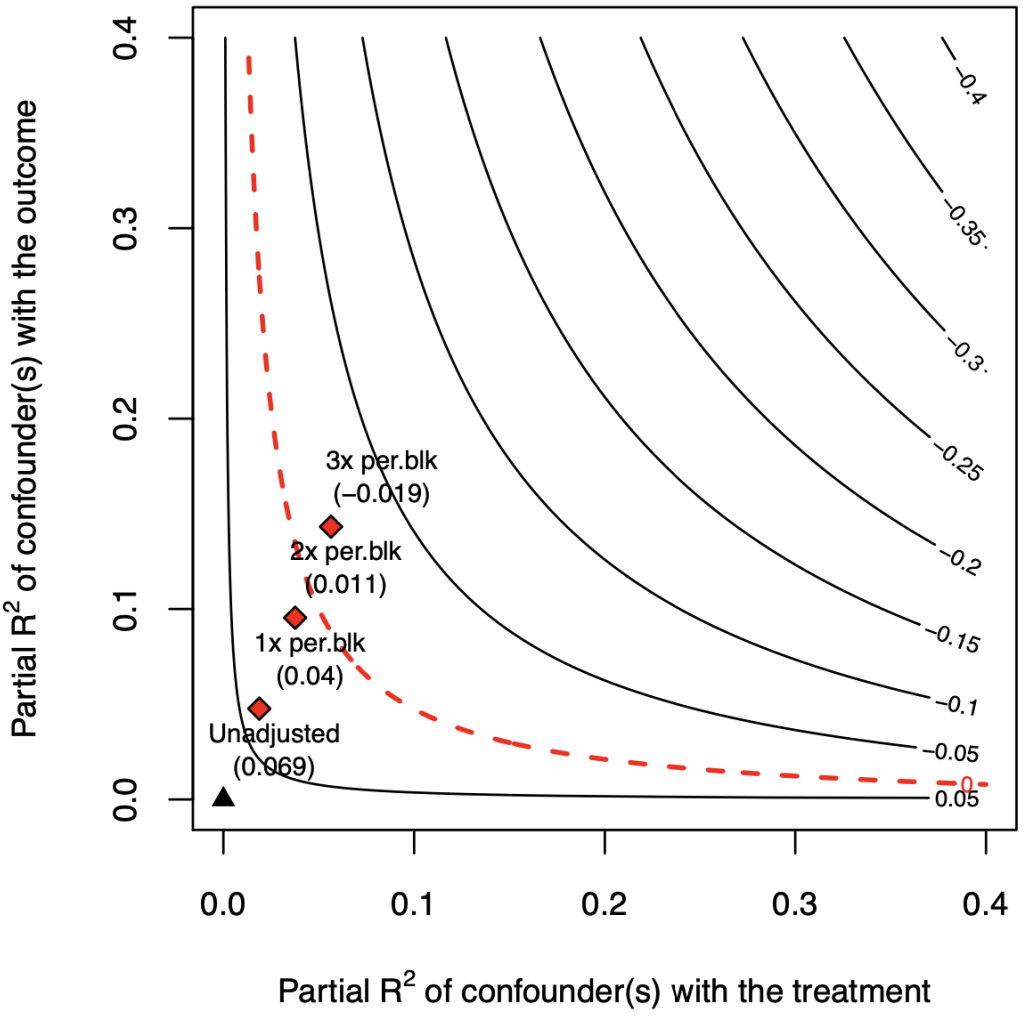

Outcome: *log(deaths + 1/ population)*

Treatment:	Est.	S.E.	t-value	$R^2_{Y\sim D\|\mathbf{X}}$	$RV_{q=1}$	$RV_{q=1,\alpha=0.05}$
mean.pm25	0.069	0.017	3.985	0.5%	7%	3.6%
df = 3017		*Bound (1x per.blk)*: $R^2_{Y\sim Z\|\mathbf{X},D}$ = 4.8%, $R^2_{D\sim Z\|\mathbf{X}}$ = 1.9%				

Table A and Plot A$_i$: Sensitivity of OLS Main Model treatment effect to confounding w/ influential, pre-treatment covariate *percent Black residents* (per.blk) bound.

Using works on sensitivity analysis by Hazlett (2021) and Cinelli and Hazlett (2020) for reference, the partial R^2 and robustness values expressed in Table A show that the OLS Main Model treatment effect estimate for the long term exposure to $PM_{2.5}$ is very fragile to

unobserved confounding. Robustness values close to 1 would describe a treatment effect estimate that is robust to strong unobserved confounding while values close to zero would indicate that even weak confounding could eliminate the treatment effect estimate (Cinelli and Hazlett, 2020). The Robustness Value ($RV_{q=1}$) that would move the OLS Main Model treatment effect estimate to zero is 7.0% (Table A), indicating that if an unobserved confounder, or group of confounders, existed that could explain just 7% of the residual variance in *both* the treatment and the outcome, they would explain away the entire estimated treatment effect. One would then conclude that, if such a confounder, or group of confounders, existed, the observed treatment effect estimate is entirely attributable to bias (Hazlett and Parente, 2020).

A confounder of this strength, however, isn't necessary to undermine the relevancy of the observed treatment effect estimate. The $RV_{q=1,\alpha=0.05}$ value of 3.6% (Table A) tests the null hypothesis that *mean.pm25* is zero. It describes the strength of confounding that would be necessary to reduce the estimated effect to the boundary of statistical significance at the $\alpha = 0.05$ level. While considering the possible existence of an unobserved confounder, or group of confounders, in this study that account for 7% of the residual variation in the treatment and outcome may prove a daunting task, considering confounding that explains only 3.6% of this variation is likely achievable. For example, the existence of a prominent co-pollutant, such as ozone, with health ramifications for pulmonary health (American Lung Association, 2020), may be able to account for this much unobserved confounding. Finally, the partial R^2 value, $R^2_{Y\sim D|X}$, describes an "extreme scenario" where the treatment variable explains only 0.5% (Table A) of the residual variation in the outcome variable after accounting for the other model covariates. This means that if unobserved confounding can explain 100% of the residual variation in COVID-19 mortality, it would have to also only explain 0.5% of the residual variation in the long term exposure to $PM_{2.5}$ in order to wipe out the estimated treatment effect. Though all

three measurements can be taken into account in order to consider the reliability of the treatment effect estimate, the $RV_{q=1,\alpha=0.05}$ value of 3.6% shows that the OLS re-estimation of the Wu et al. (2020) treatment effect is indeed fragile to the level of confounding required to render the study findings not sufficiently significant to publish.

In addition to the partial R^2 and robustness values, accompanying plots help to visualize the relationship between the strength of a hypothetical confounder and a known, influential covariate. The fraction of residual variation in the treatment that is explained by hypothetical confounding can be found on the horizontal axis while the fraction of residual variation in the outcome that is explained by hypothetical confounding can be found on the vertical axis (Cinelli and Hazlett, 2020).

The points in Plot A_i represent the bounds on the partial R^2 of the hypothetical confounder if it were 1, 2 or 3 times as strong as the observed covariate *percent Black residents*. The contour lines show the range of possible adjusted treatment effect estimates in the presence of confounders of varying strengths if they had been instead expressed as model covariates in a hypothetical, “ideal model” (Cinelli and Hazlett, 2020). The red, dashed contour line indicates where such a confounder would be able to reduce the treatment effect to zero (Cinelli and Hazlett, 2020). The 1 x *per.blk* bound shows the worst confounding that can exist if the model assumption was that confounding is no worse than the benchmark covariate *percent Black residents* in predicting treatment ($R^2_{D\sim Z|X}$:1.9%) and no worse than *percent Black residents* in predicting the outcome ($R^2_{Y\sim ZX|D}$: 4.8%). If such a confounder did exist, then Plot A_i reveals that the OLS Main Model treatment effect estimate would be robust to confounding, however, it would be reduced by over 40%. A confounder twice as strong would nearly eliminate

the treatment effect estimate and one three times as strong would change the sign of the estimate.

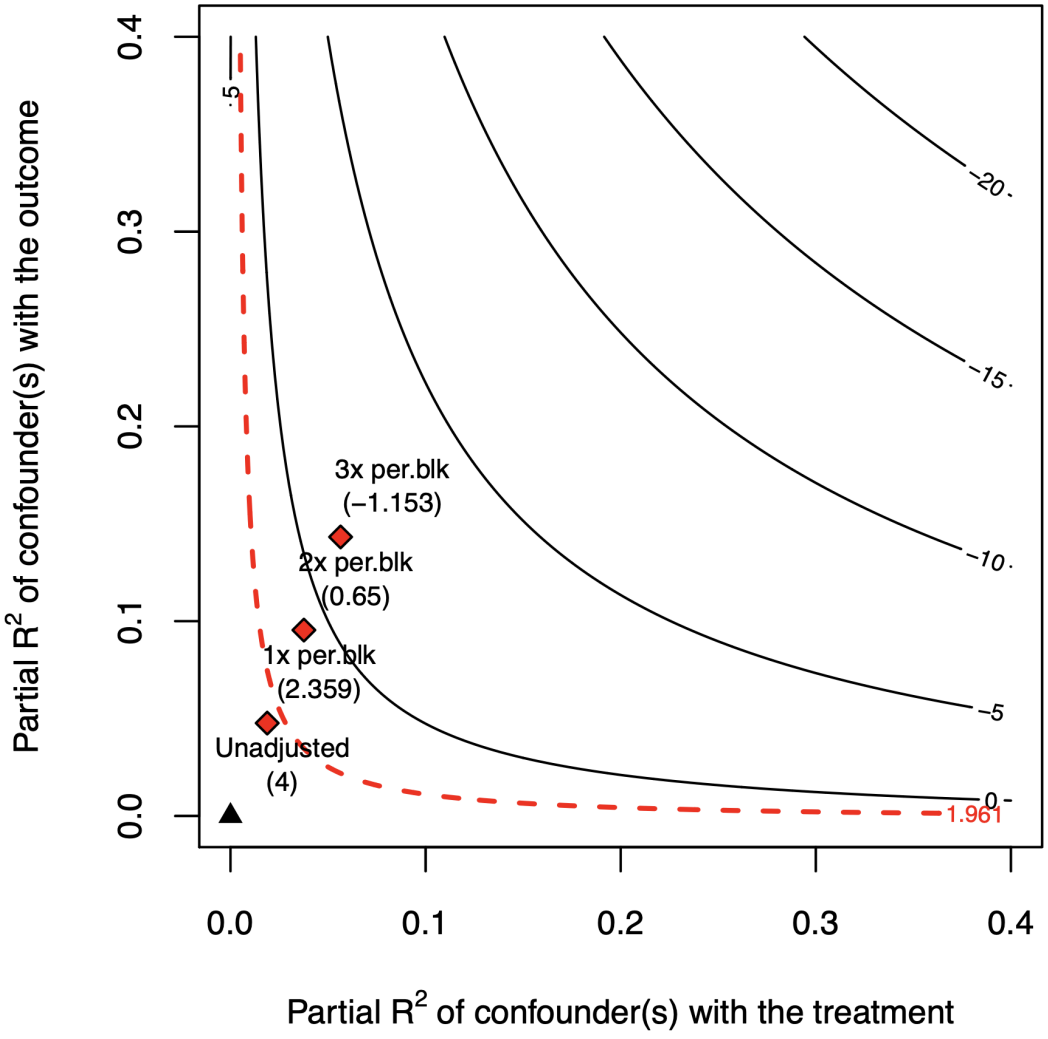

Plot A_{ii}: Sensitivity of OLS Main Model t-value of the treatment effect to confounding w/ influential, pre-treatment covariate *percent Black residents* (per.blk) bound.

With reference to Plot A_{ii}, the sensitivity of the t-value of the treatment effect estimate comes into view. With the red dashed contour now referring to a t-value of approximately 1.96, typically used for standard inferential statistics, it is clear that it would take an unobserved confounder twice as strong as the benchmark covariate *percent Black residents* to move the

treatment effect beyond the boundary of statistical significance. However, unobserved confounding as strong as *percent Black residents* brings it precariously close.

Moving on to the model inclusive of ozone expressed as covariate in an effort to bolster the treatment effect estimate against confounding, the sample used for modeling was necessarily reduced in size due to limitations in continuously monitored ozone data. The shift in the population density between the original sample used by Wu et.al with over 3000 county-level observations and the ozone subset sample with approximately 790 county level observations, is visualized in Population Density plot (Plot 1). The mean log of the population from the original sample to the ozone subset shifts from 11.6 to 10.3 indicating that the ozone subset is skewed towards more populous counties.

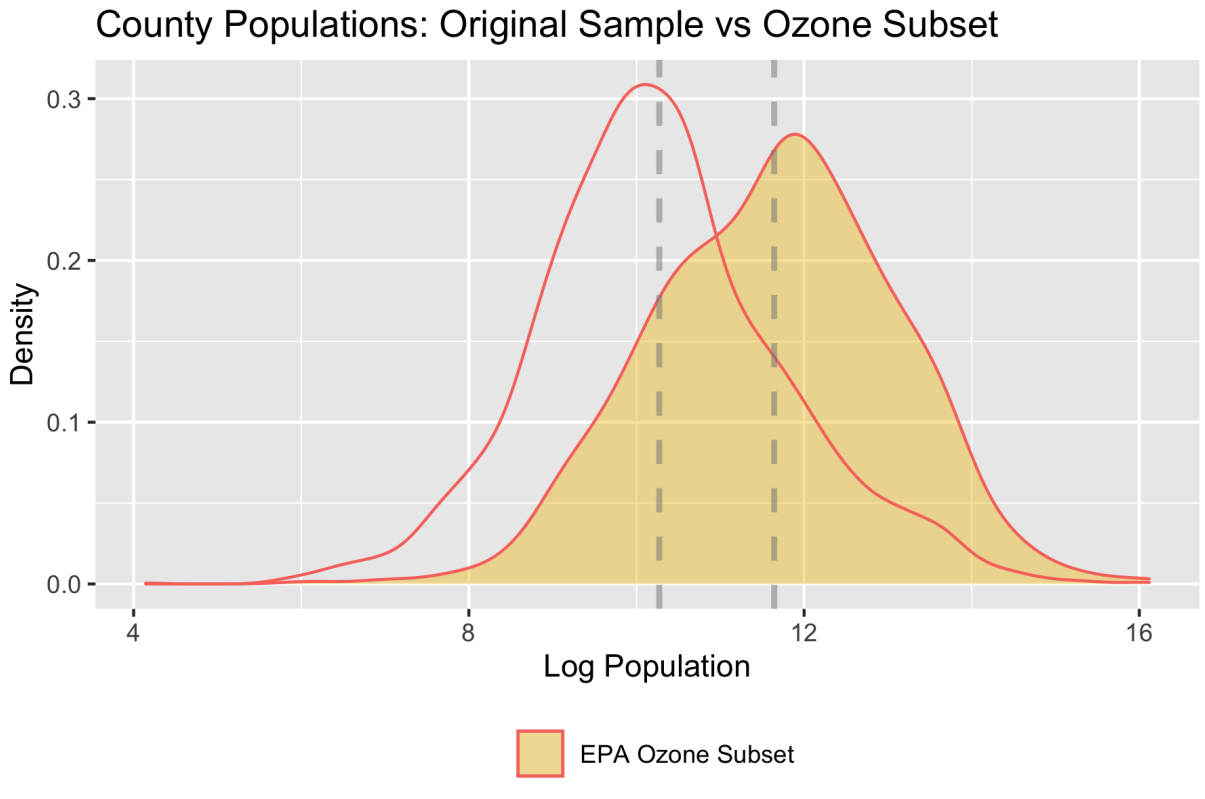

Plot 1: Original sample vs. Ozone subset. More populous counties are monitored by the EPA for ozone.

Table 4: OLS Model with Ozone ppb

	Dependent variable:
	log(deaths+1/population)
mean.pm25	0.134^{***} (0.032)
ozoneppb	-0.027^{**} (0.012)
factor(q_popdensity)2	-0.689^{***} (0.182)
factor(q_popdensity)3	-0.891^{***} (0.181)
factor(q_popdensity)4	-1.046^{***} (0.184)
factor(q_popdensity)5	-0.792^{***} (0.196)
scale(poverty)	0.052 (0.043)
scale(log(medianhousevalue))	0.215^{**} (0.089)
scale(log(medhouseholdincome))	0.270^{***} (0.084)
scale(pct_owner_occ)	0.120^{**} (0.053)
scale(education)	0.208^{***} (0.055)
scale(pct_blk)	0.412^{***} (0.052)
scale(hispanic)	0.103^{*} (0.062)
scale(older_pecent)	0.006 (0.070)
scale(prime_pecent)	-0.289^{***} (0.081)
scale(mid_pecent)	-0.107 (0.071)
scale(date_since_social)	0.160 (0.188)
scale(date_since)	-0.052 (0.040)
scale(beds/population)	0.025 (0.034)
scale(obese)	-0.111^{**} (0.052)
scale(smoke)	0.082 (0.077)
scale(mean_summer_temp)	0.145 (0.099)
scale(mean_winter_temp)	-0.362^{**} (0.172)
scale(mean_summer_rm)	-0.049 (0.132)
scale(mean_winter_rm)	-0.124^{*} (0.070)
Constant	-8.945^{***} (0.600)
Observations	788
R^2	0.576
Adjusted R^2	0.533
Residual Std. Error	0.836 (df = 715)
F Statistic	13.468^{***} (df = 72; 715)
Note:	*p<0.1; **p<0.05; ***p<0.01

Table 4: Ozone subset OLS Model

Table 5: OLS Treatment Model, w/ Ozone ppb

	Dependent variable:
	mean.pm25
ozoneppb	0.079^{***} (0.014)
factor(q_popdensity)2	0.464^{**} (0.212)
factor(q_popdensity)3	0.747^{***} (0.210)
factor(q_popdensity)4	1.085^{***} (0.212)
factor(q_popdensity)5	1.676^{***} (0.222)
scale(poverty)	−0.012 (0.050)
scale(log(medianhousevalue))	−0.065 (0.104)
scale(log(medhouseholdincome))	0.377^{***} (0.098)
scale(pct_owner_occ)	-0.268^{***} (0.061)
scale(education)	0.267^{***} (0.063)
scale(pct_blk)	0.234^{***} (0.061)
scale(hispanic)	0.106 (0.073)
scale(older_pecent)	0.009 (0.082)
scale(prime_pecent)	−0.062 (0.095)
scale(mid_pecent)	-0.198^{**} (0.083)
scale(date_since_social)	1.865^{***} (0.210)
scale(date_since)	0.116^{**} (0.047)
scale(beds/population)	−0.024 (0.040)
scale(obese)	0.063 (0.061)
scale(smoke)	−0.021 (0.090)
scale(mean_summer_temp)	0.354^{***} (0.115)
scale(mean_winter_temp)	0.048 (0.202)
scale(mean_summer_rm)	0.347^{**} (0.154)
scale(mean_winter_rm)	-0.431^{***} (0.081)
Constant	5.565^{***} (0.672)
Observations	788
R^2	0.873
Adjusted R^2	0.860
Residual Std. Error	0.980 (df = 716)
F Statistic	69.226^{***} (df = 71; 716)
Note:	*p<0.1; **p<0.05; ***p<0.01

Table 5 Ozone subset OLS Treatment Model

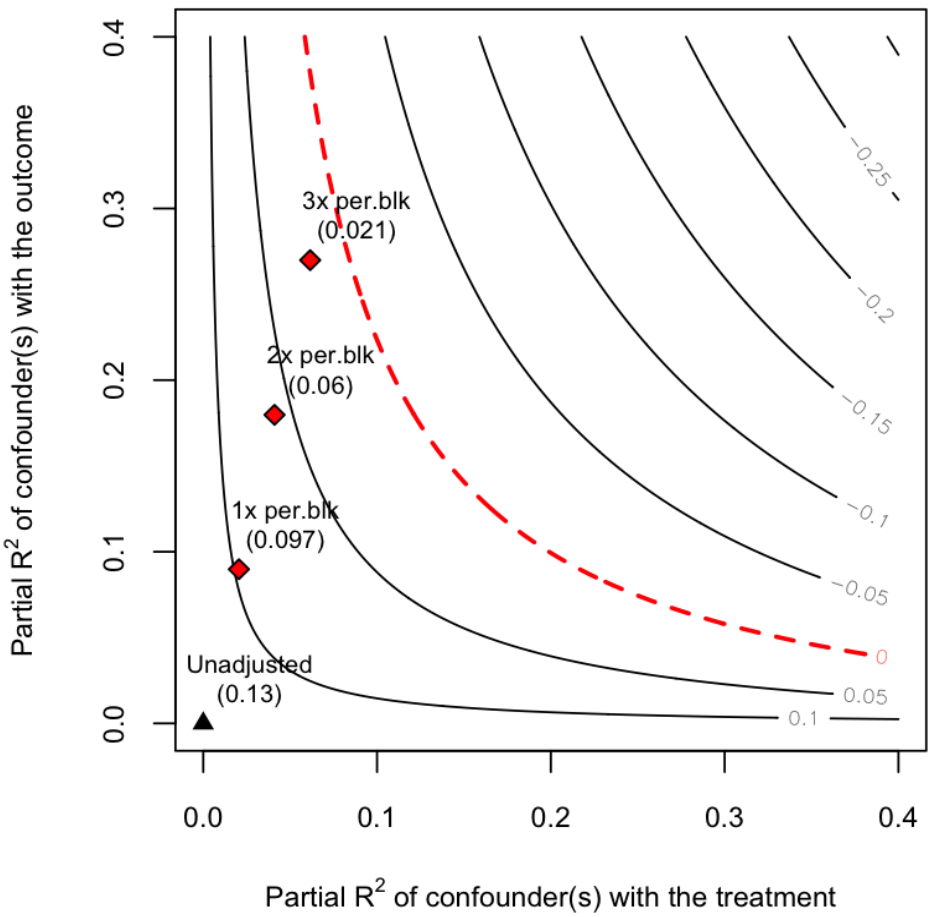

Outcome: *log(deaths + 1/ population)*

Treatment:	Est.	S.E.	t-value	$R^2_{Y\sim D\|\mathbf{X}}$	$RV_{q=1}$	$RV_{q=1,\alpha=0.05}$
mean.pm25	0.134	0.032	4.213	2.4%	14.6%	8.1%
df = 715		*Bound (1x per.blk):* $R^2_{Y\sim Z\|\mathbf{X},D}$ = 9%, $R^2_{D\sim Z\|\mathbf{X}}$ = 2.1%				

Table B and Plot B_i: Sensitivity of the Ozone Subset to confounding no worse than the benchmark covariate *percent Black residents* (*per.blk*).

The OLS Results in the ozone inclusive model presented in Table 4 and Table B shows that the inclusion of ozone in the model both bolstered the treatment effect and reduced its sensitivity to confounding: a 1 ug/m^3 increase in the long term average $PM_{2.5}$ is associated with a statistically significant 14.37% (p<0.00) increase in in COVID-19 mortality, almost double the OLS estimate in the model without ozone (7.16%; p<0.01) and approximately three percent

higher than the estimate derived from Wu et al.'s (2020) original model. The partial R^2 values in Table B $R^2_{Y\sim D|X}$, $RV_{q=1}$, $R^2_{q=1\ ,\ \alpha=0.05}$ all indicate an increase (1.9, 7.6, 4.5%, respectively) in the strength of confounding necessary to reduce the estimate to zero ($R^2_{Y\sim D|X}$: 2.4%, $RV_{q=1}$: 14.6%), or to the boundary of statistical significance ($R^2_{q=1\ ,\ \alpha=0.05}$: 8.1%).

The *percent Black residents* bound, expressed as *per.blk*, in Table B was selected from our OLS Treatment Model with ozone as a strong predictor of treatment (Table 5) and outcome (Table 4). The *per.blk* bound is visualized in Plot B_i and shows the worst confounding that can exist if the model assumption is that confounding is no worse than 1, 2, and 3 times the benchmark covariate *percent Black residents* in predicting treatment ($R^2_{D\sim Z|X}$:2.1%) and outcome ($R^2_{Y\sim ZX|D}$: 9%). Plot B_i reveals that in the ozone inclusive model, the treatment effect estimate is much more robust to confounding. In this model, an unobserved confounder, or group of confounders, that are three times as strong as the benchmark covariate *percent Black residents* are still not strong enough to move the treatment effect estimate to zero. Plot B_{ii} reveals, however, that it would take unobserved confounding twice as strong as the benchmark covariate *percent Black residents* to move the treatment effect just inside of the boundary of statistical significance. Though the ozone subset OLS model does bolster the treatment effect estimate against confounding, both tables indicate there is room to explore other sources of confounding, such as spatial effects, or the differential effects of place, in order to improve the model's explanatory power.

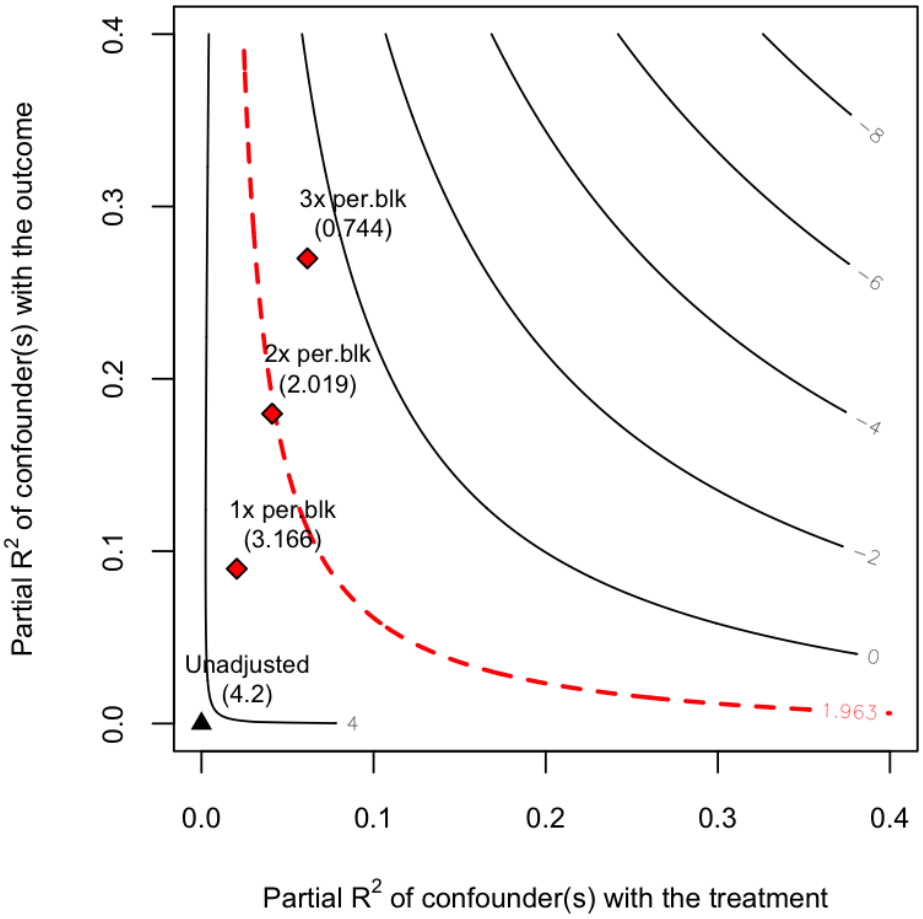

Plot B_{ii}: Sensitivity of OLS Ozone Model t-value of the treatment effect to confounding w/ influential, pre-treatment covariate *percent Black residents*(per.blk) bound.

Unexpectedly, Table 4 also shows us that ozone returned a negative relationship with COVID-19 mortality: a one part per billion increase in ozone exposure is associated with a 2.7% decrease ($p<0.05$) in COVID-19 mortality. In order to visualize this unexpected result, ozone ppb was plotted against the COVID-19 mortality rate (Plot 2) and a weakly negative association between ozone and Covid-19 mortality is revealed. In response, the potential correlation between $PM_{2.5}$ and ozone was further examined with the plot "Correlation Between $PM_{2.5}$ and Ozone" (Plot 3, see appendix) and its associated Pearson Correlation Coefficients of $R = -0.073$ [95% CI: -0.142, -0.003], p-value(0.04) confirming a very weakly negative correlation between the two pollutants. This is surprising given the co-occurrences of ozone and

$PM_{2.5}$ as well as ozone's influence over secondary particle formation and may speak to differences in the temporal and spatial resolution of the monitoring of the two pollutants. This unexpected result opens the door to further investigation of the potentially confounding effects of space and place on the long term exposure to $PM_{2.5}$ and COVID-19 mortality.

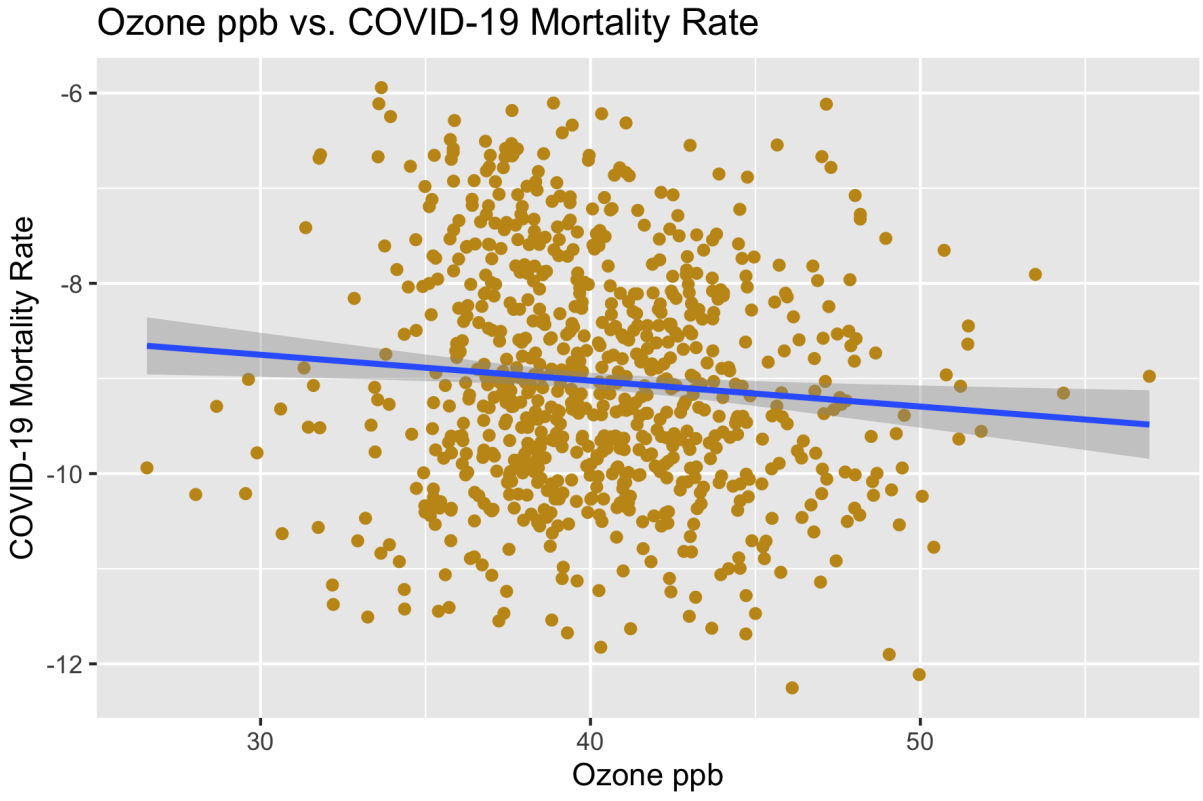

Plot 2: Ozone ppb vs. COVID-19 Mortality Rate

5.2 ESDA: Visualizing Treatment, Outcome, and Main Model OLS Residual Distribution

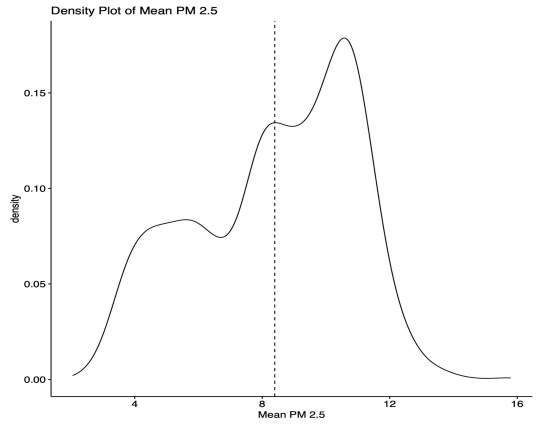

Plot 4a: Density Distribution of Mean $PM_{2.5}$ values

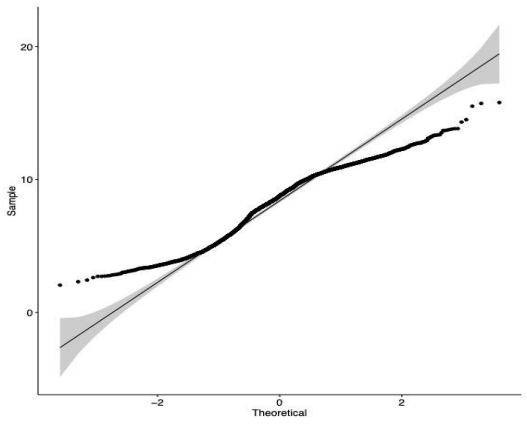

Plot 4b: Q-Q plot of the distribution of observed $PM_{2.5}$ values vs a normal distribution

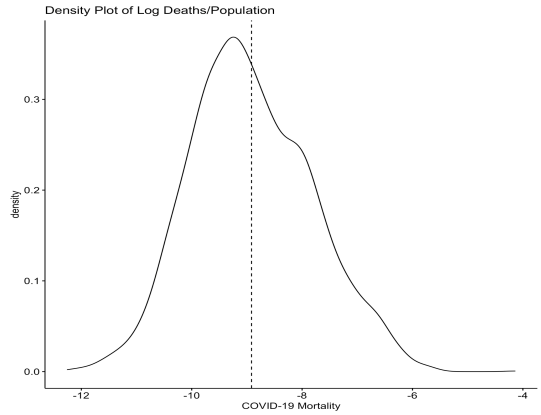

Plot 4c: Density Distribution of COVID-19 mortality values

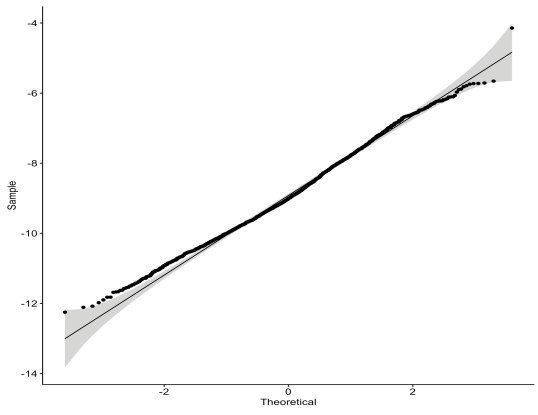

Plot 4d: Q-Q plot of the distribution of observed COVID-19 mortality values vs a normal distribution

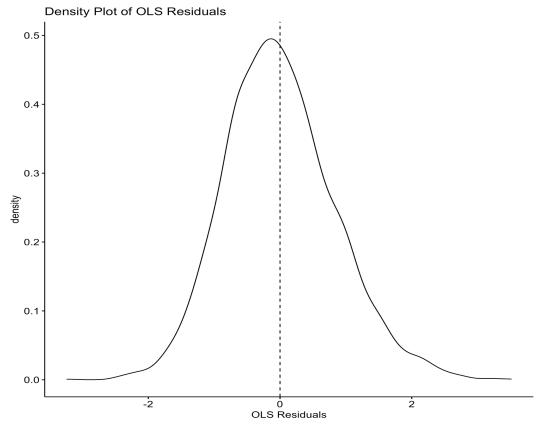

Plot 4e: Density Distribution of Main Model OLS residuals

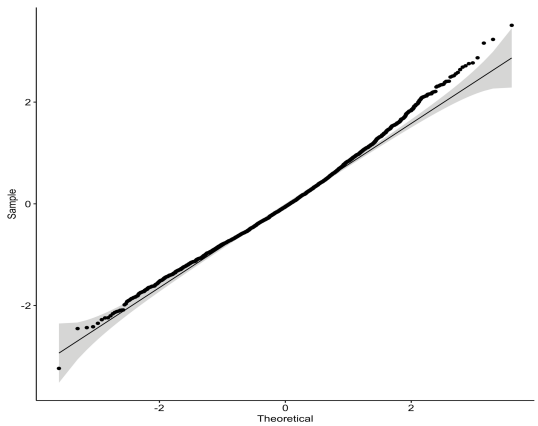

Plot 4f: Q-Q plot of the distribution of observed Main Model OLS residual values vs a normal distribution

Although the ozone inclusive model in Section 5.1 was able to strengthen the treatment effect estimate of long term exposure to $PM_{2.5}$ on COVID-19 mortality against confounding, the results beg further investigation as both models indicate room for explanatory improvement. Additionally, the negative influence of ozone on COVID-19 mortality suggests that there may be other limitations to modeling primarily populous counties or a misalignment between the scale of the grid cell, U.S. counties, and the scale at which the negative health effects of atmospheric ozone exposure occur, otherwise known as MAUP. Returning to the original sample and the model parameters contained within the OLS Main Model, ESDA methods were then deployed in order to uncover other potential sources for unmeasured confounding, such as spatial regimes in the treatment and outcome variables.

In order to begin the spatial sensitivity portion of the analysis, it is important to gain an initial sense of the distribution of the three OLS Main Model parameters of interest: long term exposure to $PM_{2.5}$, COVID-19 mortality and the OLS Main Model residuals. Plots 4a-4f characterize the probability distribution of the treatment variable, long term exposure to $PM_{2.5}$, the outcome variable, COVID-19 Mortality, and the Main Model OLS residuals and compare their distribution to a normal distribution with Density Distribution Plots and Quantile Quantile Plots, respectively. From Plot 4a, it is apparent that long term exposure to $PM_{2.5}$ has a somewhat left skewed distribution. This is likely due to a high number of East Coast and mid-Atlantic counties that are smaller in area and contain high long exposure to $PM_{2.5}$ values. Plot 4b indicates a deviation from a normal distribution at the lower and higher values of long exposure to $PM_{2.5}$ suggesting that there are more counties with lower long exposure to $PM_{2.5}$ values than would be expected in a normal distribution and there are less counties with a higher long exposure to $PM_{2.5}$ than would be expected in a normal distribution. Since industries and urban areas tend to be concentrated, for example, in areas of the Midwest, East and West

Coasts, one would not expect a normal distribution of long exposure to $PM_{2.5}$ values amongst U.S. counties.

In contrast to the distribution of the long term exposure to $PM_{2.5}$, COVID-19 mortality has a slightly right skewed distribution (Plot 4c). A similar logic can be applied to the outcome variable at this early stage in the COVID-19 pandemic, with the "cumulative number of deaths for each county up to and including June 18, 2020" (Wu et al., 2020, "Supplementary Materials"). There are more counties with low COVID-19 mortality rates and less counties with high COVID-19 mortality rates than would be expected in a normal distribution (Plot 4c). Plot 4d also reveals a similar trend aligning with the expectations of early pandemic mortality counts. Plot 4e gives the impression that the OLS residuals are approximately normally distributed (Plot 4e), however, the Q-Q Plot 4f shows that there are more positive sample values than would be expected. This entails slightly right skewed distribution in the OLS residuals indicating that the model may be biased, or underestimating parameters. Once the distribution of the important parameters is understood, the next step in ESDA methods is to geographically visualize the distribution of these values.

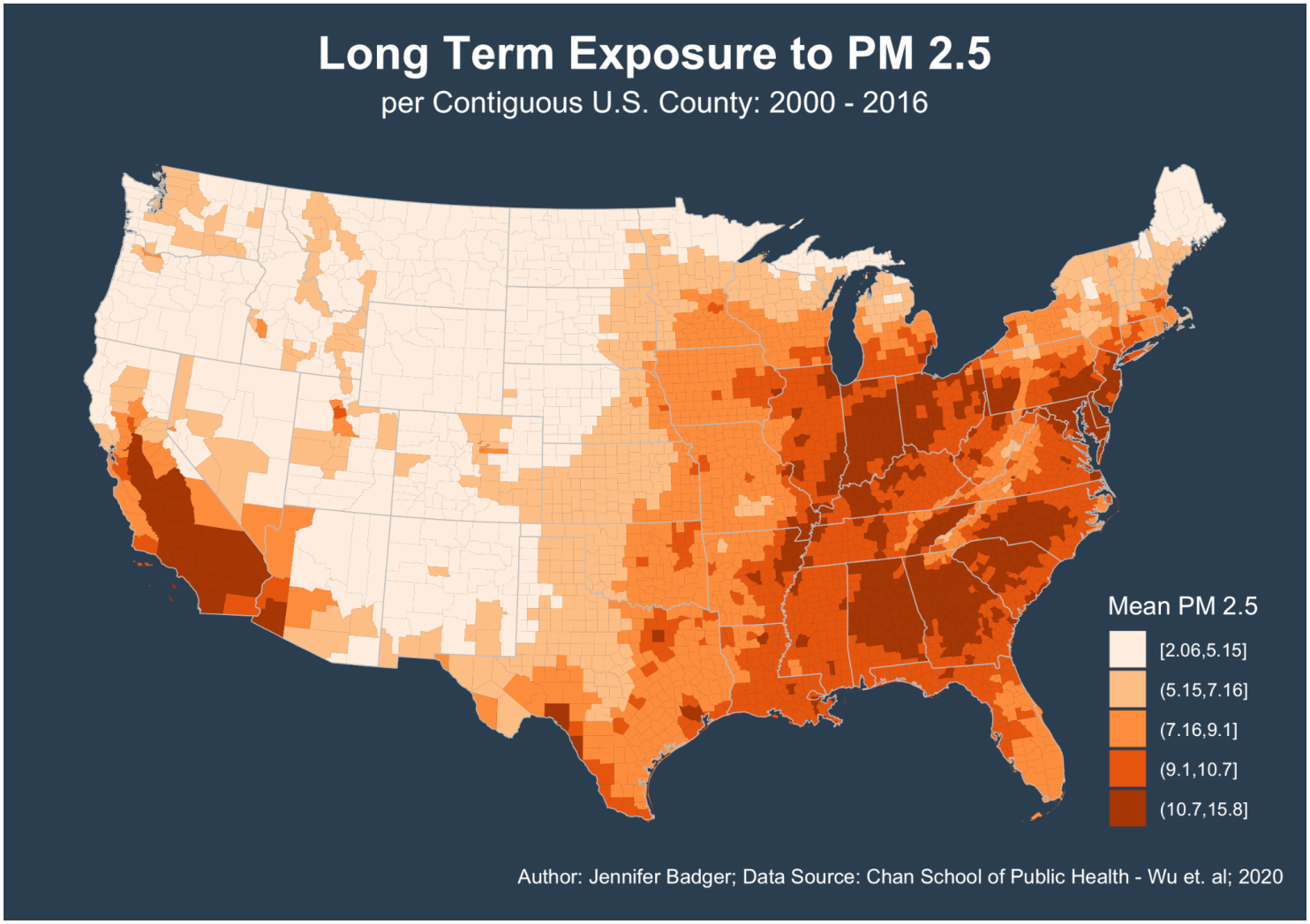

Plot 5a: Long term Exposure to $PM_{2.5}$ (Mean $PM_{2.5}$) Amongst U.S. Counties and D.C. in the Contiguous U.S.

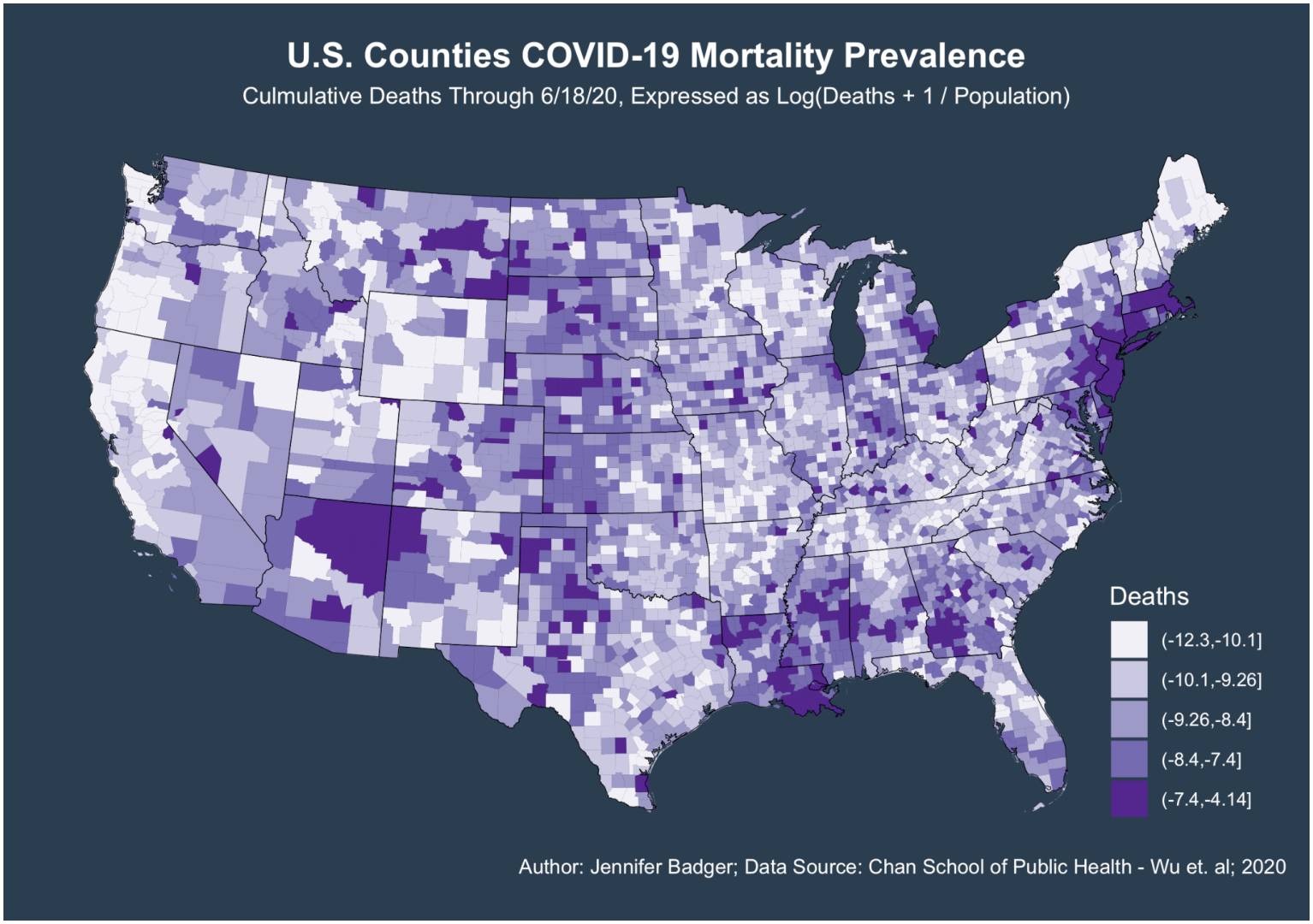

Plot 5b: COVID-19 Mortality Prevalence Amongst U.S. Counties and D.C.in the Contiguous U.S.

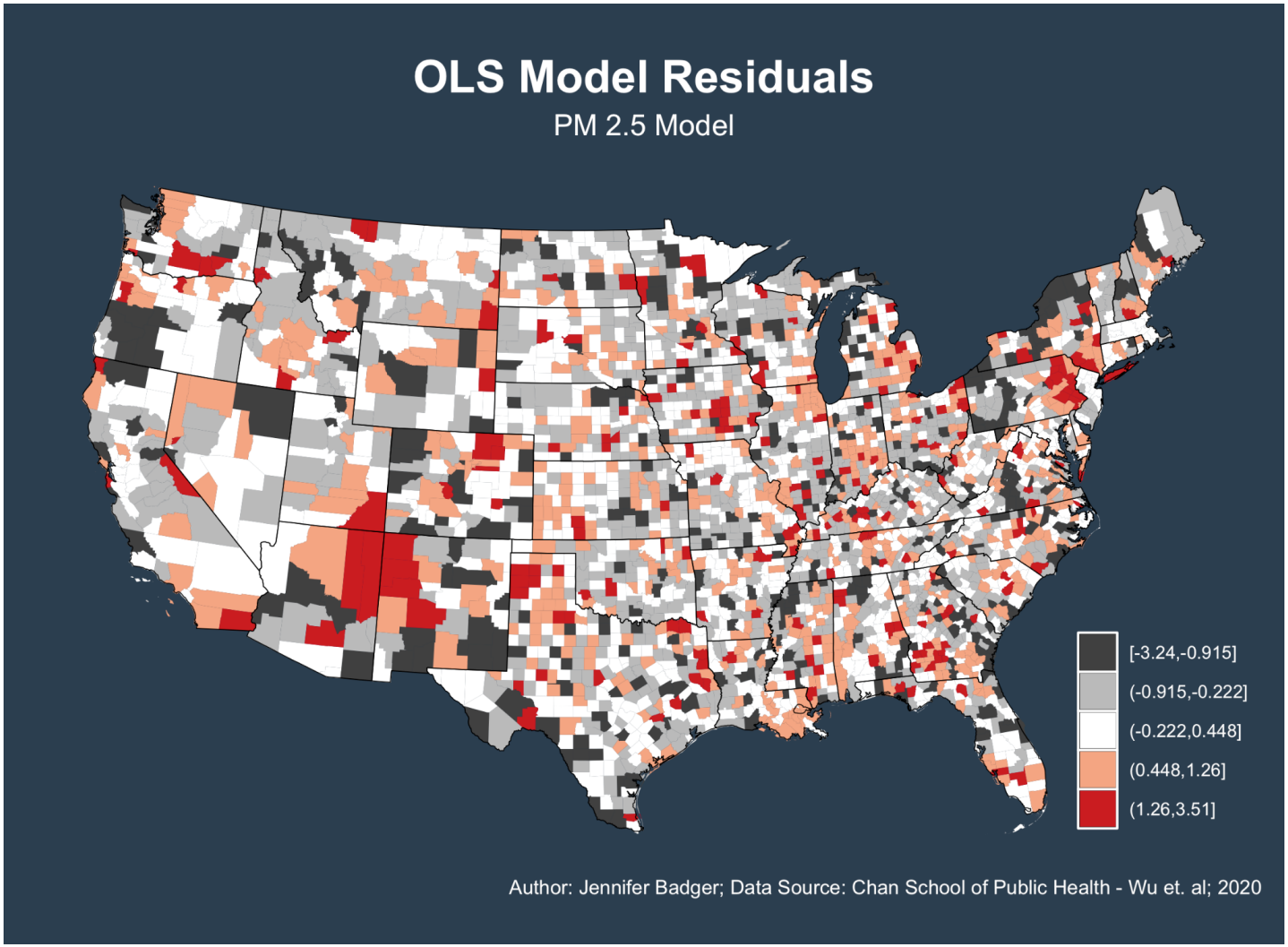

Plot 5c: OLS Main Model Residuals Amongst U.S. Counties and D.C. in the Contiguous U.S.

The geographic visualization of the treatment and outcome variables and residuals help to discern the diverse spatial patterns of these parameters across the contiguous U.S. The distribution maps of the long term exposure to $PM_{2.5}$ and COVID-19 mortality display varying degrees of spatial autocorrelation while the map of the OLS Main Model residuals suggests spatial randomness. Plot 5a shows strong patterns of spatial clustering of high long term exposure to $PM_{2.5}$ values with the highest values clustered in Southern California, the San Joaquin Valley, the southeastern portion of the Midwest Census Region, the eastern portion of the South Census Region, and the Northeast. With the exception of California, these high-high clusters cross state boundaries and occupy areas of the U.S. Census regions that generally track with populous areas (Plot 5d, see appendix) and areas of industry (Plot 5e, see appendix). Two areas of high-high clusters also track quite closely with the boundaries of the EPA Climatically Consistent Regions of the Ohio Valley and the Southeast suggesting that considering the influence of alternate definitions of place may relate regionally differential treatment effect estimates.

A more mild level of clustering of high and low COVID-19 Mortality values can be found throughout the contiguous U.S. in Plot 5b. Though less distinctive patterns emerge here than the clear patterns of clustering in county level $PM_{2.5}$ exposure values, there are some areas where COVID-19 mortality value trends transcend county borders. For instance, clustering of high values is evident in the state of Louisiana, along the shared border areas of NE Arizona and NW New Mexico, and along the urban, coastal areas of the Northeast Census Region. This somewhat tracks with expectations given the early stage of the pandemic in which the morality count was made (June 2020) and with NYC considered an early COVID-19 epicenter. Despite the exclusion of the five NYC boroughs, it is conceivable that there would be early COVID-19 spread along the very populous port cities of the Northeast coast. Additionally, Louisiana has one of the consistently highest poverty rates in the Nation (Roussel and Butkus, 2020), three

major port cities and a high percentage of Black residents (U.S. Census Bureau, 2021b). All of which could create the possibility for high COVID-19 Mortality rates early in the pandemic, before social distancing measures were enacted and before vaccines were available.

With regard to the OLS Main Model residuals, Plot 5c mainly shows a checkerboard pattern throughout most of the contiguous U.S. suggesting spatial randomness. Notably, some of the areas with higher COVID-19 mortality counts also have higher residual values indicating a further distance from the line of fit for these areas, e.g. Long Island, southern Louisiana, southeastern Michigan, Los Angeles County and a contiguous cluster of counties spanning the northeastern area of Arizona, southeastern area of Utah and western New Mexico. OLS residual clusters that are close to zero (white counties, (- 0.537, 0.812]) are found throughout the map, indicating that the line of fit closely matches the observed values for these particular counties. Though this range of OLS residual values is peppered throughout the map, it does not dominate the map therefore indicating that there is room for model improvement.

5.3 ESDA: Global Measures of Spatial Autocorrelation

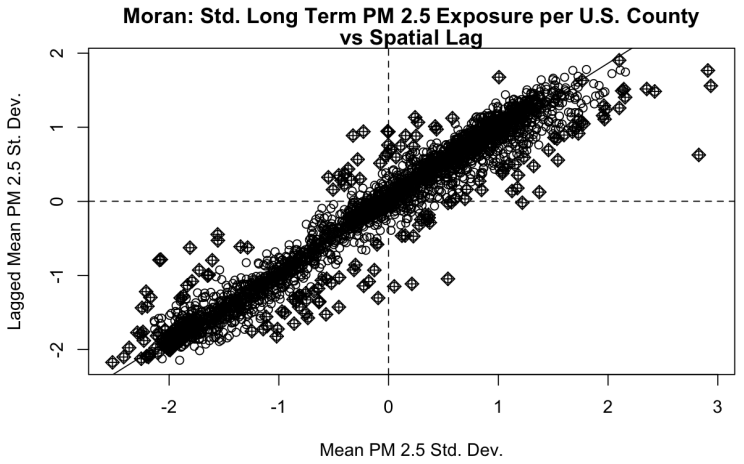

Plot 6a: Global Moran's I $PM_{2.5}$ (standardized).

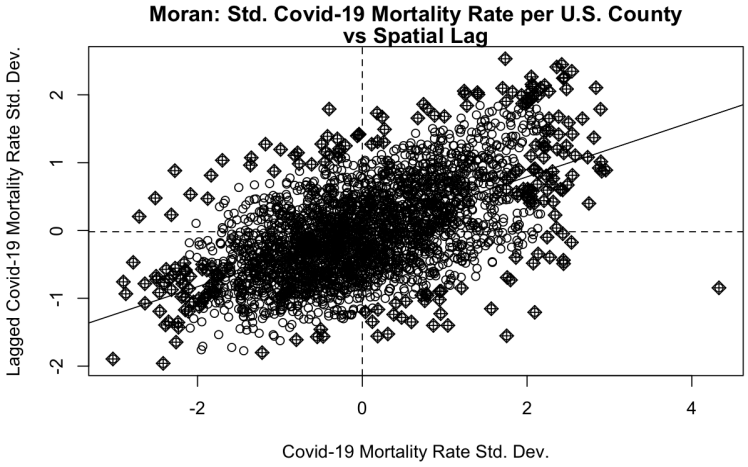

Plot 6b: Global Moran's I COVID-19 Mortality (standardized).

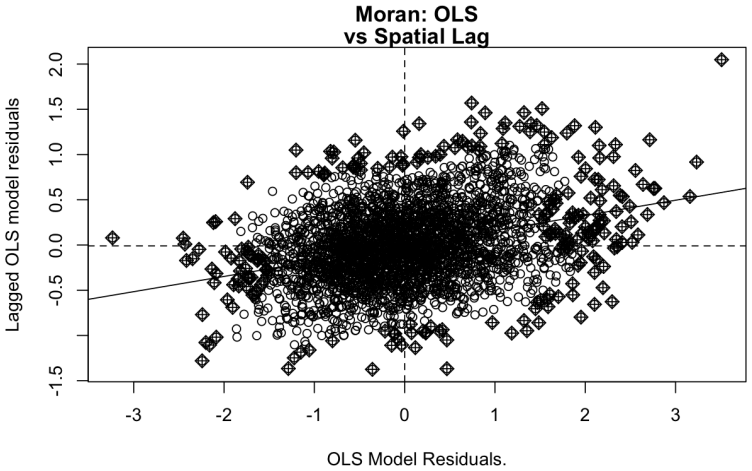

Plot 6c: Global Moran's I OLS Main Model Residuals.

While trends in the distribution of long term exposure to to $PM_{2.5}$, COVID-19 Mortality, and residuals can be visually inferred through maps, global Moran's I statistics and scatterplots can next be invoked in order to quantify or visualize the degree of clustering across the dataset. The Moran's I scatter plot is complementary to the global Moran's I statistic and can be used to determine "the extent to which the linear regression line reflects the overall pattern of association between W_y and y" (Anselin, 1996b, p. 116). While Moran's scatter plots cannot be used to assess the significance of the spatial association between the spatial lag and the variable of interest, a quantification of the degree of spatial dependence can be obtained with the Moran's I statistic.

	Moran I statistic	Expectation	Variance	p-value	z-stat
Mean PM 2.5	0.9312446	-0.0003226847	0.0001160140	2.2e-16	86.489
COVID-19 Mortality Rate	0.4053412	-0.0003226847	0.0001159889	2.2e-16	37.667
OLS Residuals	0.1685844	-0.0149008123	0.0001092906	2.2e-16	17.551

Table 6a: Global Moran's I for treatment, outcome and model residuals

In congruence with the informal map visualizations, similar patterns of spatial regimes are revealed in Table 6a and Plots 6a-6c. Table 6a and Plot 6a shows a strong, positive spatial autocorrelation between the standardized long term exposure to $PM_{2.5}$ and the weighted neighborhood average (spatial lag) as related by the global Moran's I value of 0.93 (p-value< 0.001) and the distribution of points in Moran's scatterplot. This is likely due to the transboundary nature of $PM_{2.5}$; i.e. the higher a given county's long term exposure to $PM_{2.5}$, the higher the neighborhood's long term exposure to $PM_{2.5}$ (upper right quadrant) and vice versa (lower right quadrant). Most observations are within two standard deviations of the mean. Diamonds indicate points with high influence measures. The three diamonds in the upper right quadrant represent observations with very high long term average values $PM_{2.5}$, almost three

standard deviations from the mean: Fresno (+2.8 st.dev), Los Angeles (+2.9 st. dev) and Orange (+2.9 st. dev) counties. From Plot 6a it is also evident that there are a few observations which represent spatial outliers, counties with high mean $PM_{2.5}$ surrounded by neighbors with low mean $PM_{2.5}$ (lower right quadrant) and vice versa (upper right quadrant).

This spatial relationship weakens as one moves to the outcome variable, COVID-19 mortality rate, in Table 5 (0.41, p-value< 0.001) and Plot 6b, yet still indicates some moderate spatial dependence with many more observations exhibiting negative spatial autocorrelation. A prominent spatial outlier and high influence measure can be found in the lower right quadrant of Plot 6b, which holds spatial outlier counties of high values surrounded by low values of COVID-19 Mortality. This spatial outlier represents the COVID-19 mortality rate in Loving County, Texas which bears the interesting distinction of the least populated county in the lower 48 and has been referred to as the “Last COVID-Free County” (Wallace, 2020). Digging further into the data reveals that this county has zero deaths at the time of the data accumulation. Its outlier status is then due to the addition of one death in relation to its very low population in the calculation of the outcome variable. Section 5.4 further shows that the Local Moran’s I estimate for this county, in terms of spatial outlier status, is statistically insignificant.

The OLS residuals show an even weaker yet statistically significant, positive spatial autocorrelation in Table 6a (0.17, p-value< 0.001) and Plot 6c with points more evenly spread across all quadrants. There are three prominent (+3 st. dev), high influence outliers in the upper right quadrant with the furthest from the (0,0) point representing McKinley County in NW New Mexico (3.5 st. dev). This county, once considered a COVID-19 hotspot, also became known as the first county in New Mexico to have 100% of its residents get vaccinated (Norwood, 2021). The high influence county approximating outlier status (- 3 st. dev) in the upper left quadrant represents Mesa County, Colorado. The Monte-Carlo simulation of Moran’s I found in Table 6b

(Appendix) shows that the observed Moran's I for the treatment, outcome and OLS Main Model Residuals, all rank higher than the 999 simulations (p-values: 0.001) for the null hypothesis of spatial randomness confirming that it is unlikely that the observed value for the Moran's I statistic has randomly occurred.

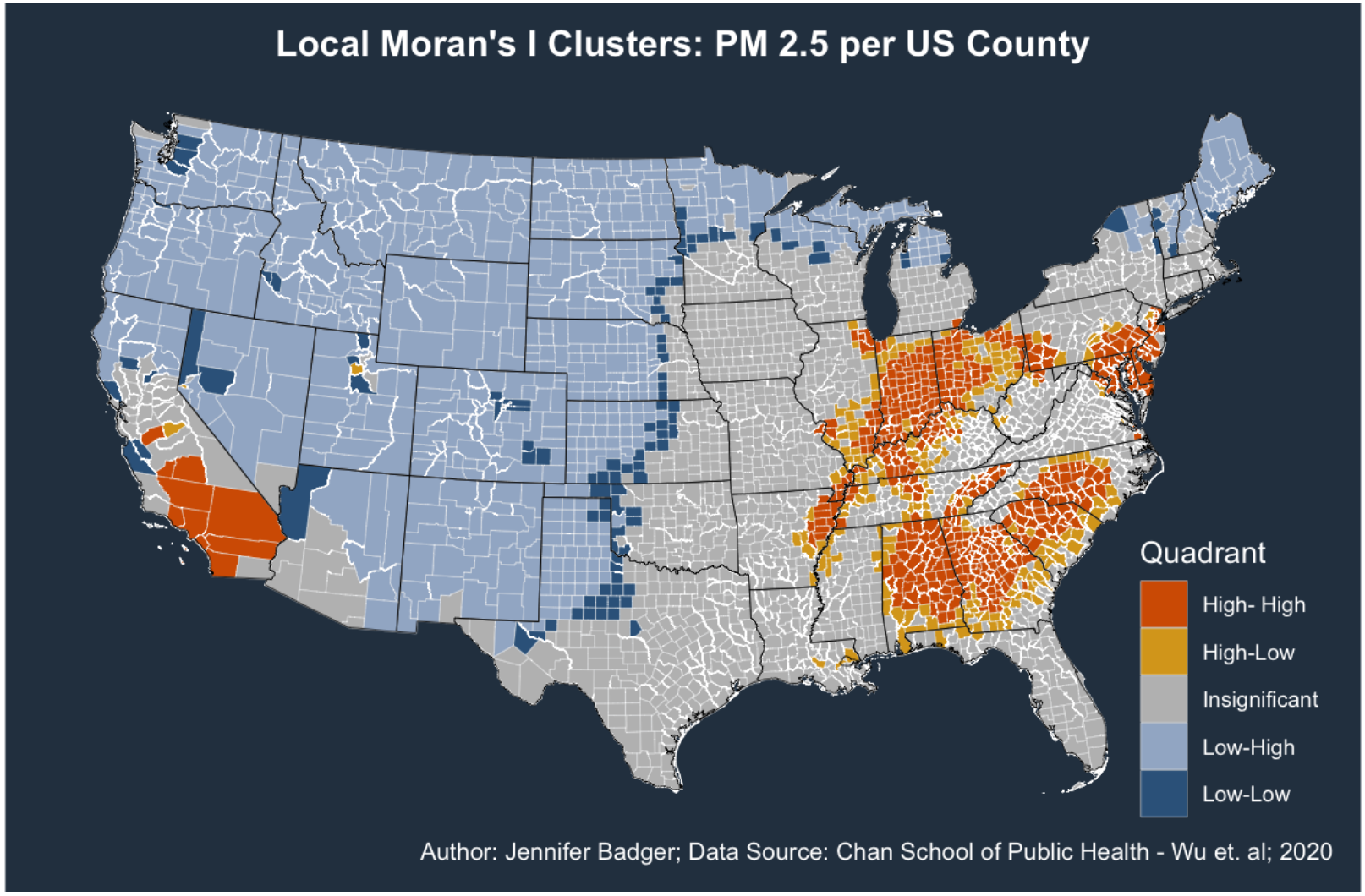

Plot 7a: Local Moran's I $PM_{2.5}$

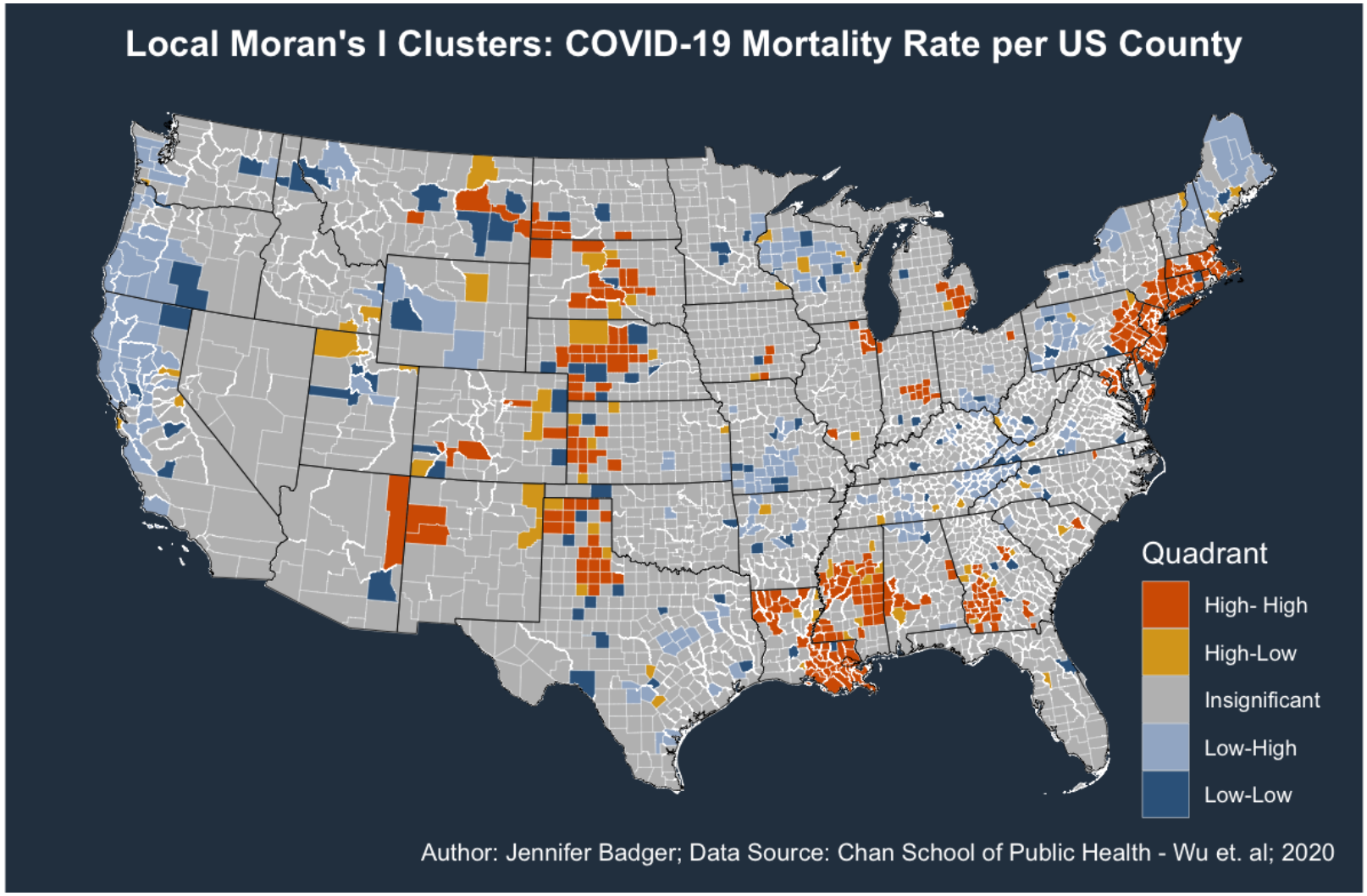

Plot 7b: Local Moran's I COVID-19 Mortality

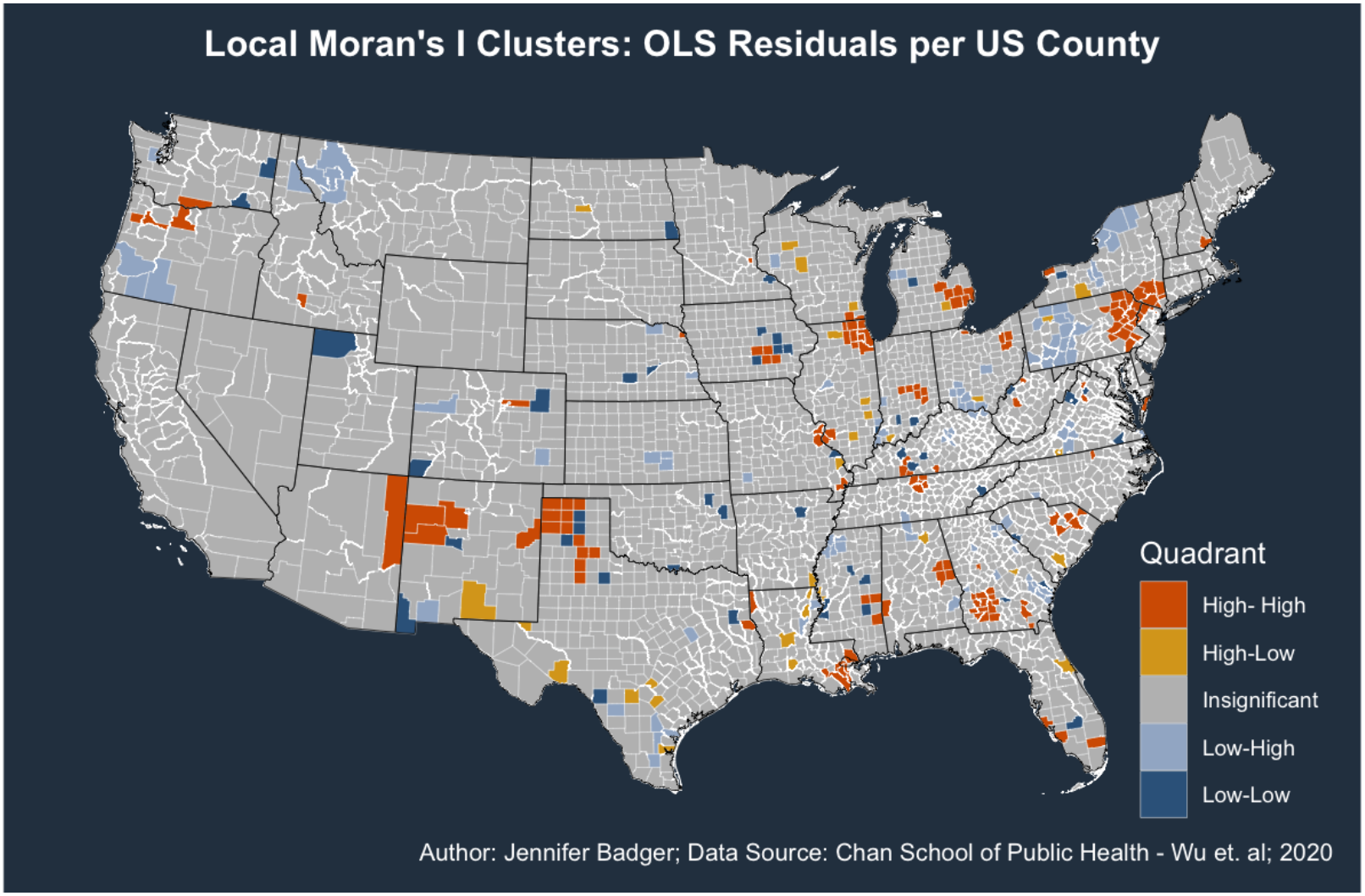

Plot 7c: Local Moran's I OLS Main Model Residuals

The Local Moran's I (LMI) output in Plots 7a-7b reveals statistically significant hotspots, coldspots, regional spatial regimes, as well as spatial outliers. Positive spatial autocorrelation hotspots, where high values are surrounded by high values, are symbolized in red-orange (High-High), and negative spatial autocorrelation coldpots, where low values are surrounded by low values, are symbolized in dark blue (Low-Low). The long term exposure to $PM_{2.5}$ LMI map (Plot 7a) shows the strongest evidence of clustering and clearly defined, differential spatial regimes among regions.

With reference to EPA Climatically Consistent Regions, Plot 7a shows large swaths of statistically significant High-High long term exposure to $PM_{2.5}$ hotspots in the Ohio Valley, the Southeast, and the southern portion of the Northeast. These regions, in addition to the High-High counties of California, track closely to the areas of high long term exposure to $PM_{2.5}$ detected in Plot 5a, and again track with population centers and areas of industry. In considering the treatment-outcome relationship, $PM_{2.5}$ hotspots track with COVID-19 Mortality hotspots among counties in a swath of the North Atlantic Coast known as the Megalopolis (Florida, 2019).

The Northeast Megalopolis extends from Northern Virginia to Southern New Hampshire and is bounded by major cities Boston and D.C. (U.S. Census Bureau, 2021a; Figure 11, see Appendix). It is characterized as an area with incredibly high population density (U.S. Census Bureau, 2021a) and is considered the world's largest megaregion, in terms of population and economic output (Florida, 2019). Given the transboundary nature of air pollution, the concentration of population and industry, the density of interstate transportation networks, and the early spread of COVID-19 in this area, the overlapping of treatment and outcome hotspots is likely evidence of spatial spillover, where long term exposure to $PM_{2.5}$ in a given county, results in a COVID-19 mortality in another. One could, for instance, imagine a scenario where a

resident of Trenton, New Jersey travels to Philadelphia for work and is exposed to a higher level of $PM_{2.5}$ while in Philadelphia, and potentially also COVID-19 while in this more populous place, but the associated COVID-19 mortality is attributed to their county of residence in New Jersey. Additionally, the treatment, long term exposure to $PM_{2.5}$, in a given county within the Megalopolis is likely not independent of treatment in another county within the Megalopolis given continuum of highly urban areas and that a large share of the health burden from $PM_{2.5}$ emissions can "occur more than 256 km away" (Goodkind et al. 2019, p. 8775). The Northeast is also where a High-High cluster of OLS Main Model residuals can be found (Plot 7c) suggesting that there is room for improvement in model specifications for this area.

In contrast to the northeastern Megalopolis, Low-High long term exposure to $PM_{2.5}$ spatial outliers dominate the Western half of the contiguous U.S. (Plot 7a). The exception in the West is a large High-High hotspot covering Southern California, another megalopolis among the world's top twenty economies (Florida, 2019) and the San Joaquin Valley, again tracking with population centers and industry. Unsurprisingly, a perimeter of Low-Low coldspots track along counties mainly in the Great Plains (Plot 7a) that are characterized by low population density (Stewart and Kennelly, 2010). Interestingly, a few of these coldspot perimeter counties, particularly in northern Texas, align with COVID-19 Mortality hotspots suggesting that in the absence of $PM_{2.5}$ emissions, perhaps there are other pollutants at play, healthcare access issues, or perhaps attitudes towards mask mandates and social distancing that promoted a more rapid spread of COVID-19 in this area early in the pandemic. Some of these north Texas counties, however, also exhibit High-High clusters of OLS Main Model residuals exposing more potential for misestimation in this area. Finally, an overlapping area of High-High clusters of OLS Main Model residuals and High-High hotspots of COVID-19 mortality can be found in the Southwest Region along the Arizona, New Mexico border indicating higher uncertainty in the treatment effect estimates for these counties. Though significant clustering is generally not

exhibited by the OLS Main Model Residuals (Plot 7c), areas of potential model misspecification and strong spatial dependence in the long term exposure to $PM_{2.5}$ suggest that the effects of space and place should be accounted for in model specifications.

5.5 Spatial Econometrics

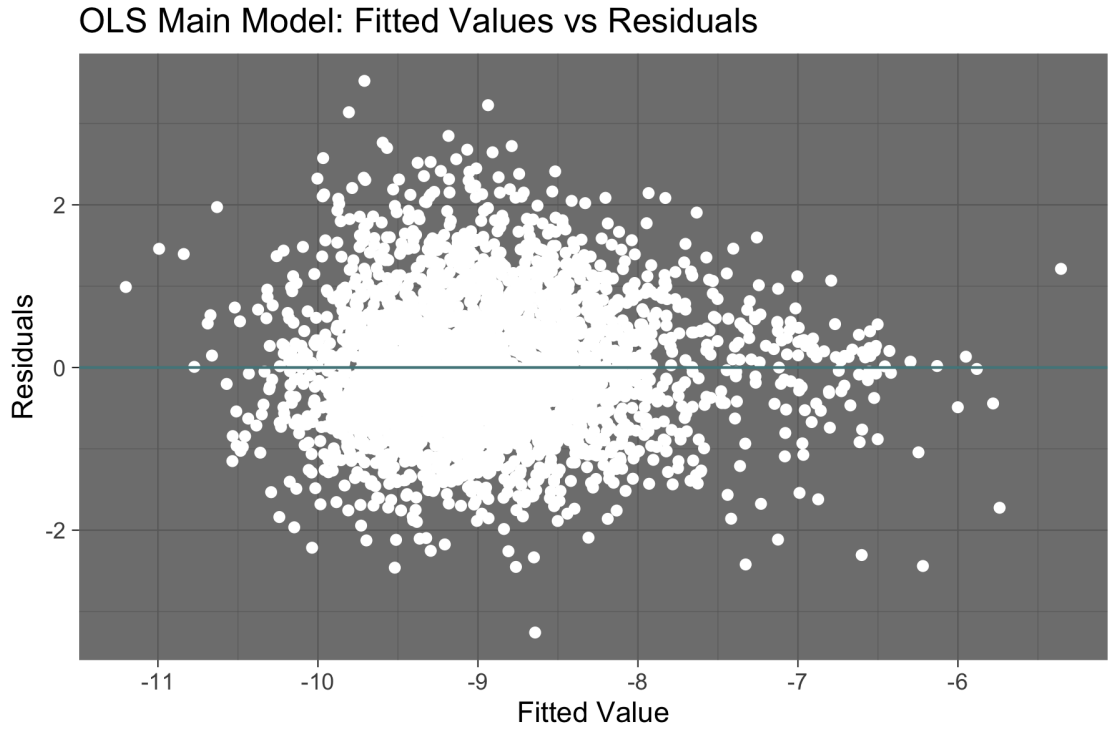

Plot 8: OLS Main Model Fitted Values vs. Residuals

Bruesch-Pagan Test

	BP	df	p-value
OLS Main Model	207.11	71	3.041e-15

Table 7 : OLS Main Model Test Results

The overlap of statistically significant long term exposure to $PM_{2.5}$ and COVID-19 Mortality hotspots in the northeast Megalopolis and the strong indicators of positive spatial autocorrelation in these treatment and outcome variables, indicate that the effects of space should be accounted for in subsequent modeling attempts. Regional spatial regimes evident in both the treatment and outcome variables also beg an accounting for the influence of place, other than the state variable, which cannot capture regional effects.

Table 8: Lagrange multiplier diagnostics for spatial dependence

	statistic	parameter	p.value
LMerr	244.5864	1	2.200e-16
LMlag	281.5569	1	2.200e-16
RLMerr	3.5167	1	6.075e-02
RLMlag	40.4871	1	1.979e-10
SARMA	285.0736	2	2.200e-16

Table 8: LM Tests for spatial dependence OLS Main Model

Though there is evidence of only weak, positive spatial autocorrelation in the OLS Main Model residuals, this suggests that the treatment effect estimate could be inefficient and that the treatment effect would be better estimated with models incorporating spatial dependence (Chi and Zhu, 2019). Additionally, one of the main assumptions of linear regression is that model residuals have equal variance, otherwise known as homoscedasticity. Unequal variances in OLS residuals, known as heteroscedasticity, can result in poorly estimated standard errors and related miscalculated confidence intervals, which can complicate hypothesis tests (Astivia and Zumbo, 2019). Fitted values from the OLS Main Model were plotted against the model residuals (Plot 8), followed up with a Bruesch-Pagan test in order to test for the presence of heteroscedasticity. With regard to Plot 8, there are not any clear patterns of spread. The OLS Main Model residuals are mostly clustering between y-axis interval of [-2,2], visually indicating no pronounced heteroskedasticity, however, the Bruesch-Pagan Test in Table 7 with

p-value<0.001 indicates that error variances of the OLS Main Model are not equal, implying the presence of heteroskedasticity and the possibility that confidence intervals may have been incorrectly estimated. From here, Lagrange Multiplier tests are used to determine which type of regression model, including spatial lag and error models, best address the spatial processes occurring in the data.

The Lagrange Multiplier diagnostics for spatial dependence in linear models (Table 8) show significant results for a missing, spatially lagged outcome variable, COVID-19 Mortality, for all versions of the outcome variable tests (LMlag p-value< 0.001; RLMlag p-value< 0.001; SARMA: LMerr + RLMlag p-value< 0.001). Spatial dependence in an outcome variable can result in OLS estimates that are biased and inconsistent. The RLMerr test for error dependence which is robust to the "possible presence of a missing, lagged dependent variable" (Bivand, n.d.) falls just outside of significance (p-value: 0.06) indicating that a spatial lag model is preferred over a spatial error model. As the null hypothesis of no spatial dependence was rejected in all of the model tests and nearly rejected in the RLMerr test, both spatial lag and spatial error models were estimated. Additionally, a spatial Durbin model was estimated in order to account for the possible spatial spillover effects of long term exposure to $PM_{2.5}$ on COVID-19 Mortality.

The coefficient of multiple determination, R^2 (Table 9) shows that only 43 percent of the COVID-19 mortality rate variation can be explained by the demographic, socioeconomic, and environmental variables in the OLS Main Model suggesting that there is room for improvement in its ability to fit the data. The difference in treatment effect estimates between OLS Main Model results listed in Table 9 (0.074) and the OLS Main Model results listed in Table 2 (0.069) are likely due to the use of a continuous surface for the Table 9 estimation.

In the spatial lag model, the spatial lag parameter estimate, Rho, is strongly positive and highly significant (Table 9: 0.36, p-value< 0.01) as is the spatial error parameter estimate, Lambda (Table 9: 0.42, p-value< 0.01), indicating that the spatial process needs to be accounted for. The spatial lag effect, as captured by Rho, comes from the spatially lagged outcome variable, meaning that the COVID-19 mortality rate in a given county is strongly affected by the COVID-19 mortality rate of its neighbors. If each neighbor, as defined by the Queen's contiguity matrix, experiences a one percent increase in the COVID-19 mortality rate, the spatial lag effect is associated with a 0.44 percent increase in the COVID-19 mortality rate of a given county, with all of the explanatory variables held constant. This result is in line with the expectation of COVID-19 community spread and "the free movement of people across US counties and states" (Chih and Ojede, 2020, p.6). In addition to the spatial lag effect, the spatial error effect is positive and statistically significant which may be the result of the absence of an important explanatory variable such as the lagged outcome variable or a missing co-pollutant.

Table 9: Title: Spatial Regression vs OLS Results

	Dependent variable:		
	log(deaths+1/population)		
	OLS	*spatial autoregressive*	*spatial error*
	(1)	(2)	(3)
mean.pm25	0.074*** (0.017)	0.083*** (0.016)	0.079*** (0.020)
Rho (spatial lag)		0.3615*** (0.022)	
Lambda (spatial error)			0.41575*** (0.024)
factor(q_popdensity)2	−0.583*** (0.061)	−0.505*** (0.058)	−0.543*** (0.058)
factor(q_popdensity)3	−0.818*** (0.066)	−0.703*** (0.063)	−0.744*** (0.064)
factor(q_popdensity)4	−0.975*** (0.071)	−0.833*** (0.067)	−0.860*** (0.069)
factor(q_popdensity)5	−0.741*** (0.085)	−0.608*** (0.081)	−0.682*** (0.083)
scale(poverty)	0.026 (0.020)	0.020 (0.019)	0.021 (0.019)
scale(log(medianhousevalue))	0.022 (0.034)	0.014 (0.032)	−0.018 (0.035)
scale(log(medhouseholdincome))	0.081** (0.035)	0.037 (0.033)	0.032 (0.034)
scale(pct_owner_occ)	0.002 (0.022)	0.009 (0.021)	0.011 (0.021)
scale(education)	0.044* (0.026)	0.041* (0.024)	0.030 (0.025)
scale(pct_blk)	0.313*** (0.026)	0.237*** (0.025)	0.282*** (0.029)
scale(hispanic)	0.043 (0.026)	0.029 (0.025)	0.062** (0.029)
scale(older_pecent)	−0.045 (0.029)	−0.052* (0.027)	−0.038 (0.029)
scale(prime_pecent)	−0.308*** (0.024)	−0.291*** (0.022)	−0.290*** (0.023)
scale(mid_pecent)	−0.063*** (0.023)	−0.048** (0.022)	−0.057** (0.023)
scale(date_since_social)	0.192 (0.335)	0.142 (0.314)	0.076 (0.321)
scale(date_since)	−0.116*** (0.020)	−0.116*** (0.019)	−0.137*** (0.019)
scale(beds/population)	0.009 (0.017)	0.003 (0.015)	0.004 (0.016)
scale(obese)	−0.069*** (0.021)	−0.061*** (0.020)	−0.071*** (0.020)
scale(smoke)	−0.006 (0.035)	−0.002 (0.033)	0.0002 (0.034)
scale(mean_summer_temp)	0.064 (0.048)	−0.024 (0.045)	−0.027 (0.050)
scale(mean_winter_temp)	−0.059 (0.069)	−0.064 (0.065)	−0.033 (0.085)
scale(mean_summer_rm)	−0.115** (0.054)	−0.071 (0.050)	−0.119* (0.063)
scale(mean_winter_rm)	−0.042 (0.035)	−0.028 (0.032)	−0.029 (0.042)
Constant	−7.931*** (0.546)	−5.397*** (0.543)	−8.677*** (0.561)
Observations	3,100	3,100	3,100
R^2	0.426		
Adjusted R^2	0.412		
Log Likelihood		-3,717.929	-3,724.212
σ^2		0.629	0.626
Akaike Inf. Crit.	7,830.029	7,587.859	7,600.425
Residual Std. Error	0.845 (df = 3026)		
F Statistic	30.771*** (df = 73; 3026)		
Wald Test (df = 1)		270.080***	306.783***
LR Test (df = 1)		244.171***	231.605***
Note:	*p<0.1; **p<0.05; ***p<0.01		

Table 9: OLS Main Model (1) vs. Spatial Lag (2) vs Spatial Error (3)

In comparing the spatial lag and error model performance (Table 9), the spatial lag model is better fit to the data based on its AIC value (7,587.859). Differences larger than 10 in the AIC values between the spatial regression models and the OLS Main Model indicate that the OLS modeling approach should not be considered further for this data (Yang, Noah, and Schoff, 2015). Overall, the coefficient magnitudes for the treatment variable, long term exposure to

$PM_{2.5}$, in the spatial lag and error models retain their significance and are slightly larger than those estimated by the OLS Main Model. In the spatial lag model, for every $1ug/m^3$ increase in the long term exposure to $PM_{2.5}$, there is a 8.65 percent increase ($p<0.01$) in the COVID-19 mortality rate with all other variables held constant. Once the effectiveness of the spatial lag model in estimating the relationship between long term exposure to $PM_{2.5}$ and COVID-19 Mortality has been established, a spatial Durbin model is then estimated to explore the possibility of spatial spillover effects of $PM_{2.5}$ exposure on COVID-19 mortality.

Interestingly, the spatial Durbin results in Table 10 show a significant and positive effect in the indirect and total impacts of the treatment variable on COVID-19 Mortality, however, the direct effects differ greatly from the OLS Main Model estimates in both the magnitude of the treatment effect estimate and its extreme lack of significance. The magnitude and significance of the indirect impacts indicate that the long term exposure to $PM_{2.5}$ has a strong spatial spillover effect on COVID-19 mortality: for every $1ug/m^3$ increase in the long term exposure to $PM_{2.5,}$ in a given county there is a 9.81 percent increase in the COVID-19 Mortality rate (p-value< 0.01) of its neighboring counties. Recalling that health risks associated with exposure to $PM_{2.5}$ has "large spatial gradients in damages, including within county and within urban" (Goodkind et al. 2019, p. 8780) these results could suggest that the direct effect of long term exposure to $PM_{2.5}$ is not adequately captured at the county level and given this level of aggregation, detecting the spatial spillover effects of $PM_{2.5}$ exposure on COVID-19 mortality is more likely. Despite its ability to detect spillover effects, the spatial Durbin model's AIC value (7824.381) is markedly higher than that of both the spatial lag and spatial error model and only marginally lower than the OLS Main Model (7830.029) suggesting that a spatial Durbin model may not be the best fitting strategy for the data. Despite this observation, the spatial spillover effect begs further consideration. With

spatial dependence accounted for in the spatial lag model, alternate definitions of place are then included as model covariates in an attempt to capture regional spatial regimes.

Table 10: Spatial Durbin Impacts

	Direct	Indirect	Total
Impacts	0.0013	0.0936	0.0948
SE	0.0317	0.0342	0.0185
Z-score	0.0404	2.7337	5.1178
P-value	0.9678	0.0063	0.0000

Table 10: Spatial Durbin Model Results

Spatial Econometrics: U.S. Census Regions

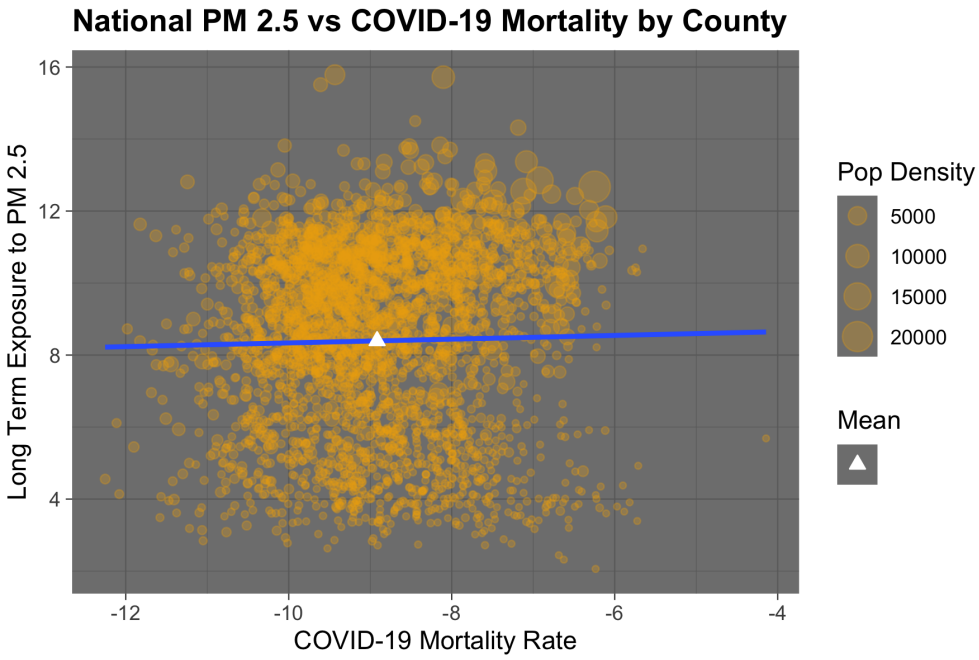

Plot 9: National Long Term Exposure to PM 2.5 vs COVID-19 Mortality by County

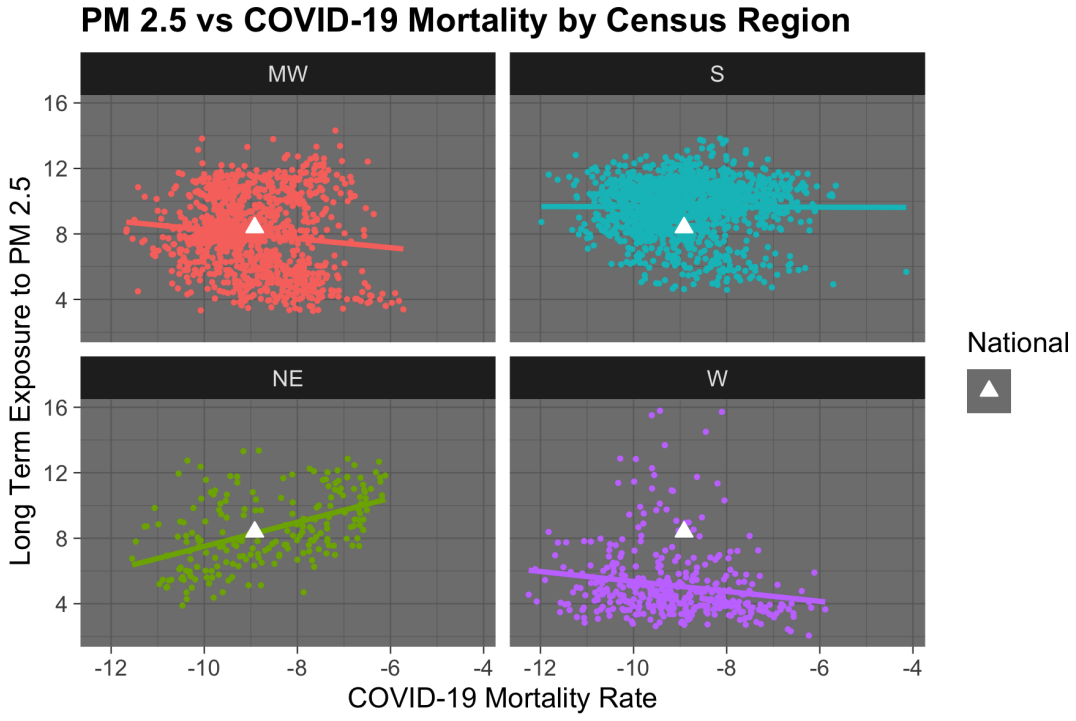

Plot 10a: Long Term Exposure to PM 2.5 vs COVID-19 Mortality by Census Region

In order to investigate the possibility of differing trends in the relationship between the treatment and outcome variable among Census Regions, long term exposure to $PM_{2.5}$ vs. COVID-19 mortality was first plotted by county on a National scale without subnational delineations (Plot 9) and then by Census Region against the National mean, expressed as *National* (Plot 10a). Plot 10a shows that the relationship between long term exposure to $PM_{2.5}$ and COVID-19 mortality varies widely by Census region with a negative association in the Census Region West and Census Region Midwest and a strongly positive association in the Census Region Northeast. This is consistent with the northeast Megalopolis as an early epicenter of the virus. Plot 10a also indicates a deviation from the National association between long term exposure to $PM_{2.5}$ and COVID-19 mortality among Census Regions South and West. The mean value set for the contiguous U.S., expressed as *National,* shows that the National

mean only approximates the Census Region mean (i.e. the centerpoint of the line of best fit) in Census Region Midwest and Census Region Northeast.

A one-way Analysis of Variance test (ANOVA) was run in order to formally assess whether there are statistically significant differences between the Census Region means and assess the effect of Census Regions as the categorical definition of place on COVID-19 Mortality. Table 11a shows that the model variable *Census Region* explains a significant amount (p-value < 0.001) of the variation in COVID-19 mortality. As the composition of $PM_{2.5}$ is highly variable, and dependent on a variety of factors including its source, its negative impact on human health may be subject to regional regimes that govern its production. For instance, wildfire generated $PM_{2.5}$ in Census Region West may have a different impact on COVID-19 Mortality than $PM_{2.5}$ generated from the 49% of U.S. coal-fired electric power plants located in the Census Region Midwest (U.S. Dept. of Energy, 2015).

	DF	Sum_Sq	Mean_Sq	F_value	Pr_F
Census Region	3	42	14.15	11.76	1.16e-07 ***
Residuals	3096	3724	1.203		

Table 11a: One Way ANOVA results, Census Regions

The Tukey Honest Significant Difference Test (Plot 10b) detects which Census Region means are significant. This test reveals differences between all Census Regions means, besides Census Region South and Census Region Midwest, as visualized in Plot 10b. The significant difference in means between all but one region pairwise comparison suggests that a model inclusive of the Census Region variables may be able to account for spatial regimes in the treatment and outcome variables.

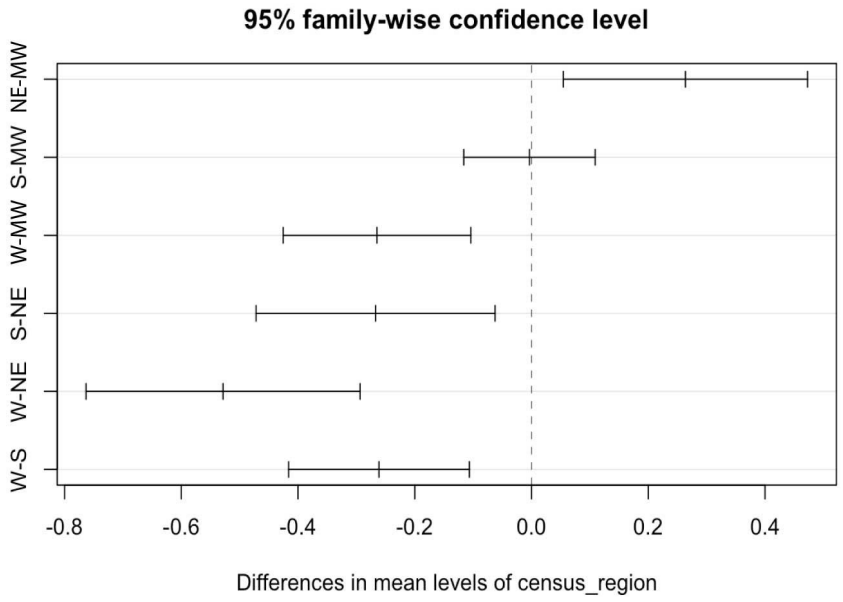

Plot 10b: Tukey Honest Significant Difference Test Census Regions

The Lagrange Multiplier diagnostics for spatial dependence in linear models for the contiguous U.S. divided into Census Regions (Table 11b) show significant results for a missing, spatially lagged outcome variable and spatial error for all versions of the tests indicating that it would be appropriate again to estimate a spatial lag, spatial error and spatial Durbin model.

	statistic	parameter	p.value
LMerr	731.416	1	2.200e-16
LMlag	760.348	1	2.200e-16
RLMerr	33.029	1	9.078e-09
RLMlag	61.962	1	3.553e-15
SARMA	793.377	2	2.200e-16

Table 11b: LM Test Results: Census Region Model

In Table 12, the spatial lag parameter estimate, Rho (0.50, p-value< 0.01) , and spatial error estimate Lamdba (0.57, p-value< 0.01) are again strongly positive and highly significant indicating that the spatial process needs to be accounted for when evaluating the treatment effect of long term exposure to $PM_{2.5}$ in this context. Again, the COVID-19 mortality rate in a given county is strongly affected by the COVID-19 mortality rate of its neighbors, as captured by Rho. Each county gains 0.64 percent in the COVID-19 mortality rate for each percentage point of weighted increase in the COVID-19 mortality rate of its neighbors with all of the explanatory variables held constant.

Table 12: Census Region: Spatial Regression vs OLS Results

	OLS	*spatial autoregressive*	*spatial error*
	OLS	Lag Model	Error Model
	(1)	(2)	(3)
mean.pm25	0.091*** (0.012)	0.083*** (0.011)	0.084*** (0.018)
Rho (spatial lag)		0.49577*** (0.019)	
Lambda (spatial error)			0.57494*** (0.020)
factor(q_popdensity)2	−0.689*** (0.063)	−0.492*** (0.057)	−0.555*** (0.059)
factor(q_popdensity)3	−0.891*** (0.069)	−0.651*** (0.061)	−0.733*** (0.064)
factor(q_popdensity)4	−1.048*** (0.074)	−0.779*** (0.066)	−0.839*** (0.069)
factor(q_popdensity)5	−0.764*** (0.088)	−0.528*** (0.078)	−0.667*** (0.083)
scale(poverty)	0.059*** (0.022)	0.038* (0.019)	0.026 (0.019)
scale(log(medianhousevalue))	−0.050 (0.033)	−0.024 (0.030)	−0.056 (0.034)
scale(log(medhouseholdincome))	0.170*** (0.034)	0.067** (0.030)	0.036 (0.034)
scale(pct_owner_occ)	0.025 (0.022)	0.018 (0.020)	0.016 (0.021)
scale(education)	0.011 (0.026)	0.014 (0.023)	0.018 (0.025)
scale(pct_blk)	0.411*** (0.024)	0.245*** (0.022)	0.296*** (0.030)
scale(hispanic)	0.022 (0.024)	0.026 (0.022)	0.059** (0.030)
scale(older_pecent)	−0.077*** (0.029)	−0.064** (0.026)	−0.045 (0.030)
scale(prime_pecent)	−0.341*** (0.025)	−0.293*** (0.023)	−0.290*** (0.023)
scale(mid_pecent)	−0.071*** (0.024)	−0.042** (0.021)	−0.061*** (0.022)
scale(date_since_social)	0.026 (0.022)	0.032* (0.019)	0.070** (0.034)
scale(date_since)	−0.095*** (0.021)	−0.100*** (0.019)	−0.143*** (0.019)
scale(beds/population)	0.011 (0.017)	−0.0005 (0.015)	0.002 (0.015)
scale(obese)	−0.076*** (0.022)	−0.062*** (0.019)	−0.066*** (0.019)
scale(smoke)	0.033 (0.029)	0.014 (0.025)	−0.015 (0.030)
scale(mean_summer_temp)	−0.054** (0.023)	−0.093*** (0.020)	−0.091*** (0.022)
scale(mean_winter_temp)	0.036 (0.036)	0.019 (0.032)	0.015 (0.056)
scale(mean_summer_rm)	−0.118*** (0.042)	−0.099*** (0.037)	−0.141** (0.061)
scale(mean_winter_rm)	−0.005 (0.026)	0.015 (0.023)	0.004 (0.040)
CR_mw	0.412*** (0.112)	0.273*** (0.099)	0.495*** (0.157)
CR_s	0.191 (0.127)	0.197* (0.112)	0.433** (0.183)
CR_ne	0.909*** (0.128)	0.569*** (0.114)	0.872*** (0.201)
Constant	−9.288*** (0.120)	−4.916*** (0.204)	−9.478*** (0.176)
Observations	3,100	3,100	3,100
R^2	0.310		
Adjusted R^2	0.304		
Log Likelihood		-3,836.007	-3,825.582
σ^2		0.662	0.644
Akaike Inf. Crit.	8,310.603	7,732.013	7,711.164
Residual Std. Error	0.920 (df = 3072)		
F Statistic	51.028*** (df = 27; 3072)		
Wald Test (df = 1)		654.792***	826.175***
LR Test (df = 1)		580.590***	601.439***
Note:	*p<0.1; **p<0.05; ***p<0.01		

Table 12: Census Region OLS(1) vs. Spatial Lag (2) and Spatial Error (3) Models

This time, however, the spatial error model is better fit to the data based on its lowest AIC value (7,711.164). The large differences between AIC values of the OLS and the spatial models again suggest that the OLS Main Model is insufficient. The coefficient of multiple determination, R^2, shows that the explanatory power of the OLS Main Model in the context of Census Regions has been reduced to 31 percent (Table 12). The positive and statistically

significant spatial error effect indicates the need to control for spatial autocorrelation in the error term and may again be the result of the absence of an important explanatory variable such as the lagged outcome variable or a missing co-pollutant.

Overall, the coefficient magnitudes for treatment variable, long term exposure to $PM_{2.5}$, in the spatial lag and error models retain their significance and are larger than those estimated by the OLS Main Model but smaller than those estimated by the OLS Census Region Model. In the spatial error model, for every $1ug/m^3$ increase in the long term exposure to $PM_{2.5}$, there is a 8.65 percent increase ($p<0.01$) in the COVID-19 mortality rate with all other variables held constant (Table 12). All Census Region dummy variables exhibit statistically significant explanatory power in the spatial error model ($p<0.05$) with varying degrees of influence, however, unexpectedly, they all show a negative relationship with the COVID-19 Mortality rate (Table 12).

The Census Region Northeast is the most influential with regard to the reference group, Census Region West, with all other explanatory variables held constant. Counties in Census Region Northeast will, on average, experience a 139% increase in the COVID-19 Mortality rate than those in the Census Region West (spatial error model, Table 12). The positive difference in COVID-19 Mortality between Census Region NE and Census Region West was expected given that New York City was considered an early pandemic epicenter and the spatial and economic contiguity of NYC and the northeast Megalopolis. However, the strongly negative effect of all Census Regions on COVID-19 Mortality is more difficult to conceive of and is perhaps due to the early stage in the pandemic at which county level deaths were counted, with over one third of the counties having logged zero deaths at the time of this study.

The negative relationship between place and COVID-19 Mortality is consistent with the OLS re-estimation of the Wu et al. (2020) model, with every state fixed effect having a negative association with COVID-19 Mortality (not reported). The author's use of the state-specific floating intercept may have been an attempt to deal with this unexpected result. The state specific coefficients in their study, however, were not reported in *Science Advances* nor in their "Supplementary Materials" (Wu et al., 2020). The approximate influence of a region on a treatment-outcome relationship for an outcome that has not yet been substantially realized in several of the regions may therefore be difficult to quantify. The significant difference between Census Region means, however, suggests that further investigation of this definition of place and the interaction of place and air pollution exposure may better account for its influence on public health in subsequent studies.

Again, the spatial Durbin results in Table 13 show a significant and positive effect in the indirect and total impacts of the treatment variable on COVID-19 mortality while the direct effects differ greatly from the OLS Main Model estimates in the magnitude and direction of the coefficient, and its extreme lack of significance. The magnitude and significance of the indirect impacts indicate that the long term exposure to $PM_{2.5}$ has a strong spatial spillover effect on COVID-19 mortality: for every $1ug/m^3$ increase in the long term exposure to $PM_{2.5}$ in a given county, there is a 12.3 percent increase in the COVID-19 Mortality rate (p-value< 0.001) of its neighboring counties. The spatial Durbin Census Regions model AIC value (8,300.895) is, however, markedly higher than that of both the spatial lag and spatial error model yet performs better than the OLS Main Model (8,310.603) suggesting that accounting for both the spatially lagged outcome and treatment variable in the model may not be the best fitting strategy for the data in the Census Region spatial context.

Table 13: Spatial Durbin Impacts: Census Regions

	Direct	Indirect	Total
Impacts	-0.0157	0.1161	0.1004
SE	0.0336	0.0341	0.0126
Z-score	-0.4691	3.4090	7.9796
P-value	0.6390	0.0007	0.0000

Table 13: Spatial Durbin Model Results- Census Results

Spatial Econometrics: EPA Climatically Consistent Regions

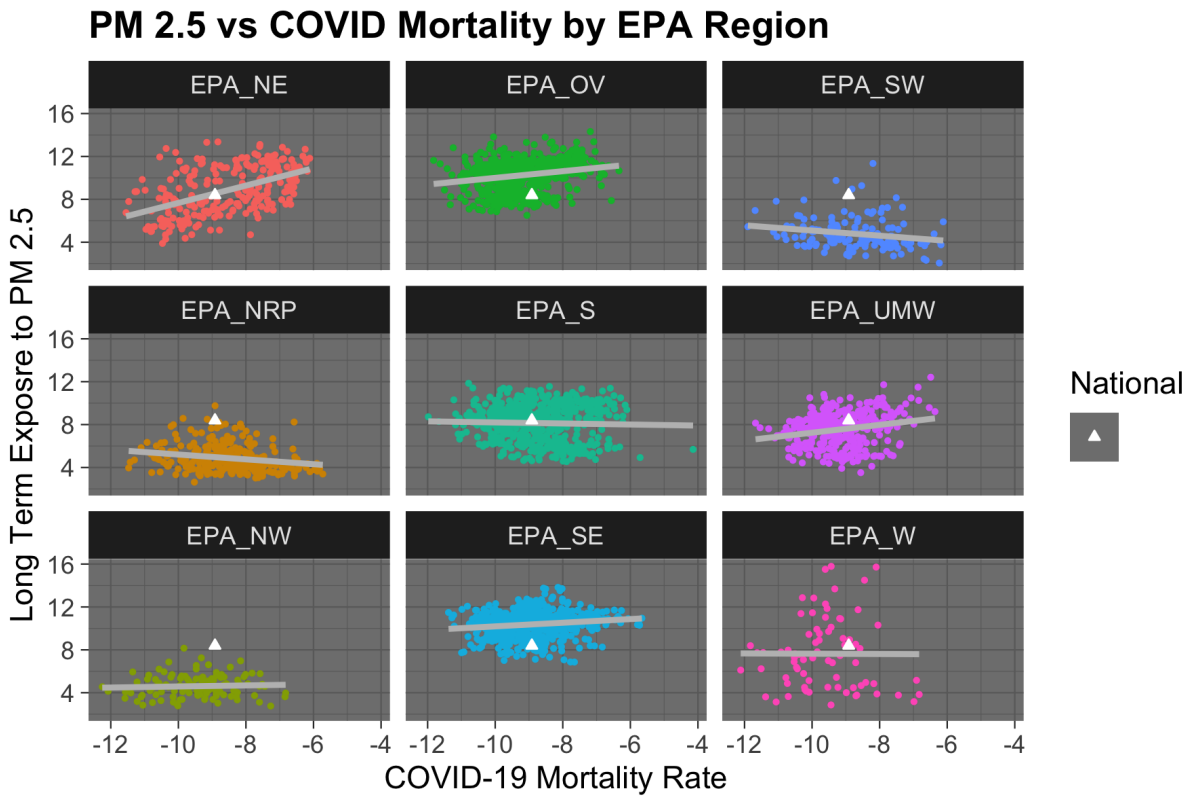

Plot 11: Long Term Exposure to PM 2.5 vs COVID-19 Mortality by EPA Climatically Consistent Region

The relationship between long term exposure to $PM_{2.5}$ and COVID-19 mortality varies widely by EPA Climatically Consistent Regions (Plot 11). Negative associations are revealed in the Regions Southwest and Northern Rocky Plain, while the strongly positive association in the

Region Northeast still holds. Plot 11 also indicates deviations from the National association between long term exposure to $PM_{2.5}$ and COVID-19 Mortality. The mean value set for the contiguous U.S., expressed as *National,* shows that the National mean only approximates the EPA Region means in Regions South, Northeast and Upper Midwest.

A one-way ANOVA was run at this conjuncture to then assess the effect of EPA Climatically Consistent Region as the categorical definition of place on COVID-19 Mortality. The results of the one-way ANOVA in Table 14a shows that the model variable *EPA Region* explains a significant amount (p-value < 0.001) of the variation in COVID-19 mortality. This likely speaks to the influential role of temperature and humidity on particle formation, as well as the relationship between particle composition and fugitive dust in more arid regions, resulting in regional differences in the composition of $PM_{2.5}$. The Tukey Honest Significant Difference Test (not reported) results reveals a significant difference in means in 56% of pairwise comparisons between EPA Regions. Again, *where* $PM_{2.5}$ is formed likely has influence over what it is comprised of, and in turn, its influence on public health.

	DF	Sum_Sq	Mean_Sq	F_value	Pr_F
EPA Region	9	246	27.28	23.94	< 2e-16 ***
Residuals	3090	3521	1.14		

Table 14a: One Way ANOVA results, EPA Regions

In the case where the EPA Climatically Consistent Regions are accounted for in the model specifications, there is a similar outcome. The Lagrange Multiplier diagnostics for spatial dependence in linear models for the contiguous U.S. divided into EPA Climatically Consistent Regions (Table 14b) show significant results for a missing, spatially lagged outcome variable

and spatial error for all versions of the tests indicating that it would be appropriate again to estimate a spatial lag, spatial error and spatial Durbin model.

	statistic	parameter	p.value
LMerr	639.416	1	2.200e-16
LMlag	682.975	1	2.200e-16
RLMerr	18.965	1	1.332e-05
RLMlag	62.524	1	2.665e-15
SARMA	701.940	2	2.200e-16

Table 14b: LM Test Results: EPA Region Model

In Table 15, the spatial lag parameter estimate, Rho (0.48, p-value< 0.01) , and spatial error estimate Lamdba (0.56, p-value< 0.01) are again strongly positive, highly significant and very similar to the Census Region spatial model estimates. Again, the COVID-19 mortality rate in a given county is strongly affected by the COVID-19 mortality rate of its neighbors, as captured by Rho. Each county gains 0.62 percent in the COVID-19 mortality rate for each percentage point of weighted increase in the COVID-19 mortality rate of its neighbors with all of the explanatory variables held constant. The large differences (greater than 10) between AIC values and the spatial models again suggest that the OLS Main Model (AIC: 8245.739) is again insufficient with the coefficient of multiple determination, R^2, indicating that the explanatory power of the OLS Main Model in the context of EPA Regions has been reduced to 31 percent (Table 15). The spatial error model is better fit to the data based on its lowest AIC value (Table 15: 7,707.665). The positive and statistically significant spatial error effect indicates the need to control for spatial autocorrelation in the error term and may be the result of the absence of an important explanatory variable such as the lagged treatment variable or a missing, climatically dependent pollutant such as ozone.

Table 15: EPA Regions: Spatial Regression vs OLS Results

	OLS	*spatial autoregressive*	*spatial error*
	OLS	Lag Model	Error Model
	(1)	(2)	(3)
mean.pm25	0.151*** (0.014)	0.112*** (0.013)	0.126*** (0.020)
Rho (spatial lag)		0.48378*** (0.020)	
Lambda (spatial error)			0.5585*** (0.020)
factor(q_popdensity)2	−0.649*** (0.064)	−0.504*** (0.058)	−0.547*** (0.059)
factor(q_popdensity)3	−0.862*** (0.070)	−0.669*** (0.063)	−0.727*** (0.064)
factor(q_popdensity)4	−1.038*** (0.074)	−0.802*** (0.067)	−0.839*** (0.069)
factor(q_popdensity)5	−0.796*** (0.088)	−0.570*** (0.079)	−0.681*** (0.084)
scale(poverty)	0.058*** (0.022)	0.037* (0.019)	0.027 (0.019)
scale(log(medianhousevalue))	−0.102*** (0.032)	−0.053* (0.029)	−0.070** (0.034)
scale(log(medhouseholdincome))	0.209*** (0.033)	0.095*** (0.030)	0.046 (0.034)
scale(pct_owner_occ)	−0.006 (0.023)	0.0002 (0.021)	0.016 (0.021)
scale(education)	0.011 (0.026)	0.016 (0.023)	0.019 (0.025)
scale(pct_blk)	0.356*** (0.026)	0.225*** (0.023)	0.280*** (0.030)
scale(hispanic)	0.017 (0.025)	0.015 (0.022)	0.055* (0.030)
scale(older_pecent)	−0.048* (0.029)	−0.051** (0.026)	−0.042 (0.029)
scale(prime_pecent)	−0.327*** (0.025)	−0.292*** (0.023)	−0.293*** (0.023)
scale(mid_pecent)	−0.065*** (0.023)	−0.042** (0.021)	−0.059*** (0.022)
scale(date_since_social)	0.105*** (0.023)	0.056*** (0.020)	0.105*** (0.035)
scale(date_since)	−0.107*** (0.021)	−0.108*** (0.019)	−0.146*** (0.019)
scale(beds/population)	0.001 (0.017)	−0.006 (0.015)	−0.002 (0.016)
scale(obese)	−0.084*** (0.022)	−0.068*** (0.019)	−0.072*** (0.020)
scale(smoke)	0.035 (0.031)	0.023 (0.028)	−0.0002 (0.031)
scale(mean_summer_temp)	−0.066*** (0.023)	−0.098*** (0.020)	−0.101*** (0.022)
scale(mean_winter_temp)	0.053 (0.040)	0.017 (0.036)	−0.011 (0.061)
scale(mean_summer_rm)	−0.074* (0.041)	−0.044 (0.036)	−0.084 (0.059)
scale(mean_winter_rm)	0.007 (0.028)	0.005 (0.025)	0.001 (0.041)
EPA_NW_dum	0.650*** (0.150)	0.311** (0.134)	0.249 (0.245)
EPA_NRP_dum	1.033*** (0.173)	0.335** (0.156)	0.703*** (0.262)
EPA_SW_dum	0.994*** (0.144)	0.416*** (0.129)	0.460** (0.229)
EPA_S_dum	0.695*** (0.158)	0.324** (0.142)	0.611** (0.240)
EPA_OV_dum	0.444*** (0.170)	0.162 (0.152)	0.274 (0.253)
EPA_UMW_dum	0.817*** (0.178)	0.375** (0.159)	0.481* (0.270)
EPA_SE_dum	0.370** (0.166)	0.125 (0.149)	0.332 (0.253)
EPA_NE_dum	1.240*** (0.175)	0.601*** (0.158)	0.922*** (0.272)
Constant	−10.179*** (0.189)	−5.297*** (0.260)	−9.869*** (0.271)
Observations	3,100	3,100	3,100
R^2	0.326		
Adjusted R^2	0.319		
Log Likelihood		-3,825.400	-3,818.832
σ^2		0.659	0.644
Akaike Inf. Crit.	8,245.739	7,720.800	7,707.665
Residual Std. Error	0.910 (df = 3067)		
F Statistic	46.378*** (df = 32; 3067)		
Wald Test (df = 1)		592.631***	747.308***
LR Test (df = 1)		526.938***	540.074***
Note:	*p<0.1; **p<0.05; ***p<0.01		

Table 15: EPA Climatically Consistent Region OLS(1) vs. Spatial Lag (2) and Spatial Error (3) Models

Overall, the coefficient magnitudes for treatment variable, long term exposure to $PM_{2.5}$, in the spatial lag and error models retain their significance and are larger than those estimated by the Census Region spatial error model. In the EPA Region spatial error model, for every $1ug/m^3$ increase in the long term exposure to $PM_{2.5}$, there is a 13.43 percent increase ($p<0.01$) in the COVID-19 mortality rate with all other variables held constant (Table 15).

All but two EPA Climatically Consistent Regions (Ohio Valley and Southeast) exhibit statistically significant explanatory power in the spatial error model with varying degrees of influence with respect to the reference group, EPA Region West (Table 15). As expected, the EPA Region Northeast, which closely tracks geographically with Census Region Northeast and includes most of the extent of the northeast Megalopolis, is the most influential with respect to the reference group. After the effects of all other explanatory variables are taken into account, counties within EPA Region Northeast will experience an 151 percent average increase in COVID-19 mortality with respect to EPA Region West. Similar to the models with Census Regions defining place, EPA Regions also show a strongly negative relationship with COVID-19 Mortality, speaking to the difficulty of obtaining place sensitive estimates when the outcome variable is still in the process of being realized.

Table 16: Spatial Durbin Impacts: EPA Regions

	Direct	Indirect	Total
Impacts	-0.0160	0.1919	0.1759
SE	0.0333	0.0344	0.0150
Z-score	-0.4819	5.5780	11.6861
P-value	0.6299	0.0000	0.0000

Table 16: Spatial Durbin Impacts- EPA Region

The spatial Durbin EPA Regions results in Table 16 show a significant and positive effect in the indirect and total impacts of the treatment variable on COVID-19 mortality while the direct

effects differ greatly from the OLS Main Model estimates in the magnitude and direction of the coefficient, and its extreme lack of significance. The magnitude and significance of the indirect impacts indicate that with respect to the long term exposure to $PM_{2.5}$ has a strong spatial spillover effect on COVID-19 mortality: for every $1ug/m^3$ increase in the long term exposure to $PM_{2.5}$ of a given county, there is a 21.15 percent increase in the COVID-19 Mortality rate (p-value< 0.001) of its neighboring counties. The spatial Durbin EPA regions model AIC value (8,216.438) shows that this model performs better than the spatial Durbin Census Regions model and the EPA OLS Main Model, however it doesn't outperform either the spatial lag or error model.

The predictive power of models accounting for space in the form of a spatial lag or spatial error term are evident in the preceding analysis. Model specifications including the effects of space help to uncover the Euclidean dimension of the Geography of $PM_{2.5}$ and its spatial relationship with COVID-19 Mortality, however, accounting for place has proven more difficult. The significant difference in place based means among Census Regions and among EPA Climatically Consistent Regions suggests that both space and place need to be accounted for when estimating air pollution effects on public health. While the effects of space can be accounted for econometrically, the influence of place on the relationship between air pollution exposure and public health is likely to require a deeper consideration, beyond econometric techniques. The substantive influence of the Geography of $PM_{2.5}$, and its effect on public health, would be best considered *a priori*, in the overall research design, hypotheses and sampling strategy.

6. Discussion

6.1 Sensitivity Analysis

A novel result was produced when the fragility of a widely received treatment effect estimate of the long term exposure to $PM_{2.5}$ on COVID-19 mortality was assessed utilizing an alternate sensitivity analysis framework. When the robustness values and partial R^2 values produced by this framework were considered within the context of plausible confounding, it was revealed that the estimate derived by Wu et al. (2020) is much more fragile to confounding than reported by the authors. Though accounting for confounding between long term exposure to $PM_{2.5}$ and COVID-19 mortality had been considered by Wu et al. through the inclusion of an E-value in their outcome variable, *Mortality Rate Ratio,* the strength of confounding required to destabilize an estimated treatment effect with public health implications should be explicitly reported alongside estimates. These differential estimates of fragility to confounding pose an interesting debate about whether some sensitivity analysis frameworks are better suited to public health research than others.

The inclusion of ozone as a covariate was able to unmask a bigger direct effect of long term exposure to $PM_{2.5}$ on COVID-19 mortality, as well as bolster this estimated effect against confounding. However, the negative relationship between ozone and COVID-19 mortality, as derived from the ozone inclusive model, suggests that there are yet more confounding relationships to uncover. Additionally, it is likely that the occurrence of ozone and $PM_{2.5}$ are positively correlated, but not perfectly collinear due to differential vectors of production, though this relationship was not captured in this analysis. With regard to ozone's unexpected negative influence on COVID-19 mortality, it is likely that areas characterized by high levels of ozone are urban and that urbanites are more likely to have access to income opportunities, education and healthcare that reduce the potential for COVID-19 mortality than those living in rural areas.

6.2 Spatial Sensitivity & Implications of scale

In addition to the potential sources of confounding by omitted variables as discovered in the sensitivity analysis portion of this thesis, the underlying spatial structure or spatial dependence in treatment, outcome, and model residuals can produce unreliable treatment effect estimates. Strong levels of spatial dependence in the long term exposure to $PM_{2.5}$, and to a lesser extent in the COVID-19 mortality rate and OLS Main Model residuals, were confirmed by both computational and exploratory spatial data analysis. The need to account for spatial processes was clear. In the National context, where the OLS Main Model includes state fixed effects, a positive and statistically significant spatial lag effect was produced signaling that long term exposure to $PM_{2.5}$ treatment effect estimates and their associated health risk, COVID-19 Mortality, are not homogeneous across the contiguous U.S. National ESDA maps revealed spatial regimes in both the treatment and outcome variables indicating that there is indeed a geography to $PM_{2.5}$. The complex geography of this air pollutant can't be captured by averaging county values across the Nation. Instead the sub-National spatial and place based processes governing its production, distribution and related human health consequences must be considered.

The highly variable associations between long term exposure to $PM_{2.5}$ and COVID-19 mortality per U.S. Census Region or EPA Climatically Consistent Region delivers the expected result that the relationship between the treatment and outcome variable changes with changes in the spatial delineation of the Nation. Three out of four Census Regions displayed treatment effect estimate trends that diverged from the National trend of positive association while only one-third of EPA Regions held similarly positive associations of varying strength. This shows

that the treatment effect estimates at the National level are subject to spatial regimes and are affected by alternate definitions of sub-national place. The null hypothesis is therefore rejected.

Though the spatial effects were best captured by the use of a spatially lagged dependent variable in the OLS Main Model, the spatial error term, Lambda, is positive and significant in all three spatial iterations suggesting that there is some spatial relationship in the error term. When state fixed effects were replaced by U.S. Census Region or EPA Climatically Consistent Region variables, the model performance was reduced and the spatial error models were now better fit to the data than the spatial lag models. Spatial error model performance in this context may be due to, for example, spatially correlated long term exposure to $PM_{2.5}$ values among counties, or spatially correlated omitted variables such as the co-pollutant ozone.

The very high spatial dependence in the long term exposure to $PM_{2.5}$, as well as the evidence for a strong spatial spillover effects in all three spatial Durbin models where the administrative groupings of counties differed by state, Census Region, and EPA Climatically Consistent Region, suggests that further investigation of regionally specific contexts for the production and spread of $PM_{2.5}$ would be useful in informing future research questions, sampling and modeling strategies. As the OLS model specifications lost complexity - moving from controlling for administrative boundary groupings by forty-eight state fixed effects and D.C. to nine EPA Climatically Consistent Regions, to four Census Regions, they also lost explanatory power, as evidenced by their AIC values. Though the regional context better captured the spatial regimes of long term exposure to $PM_{2.5,}$ they may not accurately capture the spatial dimension of the spread of COVID-19. As the prevalence of COVID-19 Mortality is likely subject to state specific policy, such as state-wide mask mandates and stay-at-home orders, this sub-national delineation may have greater explanatory power over the outcome, despite the transboundary nature of air pollution.

The within scale variations in the estimated impact of long term exposure to $PM_{2.5}$ on COVID-19 mortality is likely from place-based variations including variations in the socioeconomic, political and historical conditions between states or regions governing air pollution regulation and enforcement, COVID-19 policy response, industrialization and the distribution of wealth and healthcare facilities. There are state by state variations at play in the governance of $PM_{2.5}$ and COVID-19 including, for example, the evidence that differential enforcement of clean air standards across the Nation and the differential timing of COVID-19 mitigation strategies, such as statewide mask mandates, follow the political affiliations of state elected officials (Beland and Boucher, 2015; Adolph et al., 2021). Among Census regions, within scale variation is likely tied to differential vectors of the production of $PM_{2.5}$ from regionally specific industry, e.g. Midwestern electricity production vs. Western wildfires. The resulting variability in the chemical composition of $PM_{2.5}$ and its health impacts links differential health outcomes from $PM_{2.5}$ pollution exposure to the historical development of a region, its present economy, and climatic differences governing its production. Differences in the estimated impact of long term exposure to $PM_{2.5}$ on COVID-19 mortality among Census regions is also likely due to population distribution, and the spatial extent of integrated economies and transit networks such as in the northeastern Megalopolis.

Variations in EPA Climatically Consistent Regions can be attributed to a host of environmental and climatic factors including topographical variations between regions that affect the $PM_{2.5}$ dispersal range, and climatic conditions such as temperature and relative humidity. For example, $PM_{2.5}$ produced from fugitive dust rather than anthropogenic sources, is more likely to be prevalent in the arid West (Park et al., 2010). Additionally, extreme heat has been named a driver of the highest levels of air pollution, including secondary particle formation in the presence of ozone during warmer seasons (Schnell and Prather, 2017; Zhu, et al., 2019). The

positive association between the long term exposure to $PM_{2.5}$ and COVID-19 mortality in California was found to be attenuated during the winter months (Garcia et al., 2022), further suggesting that climatic conditions bear influence on this health hazard relationship.

Variations between counties in a given Census or EPA Region are likely to reflect a matrix of place based factors including state policies regarding emissions limits, the effectiveness of the enforcement of these limits, the timing and uptake of state and county policies meant to curb the spread of COVID-19, or the differential distribution of healthcare facilities, wealth, and industry between urban and rural counties. For instance, Colmer et. al (2020) found that differential access to clean air is a persistent trend at the census tract level across the U.S. and that the most burdened subpopulations 1981 remained the most burdened in 2016. Similarly, there is an urban-rural divide in health outcomes. Larger $PM_{2.5}$ exposure effects on cardiovascular disease, cardiopulmonary disease and all-cause mortality were found in rural California areas when compared with urban areas by Garcia et. al (2016), linking lack of quality healthcare access and wealth to environmental risk factors for premature mortality. Differential access to clean air has also been found to be exacerbated in counties along the U.S. border where “states perform fewer enforcement actions” (Konisky and Woods 2009) and in urban areas characterized by Black, LatinX, Asian American, and immigrant communities (Miranda et al., 2011; Nardone et al., 2018, Namin et al., 2020)..

The between scale variations in the treatment effect estimates, e.g. between Census Regions and EPA Climatically Consistent Regions, may be attributed to the modifiable areal unit problem (MAUP) where the scale at which long term $PM_{2.5}$ exposure and COVID-19 mortality occurs does not match the scale that the phenomena have been aggregated to in order to make inferences about their associations. While the origination of particulate matter emissions may be

assignable to a well-defined areal unit, its pattern of spread is more complex and less likely to be able to be assigned to a neat conglomeration of administrative boundaries. Given this and the climatic variables that strongly influence the presence of $PM_{2.5}$, controlling for the EPA Climatically Consistent Regions yielded stronger treatment effects across OLS and spatial models, as suspected. The negative association between regional definitions of place and COVID-19 mortality suggest, however, that strategies beyond econometric techniques should be deployed in order to incorporate the effects of place.

The biggest issue with the county level aggregation of $PM_{2.5}$ exposure is it misses important within-area variability. With Goodkind's finding that marginal damages from $PM_{2.5}$ vary by "over an order of magnitude within a single county" (p. 8775), a sub-County analysis would be required in order to uncover the pollution exposure gradients disproportionately burdening low-income Black, LatinX, Asian-American and immigrant communities. Uncovering sociospatial gradients of air pollution exposure burdeons are essential to identifying the economic and political mechanisms that continue to perpetuate uneven burdens such as the siting of toxic facilities, discriminatory settlement patterns linked to racist 20th Century housing policies, and the "indirect and partial commoditization of air quality" (Véron, 2006, p. 2096) through urban property values.

6.3 Limitations and Future Iterations

Understanding the geographic context of the spread of air pollution can help to inform sampling strategies, data aggregation strategies, modeling strategies and inference. The geography of the relationship between $PM_{2.5}$ and COVID-19 mortality is not simply additive but provides the context for the production of the toxic emission itself, the spread of the virus, and their unevenly distributed burdens. Air pollution legislation and enforcement that varies by

political boundary, 20th and 21st Century discriminatory practices in the settlement and planning of U.S. communities, and proximity dependent, fine-scale variability in exposure are all likely contributors to the differential effects of long term exposure to air pollutants, including $PM_{2.5}$. Despite the reduction in model performance, the higher treatment effect estimates and domain knowledge regarding the relationship between the presence of $PM_{2.5}$ and climatic conditions indicates that incorporating EPA Climatically Consistent Regional boundaries into future study design begs further examination. Given these scale dependent relationships, and the need to accurately uncover the environmental justice implications of this public health crisis, future studies may wish to employ a finer-scale analysis of zip code or neighborhood-level pollution and virus exposure data within a given EPA Climatically Consistent Region for a clearer assessment of the health-risk outcomes of U.S. populations. Additionally, the economic, political, topological and spatial aspects of the distribution of $PM_{2.5}$ emissions should be considered in avoidance of a spatial spillover effect.

For future iterations of this study, there are several more ways in which it can be improved. First is to estimate the ozone inclusive analysis with ozone data mimicking the same seventeen-year timescale of exposure as the $PM_{2.5}$ data procured by Wu et al. (2020). Second, Wu et al. explicitly state in their study that the limitations of an ecological analysis in this context includes the potential misclassification of air pollution exposure due to "between-area mobility and within-area variation" (2020, p.3). Within-area variation in pollution exposure would be better captured at a much finer, sub-County geographic scale. Lastly, in consideration of the potential for the incomplete characterization of variables that might affect COVID-19 mortality such as education, healthcare access, and politically motivated attitudes towards containment measures, more or different indicators of quality of life could be used. Additional areas of improvement include, but are not limited to, exploring certain methodological pathways such as Bayseian modeling approaches or Geographically weighted regression in order to more

accurately model the spatial relationship between long-term exposure to $PM_{2.5}$ and COVID-19 mortality.

Appendix

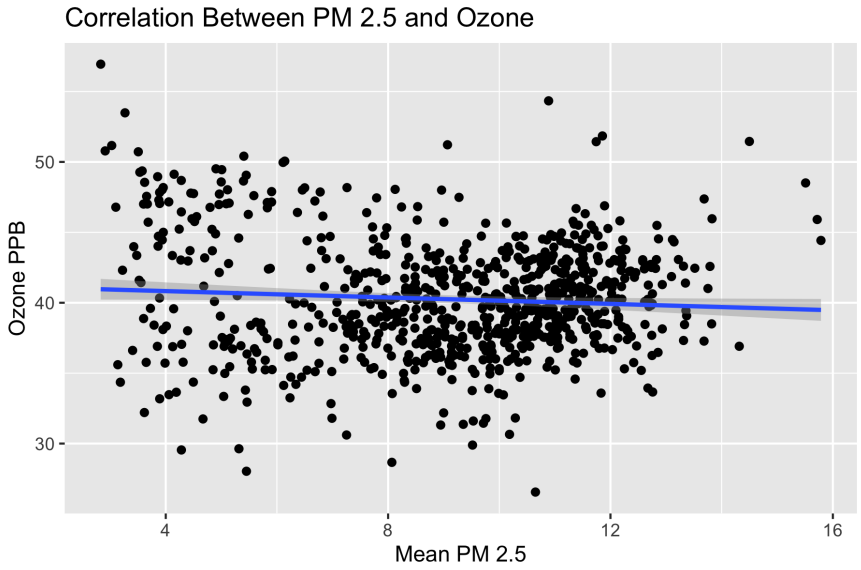

Plot 3: Correlation Between $PM_{2.5}$ and Ozone

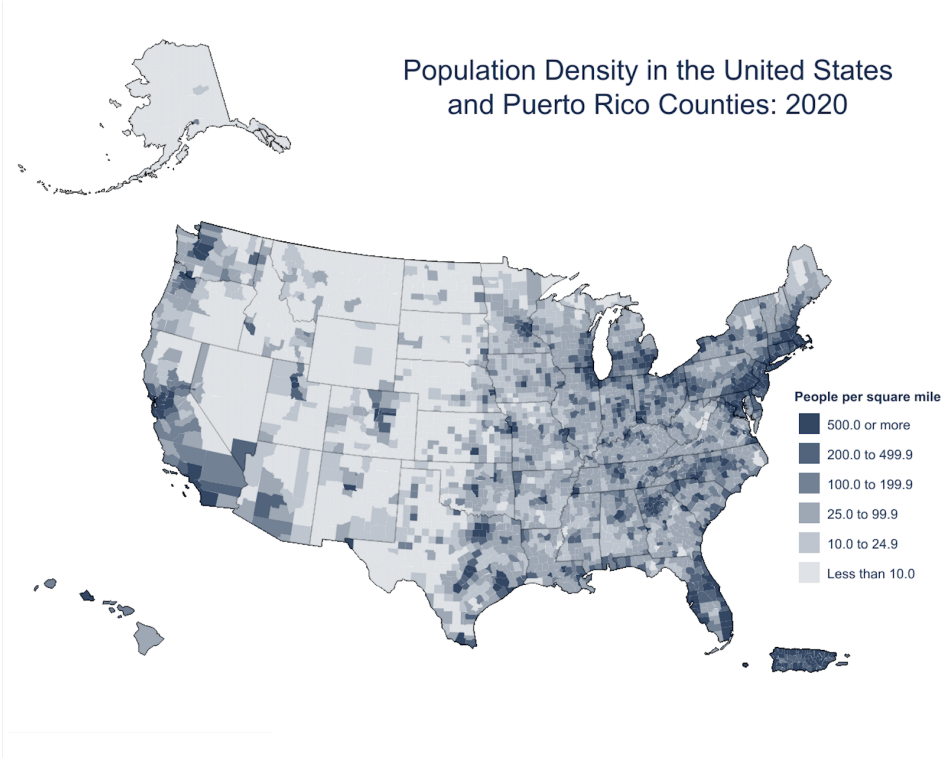

Plot 5d: 2020 Population Density per U.S. County, From Census.gov; Public Domain.

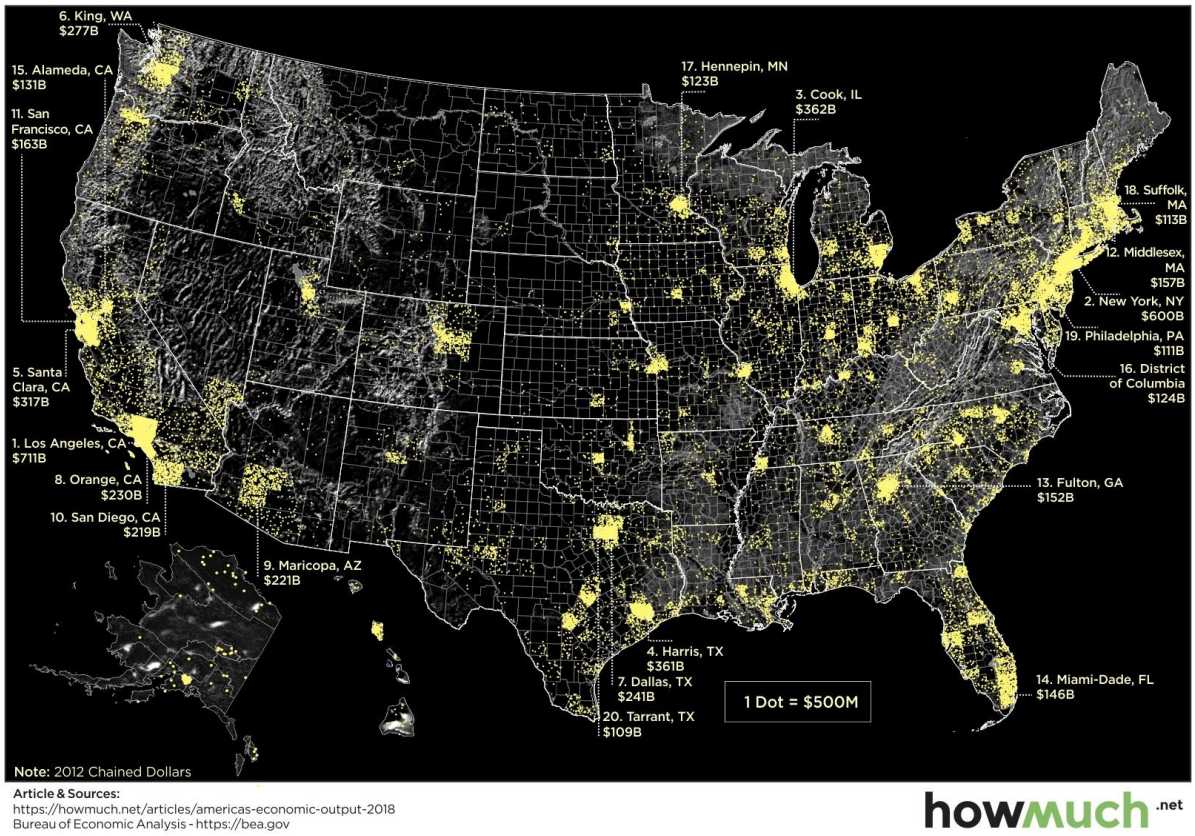

Plot 5e: *America's Economic Output in 2018*, from HowMuch.net, a financial literacy website

	# Sim	Moran's I	Rank	p-value	Alt Hyp
Mean PM 2.5	999	0.93124	1000	0.001	greater
COVID-19 Mortality Rate	999	0.40534	1000	0.001	greater
OLS Residuals	999	0.16858	1000	0.001	greater

Table 6b: Monte Carlo Simulation of Moran's I

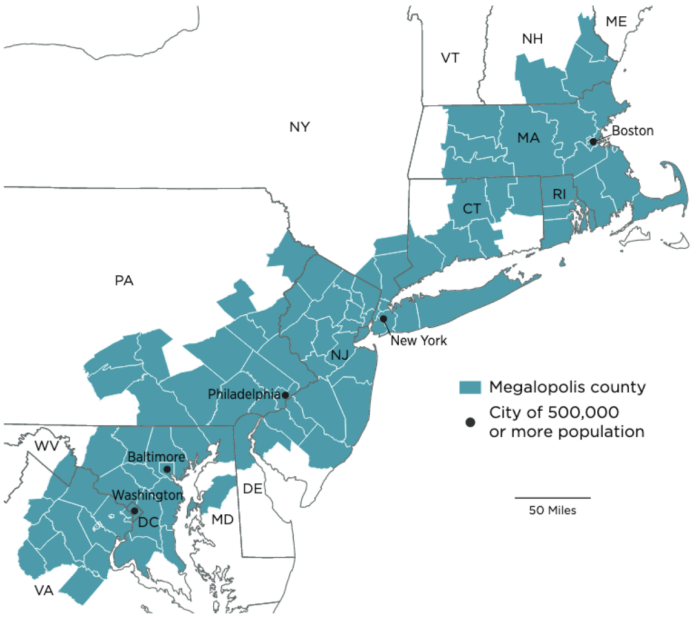

Source: U.S. Census Bureau, Vintage 2019 Population Estimates.

Megalopolis is a region within the northeastern United States that extends from northern Virginia to southern New Hampshire and is anchored by Washington, Baltimore, Philadelphia, New York, and Boston. Roughly 50 million people, nearly 1 out of every 6 Americans, live in a band of 103 counties stretching along the Atlantic coast. Geographer Jean Gottmann's 1961 in-depth study, "Megalopolis: The Urbanized Northeastern Seaboard of the United States," identified the region as a distinctive entity composed of a string of large metropolitan areas.

Figure 11: Megalopolis, U.S. Census Bureau, 2021; Public Domain.

Bibliography

Adey, P., 2013. Air/Atmospheres of the Megacity. Theory, Culture & Society 30, 291–308. https://doi.org/10.1177/0263276413501541

Adolph, C., Amano, K., Bang-Jensen, B., Fullman, N., Wilkerson, J., 2021. Pandemic Politics: Timing State-Level Social Distancing Responses to COVID-19. Journal of Health Politics, Policy and Law 46, 211–233. https://doi.org/10.1215/03616878-8802162

Agnew, J.A., 2014. 1987: Place and Politics: The Geographical Mediation of State and Society. Routledge, London. https://doi.org/10.4324/9781315756585

American Lung Association, 2001. Urban air pollution and health inequities: a workshop report. Environ Health Perspect 109, 357–374. https://doi.org/10.1289/ehp.109-1240553

American Lung Association, 2020. Ozone [WWW Document]. URL https://www.lung.org/clean-air/outdoors/what-makes-air-unhealthy/ozone (accessed 10.31.22).

American Lung Association, 2021. State of the Air 2021.

Amini, H., Danesh-Yazdi, M., Di, Q., Requia, W., Wei, Y., Abu-Awad, Y., Shi, L., Franklin, M., Kang, C.-M., Wolfson, J., James, P., Habre, R., Zhu, Q., Apte, J., Andersen, Z., kloog, I., Dominici, F., Koutrakis, P., Schwartz, J., 2022. Hyperlocal super-learned PM2.5 components across the contiguous US (preprint). In Review. https://doi.org/10.21203/rs.3.rs-1745433/v1

Anselin, L., 1988. Spatial Econometrics: Methods and Models. Kluwer Academic Publishers, The Netherlands.

Anselin, L., 1995. Local Indicators of Spatial Association—LISA. Geographical Analysis 27, 93–115. https://doi.org/10.1111/j.1538-4632.1995.tb00338.x

Anselin, L., 1996a. Interactive Techniques and Exploratory Spatial Data Analysis. Regional Research Institute Working Papers.

Anselin, L., 1996b. The Moran scatterplot as an ESDA tool to assess local instability in spatial association, in: Spatial Analytical Perspectives on GIS. Routledge.

Anselin, L., 2003. Spatial Econometrics, in: A Companion to Theoretical Econometrics. John Wiley & Sons, Ltd, pp. 310–330. https://doi.org/10.1002/9780470996249.ch15

Anselin, L., 2020. Global Spatial Autocorrelation (1) [WWW Document]. Geoda. URL https://geodacenter.github.io/workbook/5a_global_auto/lab5a.html (accessed 6.30.22).

Anselin, L., Bera, A., 1998. Spatial Dependence in Linear Regression Models with an Introduction to Spatial Econometrics: Regression Models with an Anselin Bera I. INTRODUCTION, in: Handbook of Applied Economic Statistics. CRC Press.

Anselin, L., Getis, A., 1992. Spatial statistical analysis and geographic information systems. Ann Reg Sci 26, 19–33. https://doi.org/10.1007/BF01581478

Aronow, P.M., Miller, B.T., 2019. Foundations of Agnostic Statistics. Cambridge University Press, Cambridge. https://doi.org/10.1017/9781316831762

Asthma and Allergy Foundation of America. 2015. Air Pollution and Asthma | AAFA.org [WWW Document], n.d. URL https://www.aafa.org/air-pollution-smog-asthma/(accessed 6.29.22).

Astivia, O., Zumbo, B., 2019. Heteroskedasticity in Multiple Regression Analysis: What it is, How to Detect it and How to Solve it with Applications in R and SPSS. Practical Assessment, Research, and Evaluation 24. https://doi.org/10.7275/q5xr-fr95

Bailey, Z.D., Krieger, N., Agénor, M., Graves, J., Linos, N., Bassett, M.T., 2017. Structural racism and health inequities in the USA: evidence and interventions. The Lancet 389, 1453–1463. https://doi.org/10.1016/S0140-6736(17)30569-X

Baker, C., 2020. The Trump administration's major environmental deregulations. Brookings. URL https://www.brookings.edu/blog/up-front/2020/12/15/the-trump-administrations-major-environmental-deregulations/(accessed 6.29.22).

Baller, R.D., Anselin, L., Messner, S.F., Deane, G., Hawkins, D.F., 2001. Structural Covariates of U.s. County Homicide Rates: Incorporating Spatial Effects*. Criminology 39, 561–588. https://doi.org/10.1111/j.1745-9125.2001.tb00933.x

Bashir, M.F., Ma, B., Bilal, Komal, B., Bashir, M.A., Tan, D., Bashir, M., 2020. Correlation between climate indicators and COVID-19 pandemic in New York, USA. Science of The Total Environment 728, 138835. https://doi.org/10.1016/j.scitotenv.2020.138835

Bauer, R.N., Diaz-Sanchez, D., Jaspers, I., 2012. Effects of air pollutants on innate immunity: The role of Toll-like receptors and nucleotide-binding oligomerization domain–like receptors. Journal of Allergy and Clinical Immunology 129, 14–24. https://doi.org/10.1016/j.jaci.2011.11.004

BBC News, 2022. Ella Adoo-Kissi-Debrah: Vigil to mark birthday of girl killed by toxic air - BBC News [WWW Document]. URL https://www.bbc.com/news/uk-england-london-60084882 (accessed 6.29.22).

Beland, L.-P., Boucher, V., 2015. Polluting politics. Economics Letters 137, 176–181. https://doi.org/10.1016/j.econlet.2015.11.007

Bell, M.L., HEI Health Review Committee, 2012. Assessment of the health impacts of particulate matter characteristics. Res Rep Health Eff Inst 5–38.

Berg, K., Romer Present, P., Richardson, K., 2021. Long-term air pollution and other risk factors associated with COVID-19 at the census tract level in Colorado. Environmental Pollution 287, 117584. https://doi.org/10.1016/j.envpol.2021.117584

Bivand, R., n.d. Lagrange Multiplier diagnostics for spatial dependence in linear models — lm.LMtests [WWW Document]. URL https://r-spatial.github.io/spdep/reference/lm.LMtests.html#see-also-1 (accessed 6.30.22).

Blum, M.R., Tan, Y.J., Ioannidis, J.P.A., 2020. Use of E-values for addressing confounding in observational studies—an empirical assessment of the literature. International Journal of Epidemiology 49, 1482–1494. https://doi.org/10.1093/ije/dyz261

Bocci, V.A., 2007. Tropospheric ozone toxicity vs. usefulness of ozone therapy. Arch Med Res 38, 265–267. https://doi.org/10.1016/j.arcmed.2006.09.011

Boots, B., Tiefelsdorf, M., 2000. Global and local spatial autocorrelation in bounded regular tessellations. J Geograph Syst 2, 319–348. https://doi.org/10.1007/PL00011461

Bravo, M.A., Anthopolos, R., Bell, M.L., Miranda, M.L., 2016. Racial isolation and exposure to airborne particulate matter and ozone in understudied US populations: Environmental justice applications of downscaled numerical model output. Environment International 92–93, 247–255. https://doi.org/10.1016/j.envint.2016.04.008

Cattel, F., Giordano, S., Bertiond, C., Lupia, T., Corcione, S., Scaldaferri, M., Angelone, L., De Rosa, F.G., 2021. Ozone therapy in COVID-19: A narrative review. Virus Res 291, 198207. https://doi.org/10.1016/j.virusres.2020.198207

Chen, B., Song, Y., Jiang, T., Chen, Z., Huang, B., Xu, B., 2018. Real-Time Estimation of Population Exposure to PM2.5 Using Mobile- and Station-Based Big Data. International Journal of Environmental Research and Public Health 15, 573. https://doi.org/10.3390/ijerph15040573

Chen, X., Shao, S., Tian, Z., Xie, Z., Yin, P., 2017. Impacts of air pollution and its spatial spillover effect on public health based on China's big data sample. Journal of Cleaner Production, Special Volume on Improving natural resource management and human health to ensure sustainable societal development based upon insights gained from working within 'Big Data Environments' 142, 915–925. https://doi.org/10.1016/j.jclepro.2016.02.119

Cheng, W., 2019. Measuring the Robustness of the National Basketball Association Home Court Advantage Effect. University of California, Los Angeles ProQuest Dissertations Publishing.

Cheng, Y., He, K., Du, Z., Zheng, M., Duan, F., Ma, Y., 2015. Humidity plays an important role in the PM2.5 pollution in Beijing. Environmental Pollution 197, 68–75. https://doi.org/10.1016/j.envpol.2014.11.028

Chi, G., Zhu, J., 2019. Spatial Regression Models for the Social Sciences. SAGE Publications.

Chih, Y.-Y., Ojede, A., 2020. Racial Disparity Effects of the COVID-19 Pandemic: A Spatial Diffusion Analysis Across U.S. Counties.

Chowkwanyun, M., Reed Jr., A., 2020. Racial Health Disparities and Covid-19 — Caution and Context | NEJM [WWW Document]. URL https://www.nejm.org/doi/full/10.1056/NEJMp2012910 (accessed 6.30.22).

Cinelli, C., Ferwerda, J., Hazlett, C., 2020. Sensemakr: Sensitivity Analysis Tools for OLS in R and Stata. https://doi.org/10.2139/ssrn.3588978

Cinelli, C., Hazlett, C., 2020. Making sense of sensitivity: extending omitted variable bias. Journal of the Royal Statistical Society: Series B (Statistical Methodology) 82, 39–67. https://doi.org/10.1111/rssb.12348

Cisneros, R., Bytnerowicz, A., Schweizer, D., Zhong, S., Traina, S., Bennett, D.H., 2010. Ozone, nitric acid, and ammonia air pollution is unhealthy for people and ecosystems in southern Sierra Nevada, California. Environmental Pollution 158, 3261–3271. https://doi.org/10.1016/j.envpol.2010.07.025

Clay, K., Muller, N.Z., Wang, X., 2021. Recent Increases in Air Pollution: Evidence and Implications for Mortality. Review of Environmental Economics and Policy 15, 154–162. https://doi.org/10.1086/712983

Colmer, J., Hardman, I., Shimshack, J., Voorheis, J., 2020. Disparities in PM2.5 air pollution in the United States. Science 369, 575–578. https://doi.org/10.1126/science.aaz9353

Cordes, J., Castro, M.C., 2020. Spatial analysis of COVID-19 clusters and contextual factors in New York City. Spatial and Spatio-temporal Epidemiology 34, 100355. https://doi.org/10.1016/j.sste.2020.100355

Cowan, J., Bloch, M., 2021. In Los Angeles, the Virus Is Pummeling Those Who Can Least Afford to Fall Ill - The New York Times [WWW Document]. URL https://www.nytimes.com/interactive/2021/01/29/us/los-angeles-county-covid-rates.html (accessed 6.30.22).

Cresswell, Tim, 2004. “Defining place.” Place: A Short Introduction [WWW Document]. URL https://www.northernhighlands.org/cms/lib/NJ01000179/Centricity/Domain/159/Defining%20Place%20by%20Tim%20Cresswell.pdf(accessed 9.13.22).

Currie, J., Walker, R., 2019. What Do Economists Have to Say about the Clean Air Act 50 Years after the Establishment of the Environmental Protection Agency? Journal of Economic Perspectives 33, 3–26. https://doi.org/10.1257/jep.33.4.3

Curtis, S., 2016. Space, Place and Mental Health. Routledge, London. https://doi.org/10.4324/9781315610160

Cutchin, M.P., 2007. The Need for the “New Health Geography” in Epidemiologic Studies of Environment and Health. Health Place 13, 725–742. https://doi.org/10.1016/j.healthplace.2006.11.003

Davenport, C., 2022. California Returns as Climate Leader, With Help From the White House. The New York Times.

David, L.M., Ravishankara, A.R., Brey, S.J., Fischer, E.V., Volckens, J., Kreidenweis, S., 2021. Could the exception become the rule? “Uncontrollable” air pollution events in the U.S. due to wildland fires. Environ. Res. Lett. https://doi.org/10.1088/1748-9326/abe1f3

Delmelle, E.M., Desjardins, M.R., Jung, P., Owusu, C., Lan, Y., Hohl, A., Dony, C., 2022. Uncertainty in geospatial health: challenges and opportunities ahead. Annals of Epidemiology 65, 15–30. https://doi.org/10.1016/j.annepidem.2021.10.002

Ding, P., VanderWeele, T.J., 2016. Sensitivity Analysis Without Assumptions. Epidemiology 27, 368–377. https://doi.org/10.1097/EDE.0000000000000457

Dummer, T.J.B., 2008. Health geography: supporting public health policy and planning. CMAJ 178, 1177–1180. https://doi.org/10.1503/cmaj.071783

Dyck, I., 1995. Putting chronic illness ‘in place’. Women immigrants’ accounts of their health care. Geoforum, Geographies of Women’s Health 26, 247–260. https://doi.org/10.1016/0016-7185(95)00025-9

Farzin, Y.H., Bond, C., 2013. Are Democrats Greener than Republicans? The Case of California Air Quality. https://doi.org/10.2139/ssrn.2201595

Fielding-Miller, R.K., Sundaram, M.E., Brouwer, K., 2020. Social determinants of COVID-19 mortality at the county level. PLOS ONE 15, e0240151. https://doi.org/10.1371/journal.pone.0240151

Fink, S., Kosofsky, I., 2021. Dying of Covid in a 'Separate and Unequal' L.A. Hospital. The New York Times.

Florida, R., 2019. The Real Economic Powerhouses Are Mega-Regions, Not Nations. Bloomberg.com.

Fotheringham, A.S., Wong, D.W.S., 1991. The Modifiable Areal Unit Problem in Multivariate Statistical Analysis. Environ Plan A 23, 1025–1044. https://doi.org/10.1068/a231025

Fox, M.P., Arah, O.A., Stuart, E.A., 2020. Commentary: The value of E-values and why they are not enough. International Journal of Epidemiology 49, 1505–1506. https://doi.org/10.1093/ije/dyaa093

Garcia, C.A., Yap, P.-S., Park, H.-Y., Weller, B.L., 2016. Association of long-term PM2.5 exposure with mortality using different air pollution exposure models: impacts in rural and urban California. International Journal of Environmental Health Research 26, 145–157. https://doi.org/10.1080/09603123.2015.1061113

Garcia, E., Marian, B., Chen, Z., Li, K., Lurmann, F., Gilliland, F., Eckel, S.P., 2022. Long-term air pollution and COVID-19 mortality rates in California: Findings from the Spring/Summer and Winter surges of COVID-19. Environmental Pollution 292, 118396. https://doi.org/10.1016/j.envpol.2021.118396

Glass, G.E., 2000. Update: Spatial Aspects of Epidemiology: The Interface with Medical Geography. Epidemiologic Reviews 22, 136–139. https://doi.org/10.1093/oxfordjournals.epirev.a018010

Goldhagen, J., Remo, R., Bryant, T., Wludyka, P., Dailey, A., Wood, D., Watts, G., Livingood, W., 2005. The Health Status of Southern Children: A Neglected Regional Disparity. Pediatrics 116, e746–e753. https://doi.org/10.1542/peds.2005-0366

Goodkind, A.L., Tessum, C.W., Coggins, J.S., Hill, J.D., Marshall, J.D., 2019. Fine-scale damage estimates of particulate matter air pollution reveal opportunities for

location-specific mitigation of emissions. Proceedings of the National Academy of Sciences 116, 8775–8780. https://doi.org/10.1073/pnas.1816102116

Greenland, S., 1996. Basic Methods for Sensitivity Analysis of Biases. International Journal of Epidemiology 25, 1107–1116. https://doi.org/10.1093/ije/25.6.1107-a

Grekousis, G., Feng, Z., Marakakis, I., Lu, Y., Wang, R., 2022. Ranking the importance of demographic, socioeconomic, and underlying health factors on US COVID-19 deaths: A geographical random forest approach. Health & Place 74, 102744. https://doi.org/10.1016/j.healthplace.2022.102744

Hamra, G.B., 2019. RE: "APPLYING THE E VALUE TO ASSESS THE ROBUSTNESS OF EPIDEMIOLOGIC FIELDS OF INQUIRY TO UNMEASURED CONFOUNDING." American Journal of Epidemiology 188, 1578–1580. https://doi.org/10.1093/aje/kwz128

Hazlett, C., Parente, F., 2020. Who supports peace with the FARC? A sensitivity-based approach under imperfect identification.

Hernández, A., Viñals, M., Pablos, A., Vilás, F., Papadakos, P.J., Wijeysundera, D.N., Bergese, S.D., Vives, M., 2021. Ozone therapy for patients with COVID-19 pneumonia: Preliminary report of a prospective case-control study. Int Immunopharmacol 90, 107261. https://doi.org/10.1016/j.intimp.2020.107261

Hinojosa-Baliño, I., Infante-Vázquez, O., Vallejo, M., 2019. Distribution of PM2.5 Air Pollution in Mexico City: Spatial Analysis with Land-Use Regression Model. Applied Sciences 9, 2936. https://doi.org/10.3390/app9142936

Imbens, G.W., Rubin, D.B., 2010. Rubin Causal Model, in: Durlauf, S.N., Blume, L.E. (Eds.), Microeconometrics, The New Palgrave Economics Collection. Palgrave Macmillan UK, London, pp. 229–241. https://doi.org/10.1057/9780230280816_28

Ioannidis, J.P.A., Tan, Y.J., Blum, M.R., 2019. Limitations and Misinterpretations of E-Values for Sensitivity Analyses of Observational Studies. Ann Intern Med 170, 108–111. https://doi.org/10.7326/M18-2159

Jones, J.P.A., Tan, Y.J., Blum, M.R., 2019. Limitations and Misinterpretations of E-Values for Sensitivity Analyses of Observational Studies. Ann Intern Med 170, 108–111. https://doi.org/10.7326/M18-2159

Jones, Kelvyn, Moon, Graham, 1993. Medical geography: taking space seriously - Kelvyn Jones, Graham Moon, 1993 [WWW Document]. URL https://journals.sagepub.com/doi/10.1177/030913259301700405 (accessed 9.6.22).

Kalashnikov, D.A., Schnell, J.L., Abatzoglou, J.T., Swain, D.L., Singh, D., n.d. Increasing co-occurrence of fine particulate matter and ground-level ozone extremes in the western United States. Science Advances 8, eabi9386. https://doi.org/10.1126/sciadv.abi9386

Kolak, M., Anselin, L., 2019. A Spatial Perspective on the Econometrics of Program Evaluation. International Regional Science Review 43, 128–153. https://doi.org/10.1177/0160017619869781

Konisky, D.M., Woods, N.D., 2010. Exporting Air Pollution? Regulatory Enforcement and Environmental Free Riding in the United States. Political Research Quarterly 63, 771–782. https://doi.org/10.1177/1065912909334429

Konstantinoudis, G., Padellini, T., Bennett, J., Davies, B., Ezzati, M., Blangiardo, M., 2021. Long-term exposure to air-pollution and COVID-19 mortality in England: A hierarchical spatial analysis. Environment International 146, 106316. https://doi.org/10.1016/j.envint.2020.106316

Kumar, N., Chu, A., Foster, A., 2007. An empirical relationship between PM(2.5) and aerosol optical depth in Delhi Metropolitan. Atmos Environ (1994) 41, 4492–4503. https://doi.org/10.1016/j.atmosenv.2007.01.046

Lee, D., Robertson, C., Ramsay, C., Pyper, K., 2020. Quantifying the impact of the modifiable areal unit problem when estimating the health effects of air pollution. Environmetrics 31, e2643. https://doi.org/10.1002/env.2643

Lee, D., Sarran, C., 2015. Controlling for unmeasured confounding and spatial misalignment in long-term air pollution and health studies. Environmetrics 26, 477–487. https://doi.org/10.1002/env.2348

Lee, H.J., Coull, B.A., Bell, M.L., Koutrakis, P., 2012. Use of satellite-based aerosol optical depth and spatial clustering to predict ambient PM2.5 concentrations. Environmental Research 118, 8–15. https://doi.org/10.1016/j.envres.2012.06.011

LeSage, J.P., 2008. An Introduction to Spatial Econometrics. rei 19–44. https://doi.org/10.4000/rei.3887

Lesage, J., 2014. What Regional Scientists Need to Know about Spatial Econometrics. Review of Regional Studies. https://doi.org/10.52324/001c.8081

Liang, D., Shi, L., Zhao, J., Liu, P., Sarnat, J.A., Gao, S., Schwartz, J., Liu, Y., Ebelt, S.T., Scovronick, N., Chang, H.H., 2020. Urban Air Pollution May Enhance COVID-19 Case-Fatality and Mortality Rates in the United States. The Innovation 1, 100047. https://doi.org/10.1016/j.xinn.2020.100047

Lipsitt, J., Chan-Golston, A.M., Liu, J., Su, J., Zhu, Y., Jerrett, M., 2021. Spatial analysis of COVID-19 and traffic-related air pollution in Los Angeles. Environment International 153, 106531. https://doi.org/10.1016/j.envint.2021.106531

López-Feldman, A., Heres, D., Marquez-Padilla, F., 2021. Air pollution exposure and COVID-19: A look at mortality in Mexico City using individual-level data. Science of The Total Environment 756, 143929. https://doi.org/10.1016/j.scitotenv.2020.143929

Lukermann, F., 1964. Geography as a Formal Intellectual Discipline and the Way in Which It Contributes to Human Knowledge. The Canadian Geographer / Le Géographe canadien 8, 167–172. https://doi.org/10.1111/j.1541-0064.1964.tb00605.x

Lundberg, D.J., Cho, A., Raquib, R., Nsoesie, E.O., Wrigley-Field, E., Stokes, A.C., 2022. Geographic and Temporal Patterns in Covid-19 Mortality by Race and Ethnicity in the United States from March 2020 to February 2022. medRxiv 2022.07.20.22277872. https://doi.org/10.1101/2022.07.20.22277872

Mailloux, N.A., Abel, D.W., Holloway, T., Patz, J.A., 2022. Nationwide and Regional PM2.5-Related Air Quality Health Benefits From the Removal of Energy-Related Emissions in the United States. GeoHealth 6, e2022GH000603. https://doi.org/10.1029/2022GH000603

Makar, M., Antonelli, J., Di, Q., Cutler, D., Schwartz, J., Dominici, F., 2017. Estimating the Causal Effect of Fine Particulate Matter Levels on Death and Hospitalization: Are Levels Below the Safety Standards Harmful? Epidemiology (Cambridge, Mass.) 28, 627. https://doi.org/10.1097/EDE.0000000000000690

Manjunath, S.N., Sakar, M., Katapadi, M., Geetha Balakrishna, R., 2021. Recent case studies on the use of ozone to combat coronavirus: Problems and perspectives. Environ Technol Innov 21, 101313. https://doi.org/10.1016/j.eti.2020.101313

Matisziw, T.C., Grubesic, T.H., Wei, H., 2008. Downscaling spatial structure for the analysis of epidemiological data. Computers, Environment and Urban Systems 32, 81–93. https://doi.org/10.1016/j.compenvurbsys.2007.06.002

Messner, S.F., Anselin, L., Baller, R.D., Hawkins, D.F., Deane, G., Tolnay, S.E., 1999. The Spatial Patterning of County Homicide Rates: An Application of Exploratory Spatial Data Analysis. Journal of Quantitative Criminology 15, 423–450. https://doi.org/10.1023/A:1007544208712

Miranda, M.L., Edwards, S.E., Keating, M.H., Paul, C.J., 2011. Making the Environmental Justice Grade: The Relative Burden of Air Pollution Exposure in the United States. International Journal of Environmental Research and Public Health 8, 1755–1771. https://doi.org/10.3390/ijerph8061755

Morello-Frosch, R., Lopez, R., 2006. The riskscape and the color line: Examining the role of segregation in environmental health disparities. Environmental Research, IG000012 102, 181–196. https://doi.org/10.1016/j.envres.2006.05.007

Morgan, S.L., Winship, C., 2015. Counterfactuals and Causal Inference: Methods and Principles for Social Research, 2nd ed, Analytical Methods for Social Research. Cambridge University Press, Cambridge. https://doi.org/10.1017/CBO9781107587991

Morrill, R., Gaile, G.L., Thrall, G.I., 1988. Spatial Diffusion 65.

Murthy, B.P., Sterrett, N., Weller, D., Zell, E., Reynolds, L., Toblin, R.L., Murthy, N., Kriss, J., Rose, C., Cadwell, B., Wang, A., Ritchey, M.D., Gibbs-Scharf, L., Qualters, J.R., Shaw, L., Brookmeyer, K.A., Clayton, H., Eke, P., Adams, L., Zajac, J., Patel, A., Fox, K., Williams, C., Stokley, S., Flores, S., Barbour, K.E., Harris, L.Q., 2021. Disparities in COVID-19 Vaccination Coverage Between Urban and Rural Counties — United States, December 14, 2020–April 10, 2021. MMWR Morb Mortal Wkly Rep 70, 759–764. https://doi.org/10.15585/mmwr.mm7020e3

Nagelkerke, N.J.D., 1991. A Note on a General Definition of The Coefficient of Determination. Biometrika 78, 691–692. https://www.jstor.org/stable/2337038

Nakagawa, S., Schielzeth, H., 2013. A general and simple method for obtaining R2 from generalized linear mixed-effects models. Methods in Ecology and Evolution 4, 133–142. https://doi.org/10.1111/j.2041-210x.2012.00261.x

Namin, S., Xu, W., Zhou, Y., Beyer, K., 2020. The legacy of the Home Owners' Loan Corporation and the political ecology of urban trees and air pollution in the United States. Social Science & Medicine 246, 112758. https://doi.org/10.1016/j.socscimed.2019.112758

Nardone, A., Neophytou, A.M., Balmes, J., Thakur, N., 2018. Ambient Air Pollution and Asthma-Related Outcomes in Children of Color of the USA: a Scoping Review of Literature Published Between 2013 and 2017. Curr Allergy Asthma Rep 18, 29. https://doi.org/10.1007/s11882-018-0782-x

Neelon, B., Mutiso, F., Mueller, N.T., Pearce, J.L., Benjamin-Neelon, S.E., 2021. Associations Between Governor Political Affiliation and COVID-19 Cases, Deaths, and Testing in the U.S. American Journal of Preventive Medicine 61, 115–119. https://doi.org/10.1016/j.amepre.2021.01.034

Nguyen, J.L., Benigno, M., Malhotra, D., Reimbaeva, M., Sam, Z., Chambers, R., Hammond, J., Emir, B., 2022. Hospitalization and Mortality Trends among Patients with Confirmed COVID-19 in the United States, April through August 2020. Journal of Public Health Research 11, jphr.2021.2244. https://doi.org/10.4081/jphr.2021.2244

Nordenstam, B.J., Lambright, W.H., Berger, M.E., Little, M.K., 1998. A framework for analysis of transboundary institutions for air pollution policy in the United States. Environmental Science & Policy 1, 231–238. https://doi.org/10.1016/S1462-9011(98)00021-5

Norwood, K., 2021. Former COVID hot spot is first county in NM to have 100% of residents one shot down [WWW Document]. KOAT. URL https://www.koat.com/article/mckinley-county-becomes-first-county-in-new-mexico-to-get-100-of-residents-vaccinated-with-first-shot/36948214 (accessed 11.8.22).

NY State Dept. of Health, 2018. Fine Particles (PM 2.5) Questions and Answers [WWW Document]. URL https://www.health.ny.gov/environmental/indoors/air/pmq_a.htm (accessed 6.29.22).

Oster, A.M., Kang, G.J., Cha, A.E., Beresovsky, V., Rose, C.E., Rainisch, G., Porter, L., Valverde, E.E., Peterson, E.B., Driscoll, A.K., Norris, T., Wilson, N., Ritchey, M., Walke, H.T., Rose, D.A., Oussayef, N.L., Parise, M.E., Moore, Z.S., Fleischauer, A.T., Honein, M.A., Dirlikov, E., Villanueva, J., 2020. Trends in Number and Distribution of COVID-19 Hotspot Counties — United States, March 8–July 15, 2020. MMWR Morb Mortal Wkly Rep 69, 1127–1132. https://doi.org/10.15585/mmwr.mm6933e2

Pacheco, A.I., Tyrrell, T.J., 2002. Testing spatial patterns and growth spillover effects in clusters of cities. J Geograph Syst 4, 275–285. https://doi.org/10.1007/s101090200089

Park, S.H., Gong, S.L., Gong, W., Makar, P.A., Moran, M.D., Zhang, J., Stroud, C.A., 2010. Relative impact of windblown dust versus anthropogenic fugitive dust in PM2.5 on air quality in North America. Journal of Geophysical Research: Atmospheres 115. https://doi.org/10.1029/2009JD013144

Pierce, A.M., Loría-Salazar, S.M., Holmes, H.A., Gustin, M.S., 2019. Investigating horizontal and vertical pollution gradients in the atmosphere associated with an urban location in complex terrain, Reno, Nevada, USA. Atmospheric Environment 196, 103–117. https://doi.org/10.1016/j.atmosenv.2018.09.063

Pope, C.A., Coleman, N., Pond, Z.A., Burnett, R.T., 2020. Fine particulate air pollution and human mortality: 25+ years of cohort studies. Environ Res 183, 108924. https://doi.org/10.1016/j.envres.2019.108924

Razavi, S., Jakeman, A., Saltelli, A., Prieur, C., Iooss, B., Borgonovo, E., Plischke, E., Lo Piano, S., Iwanaga, T., Becker, W., Tarantola, S., Guillaume, J.H.A., Jakeman, J., Gupta, H., Melillo, N., Rabitti, G., Chabridon, V., Duan, Q., Sun, X., Smith, S., Sheikholeslami, R., Hosseini, N., Asadzadeh, M., Puy, A., Kucherenko, S., Maier, H.R., 2021. The Future of Sensitivity Analysis: An essential discipline for systems modeling and policy support. Environmental Modelling & Software 137, 104954. https://doi.org/10.1016/j.envsoft.2020.104954

Reich, B.J., Yang, S., Guan, Y., Giffin, A.B., Miller, M.J., Rappold, A., 2021. A Review of Spatial Causal Inference Methods for Environmental and Epidemiological Applications. International Statistical Review 89, 605–634. https://doi.org/10.1111/insr.12452

Reynolds, E., 2020. Air pollution a cause of UK girl's death, coroner rules - CNN [WWW Document]. URL https://www.cnn.com/2020/12/16/uk/air-pollution-death-ella-kissi-debrah-uk-gbr-intl/index.html (accessed 9.25.22).

Romano, S.D., Blackstock, A.J., Taylor, E.V., El Burai Felix, S., Adjei, S., Singleton, C.-M., Fuld, J., Bruce, B.B., Boehmer, T.K., 2021. Trends in Racial and Ethnic Disparities in COVID-19 Hospitalizations, by Region — United States, March–December 2020. MMWR Morb Mortal Wkly Rep 70, 560–565. https://doi.org/10.15585/mmwr.mm7015e2

Rosenbaum, P.R., 2014. Sensitivity Analysis in Observational Studies, in: Wiley StatsRef: Statistics Reference Online. John Wiley & Sons, Ltd. https://doi.org/10.1002/9781118445112.stat06358

Rossen, L.M., 2020. Excess Deaths Associated with COVID-19, by Age and Race and Ethnicity — United States, January 26–October 3, 2020. MMWR Morb Mortal Wkly Rep 69. https://doi.org/10.15585/mmwr.mm6942e2

Roussel, S., Butkus, Neva, 2020. Poverty in Louisiana. Louisiana Budget Project.https://www.labudget.org/wp-content/uploads/2020/09/LBP-Census-2019.p

Schnell, J.L., Prather, M.J., 2017. Co-occurrence of extremes in surface ozone, particulate matter, and temperature over eastern North America. PNAS 114, 2854–2859. https://doi.org/10.1073/pnas.1614453114

Sergi, B., Azevedo, I., Davis, S.J., Muller, N.Z., 2020. Regional and county flows of particulate matter damage in the US. Environ. Res. Lett. 15, 104073. https://doi.org/10.1088/1748-9326/abb429

Shin, M., Agnew, J., 2011. Spatial regression for electoral studies: The case of the Italian Lega Nord. Revitalizing Electoral Geography 59–74.

Shin, M., Ward, M.D., 1999. Lost in Space: Political Geography and the Defense-Growth Trade-Off. Journal of Conflict Resolution 43, 793–817. https://doi.org/10.1177/0022002799043006006

Simon, H., Reff, A., Wells, B., Xing, J., Frank, N., 2015. Ozone Trends Across the United States over a Period of Decreasing NOx and VOC Emissions. Environ. Sci. Technol. 49, 186–195. https://doi.org/10.1021/es504514z

Sittner, T., 2021. A Case for The Curriculum: Health Geography. Teaching Geography 46, 21–24.

Stewart, J., Kennelly, P., 2010. Illuminated Choropleth Maps. Annals of the Association of American Geographers 100, 513–534. https://doi.org/10.1080/00045608.2010.485449

Thind, M.P.S., Tessum, C.W., Azevedo, I.L., Marshall, J.D., 2019. Fine Particulate Air Pollution from Electricity Generation in the US: Health Impacts by Race, Income, and Geography. Environ. Sci. Technol. 53, 14010–14019. https://doi.org/10.1021/acs.est.9b02527

Thompson, C.N., Baumgartner, J., Pichardo, C., Toro, B., Li, L., Arciuolo, R., Chan, P.Y., Chen, J., Culp, G., Davidson, A., Devinney, K., Dorsinville, A., Eddy, M., English, M., Fireteanu, A.M., Graf, L., Geevarughese, A., Greene, S.K., Guerra, K., Huynh, M., Hwang, C., Iqbal, M., Jessup, J., Knorr, J., Latash, J., Lee, E., Lee, K., Li, W., Mathes, R., McGibbon, E., McIntosh, N., Montesano, M., Moore, M.S., Murray, K., Ngai, S., Paladini, M., Paneth-Pollak, R., Parton, H., Peterson, E., Pouchet, R., Ramachandran, J., Reilly, K., Sanderson Slutsker, J., Van Wye, G., Wahnich, A., Winters, A., Layton, M., Jones, L., Reddy, V., Fine, A., 2020. COVID-19 Outbreak — New York City, February 29–June 1, 2020. MMWR Morb Mortal Wkly Rep 69, 1725–1729. https://doi.org/10.15585/mmwr.mm6946a2

Tobler, W.R., 1970. A Computer Movie Simulating Urban Growth in the Detroit Region. Economic Geography 46, 234. https://doi.org/10.2307/143141

Tsirigotis, Panagiotis (EPA), 2021. Release of the Draft Policy Assessment for the Particulate Matter National Ambient Air Quality Standards. Federal Register, National Archives. https://www.federalregister.gov/d/2021-22067

Tuan, Yi-Fu, 1979. Space and Place: Humanistic Perspective | SpringerLink [WWW Document]. URL https://link.springer.com/chapter/10.1007/978-94-009-9394-5_19 (accessed 9.6.22).

Tulchinsky, T.H., 2018. John Snow, Cholera, the Broad Street Pump; Waterborne Diseases Then and Now. Case Studies in Public Health 77–99. https://doi.org/10.1016/B978-0-12-804571-8.00017-2

U.S. Census Bureau, 2021a. Megalopolis [WWW Document]. URL https://www.census.gov/content/dam/Census/library/visualizations/2021/demo/megalopolis.pdf (accessed 11.4.22).

U.S. Census Bureau, 2021b. U.S. Census Bureau QuickFacts: Louisiana [WWW Document]. URL https://www.census.gov/quickfacts/LA (accessed 11.4.22).

U.S. Dept. of Commerce, 1994. Geographic Areas Reference Manual [WWW Document]. Census.gov. URL https://www.census.gov/programs-surveys/geography/guidance/geographic-areas-reference-manual.html (accessed 2.2.22).

U.S. Dept. of Energy, 2015. Midwest Region ENERGY SECTOR RISK PROFILE [WWW Document]. URL https://www.energy.gov/sites/prod/files/2015/10/f27/Energy_Sector_Risk_Profile_MidwestRegion.pdf (accessed 11.8.22).

US EPA, 2013. National Ambient Air Quality Standards for Particulate Matter; Final Rule. https://www.epa.gov/pm-pollution/national-ambient-air-quality-standards-naaqs-pm

US EPA, 2015. Criteria Air Pollutants 22. https://www.epa.gov/sites/default/files/2015-10/documents/ace3_criteria_air_pollutants.pdf

US EPA, 2016a. Particulate Matter (PM2.5) Trends | National Air Quality: Status and Trends of Key Air Pollutants | US EPA [WWW Document]. URL https://19january2017snapshot.epa.gov/air-trends/particulate-matter-pm25-trends_.html (accessed 6.15.22).

US EPA, 2016b. Particulate Matter (PM) Basics [WWW Document]. US EPA. URL https://www.epa.gov/pm-pollution/particulate-matter-pm-basics (accessed 6.5.21).

US EPA, 2018. EPA Report on the Environment. https://cfpub.epa.gov/roe/indicator_pdf.cfm?i=19

US EPA, 2021a. National Ambient Air Quality Standards (NAAQS) for PM [WWW Document]. URL https://www.epa.gov/pm-pollution/national-ambient-air-quality-standards-naaqs-pm (accessed 6.29.22).

US EPA, 2021b. Regional Haze Program [WWW Document]. URL https://www.epa.gov/visibility/regional-haze-program (accessed 6.29.22).

US EPA, 2021c. Reviewing National Ambient Air Quality Standards (NAAQS): Scientific and Technical Information [WWW Document]. URL https://www.epa.gov/naaqs (accessed 6.29.22).

US EPA, 2021d. Regulatory and Guidance Information by Topic: Air [WWW Document]. URL https://www.epa.gov/regulatory-information-topic/regulatory-and-guidance-information-topic-air (accessed 6.29.22).

VanderWeele, T.J., Ding, P., 2017. Sensitivity Analysis in Observational Research: Introducing the E-Value. Ann Intern Med 167, 268–274. https://doi.org/10.7326/M16-2607

VanderWeele, T.J., Martin, J.N., Mathur, M.B., 2020. E Values and Incidence Density Sampling. Epidemiology 31, e51. https://doi.org/10.1097/EDE.0000000000001238

Véron, R., 2006. Remaking Urban Environments: The Political Ecology of Air Pollution in Delhi. Environ Plan A 38, 2093–2109. https://doi.org/10.1068/a37449

Vijayan, T., Shin, M., Adamson, P.C., Harris, C., Seeman, T., Norris, K.C., Goodman-Meza, D., 2021. Beyond the 405 and the 5: Geographic Variations and Factors Associated With Severe Acute Respiratory Syndrome Coronavirus 2 (SARS-CoV-2) Positivity Rates in Los Angeles County. Clinical Infectious Diseases 73, e2970–e2975. https://doi.org/10.1093/cid/ciaa1692

Wallace, C., 2020. COVID Is Everywhere, Even in “the Last COVID-Free County” [WWW Document]. Texas Monthly. URL https://www.texasmonthly.com/news-politics/covid-loving-county/ (accessed 11.8.22).

Wu, X., Nethery, R.C., Sabath, M.B., Braun, D., Dominici, F., 2020. Air pollution and COVID-19 mortality in the United States: Strengths and limitations of an ecological regression analysis. Science Advances 6, eabd4049. https://doi.org/10.1126/sciadv.abd4049

Xu, A., Loch-Temzelides, T., Adiole, C., Botton, N., Dee, S.G., Masiello, C.A., Osborn, M., Torres, M.A., Cohan, D.S., 2022. Race and ethnic minority, local pollution, and COVID-19 deaths in Texas. Sci Rep 12, 1002. https://doi.org/10.1038/s41598-021-04507-x

Yang, T.-C., Noah, A.J., Shoff, C., 2015. Exploring Geographic Variation in US Mortality Rates Using a Spatial Durbin Approach. Population, Space and Place 21, 18–37. https://doi.org/10.1002/psp.1809

Yang, X., Ye, X., Sui, D., 2016. We Know Where You Are: International Journal of Applied Geospatial Research 7, 61–75. https://doi.org/10.4018/IJAGR.2016040105

Zalakeviciute, R., López-Villada, J., Rybarczyk, Y., 2018. Contrasted Effects of Relative Humidity and Precipitation on Urban PM2.5 Pollution in High Elevation Urban Areas. Sustainability 10, 2064. https://doi.org/10.3390/su10062064

Zhang, G., Rui, X., Fan, Y., 2018. Critical Review of Methods to Estimate PM2.5 Concentrations within Specified Research Region. ISPRS International Journal of Geo-Information 7, 368. https://doi.org/10.3390/ijgi7090368

Zhu, J., Chen, L., Liao, H., Dang, R., 2019. Correlations between PM2.5 and Ozone over China and Associated Underlying Reasons. Atmosphere 10, 352. https://doi.org/10.3390/atmos10070352

Zhu, Y., Xie, J., Huang, F., Cao, L., 2020. Association between short-term exposure to air pollution and COVID-19 infection: Evidence from China. Science of The Total Environment 727, 138704. https://doi.org/10.1016/j.scitotenv.2020.138704